COO-4570-10
MITNE-227
MIT-EL-79-022

AN EVALUATION OF TIGHT-PITCH PWR CORES

by

Francisco Corrêa
Michael J. Driscoll
David D. Lanning

DOE Contract No. EN-77-S 02-4570
Nuclear Engineering Report No. MITNE-227
Energy Laboratory Report No. MIT-EL 79-022
August 1979

AN EVALUATION OF TIGHT-PITCH PWR CORES

by

Francisco Corrêa
Michael J. Driscoll
David D. Lanning

Department of Nuclear Engineering
and
Energy Laboratory
MASSACHUSETTS INSTITUTE OF TECHNOLOGY
Cambridge, Massachusetts 02139

Sponsored by
U.S. Department of Energy

Printed in the United States of America

Available from

National Technical Information Service
U.S. Department of Commerce
5285 Port Royal Road
Springfield, VA 22161

Price: Printed Copy $9.25; Microfiche $3.00

ACKNOWLEDGEMENTS

The work presented in this report has been performed primarily by the principal author, Francisco Corrêa, who has submitted substantially the same report in partial fulfillment of the requirements for the degree of Doctor of Philosophy in Nuclear Engineering at M.I.T.

The principal author was supported during the course of this work by the Instituto de Pesquisas Energéticas e Nucleares (Brazil) and Fundação de Amparo à Pesquisa do Estado de São Paulo (Brazil) and by a Department of Energy (DOE) contract administered through the MIT Energy Laboratory. Computer calculations were carried out at the MIT Information Processing Center and Laboratory for Nuclear Science. We would specially like to thank Rachel Morton for her continuous help on computational problems, and Dale Lancaster for help with the application of fast reactor-physics methods.

The typing of this manuscript was very ably handled by Cynthia Mitaras.

ABSTRACT

The impact of tight pitch cores on the consumption of natural uranium ore has been evaluated for two systems of coupled PWR's namely one particular type of thorium system--U-235/UO_2: Pu/ThO_2: U-233/ThO_2--and the conventional recycle-mode uranium system-- U-235/UO_2: Pu/UO_2. The basic parameter varied was the fuel-to-moderator volume ratio (F/M) of the (uniform) lattice for the last core in each sequence.

Although methods and data verification in the range of present interest, 0.5 (current lattices) < F/M < 4.0 are limited by the scarcity of experiments with F/M > 1.0, the EPRI-LEOPARD and LASER programs used for the thorium and uranium calculations, respectively, were successfully benchmarked against several of the more pertinent experiments.

It was found that by increasing F/M to $\sim$3 the uranium ore usage for the uranium system can be decreased by as much as 60% compared to the same system with conventional recycle (at F/M = 0.5). Equivalent savings for the thorium system of the type examined here are much smaller ($\sim$10%) because of the poor performance of the intermediate Pu/ThO_2 core--which is not substantially improved by increasing F/M. Although fuel cycle costs (calculated at the indifference value of bred fissile species) are rather insensitive to the characteristics of the tight pitch cores, system energy production costs do not favor the low discharge burnups which might otherwise allow even greater ore savings ($\sim$80%).

Temperature and void coefficients of reactivity for the tight pitch cores were calculated to be negative. Means for implementing tight lattice use were investigated, such as the use of stainless steel clad in place of zircaloy; and alternatives achieving the same objective were briefly examined, such as the use of D_2O/H_2O mixtures as coolant. Major items identified requiring further work are system redesign to accommodate higher core pressure drop, and transient and accident thermal-hydraulics.

TABLE OF CONTENTS

LIST OF TABLES

LIST OF FIGURES

CHAPTER 1

INTRODUCTION

1.1 Foreword

The increasing dependence of world energy production on fission energy and the delay in the development and deployment of advanced fission reactors, such as the HTGR and the LMFBR (High Temperature Gas Cooled Reactor and Liquid Metal-Cooled Fast Breeder Reactor, respectively), have shortened the projected useful resource lifetime for the known low-cost reserves of natural uranium. For example, a representative recent estimate of the assured reserves of uranium for the noncommunist world ($\sim 2.42 \times 10^6$ ST U_3O_8) (N-1) would barely suffice to fuel LWR's (Light Water Reactors) already operable, under construction or on order for their entire anticipated service life of thirty-years. This would be particularly true if these LWR's continue to operate on the once-through fuel cycle (no uranium or plutonium recycling) and if no advanced converter or breeder reactors are introduced in substantial numbers in the next thirty years.

This situation has motivated, among other things, a renewed interest in the reoptimization of LWR cores to achieve better uranium ore conservation. We should stress here that as of January, 1979 about 54% and 23% of the committed nuclear power plants in the world were PWR's and BWR's (Pressurized and Boiling Water Reactors), respectively (Table 2-1).

The present work represents one subtask of a project carried out at MIT for DOE as part of their NASAP/INFCE-related efforts (Nonproliferation Alternative System Assessment Program and International Nuclear Fuel Cycle

Evaluation (G-1, F-1, A-1, A-2). Optimization studies of fuel cycle cost and the consumption of natural uranium have been done for a variety of systems of coupled PWR's for both once-through and recycle-mode fuel cycles in previously reported efforts (G-1, F-1). Building on this work, the present effort is concentrated on an evaluation of the effects of different fuel management strategies for tight-pitch PWR lattices fueled by U-233/ThO_2 or Pu/UO_2 on the ore consumption and economics of systems of coupled reactors (composed of standard and advanced tight-pitch PWR reactors). The number of core batches (N), the discharge fuel burnup (B) and the fuel-to-moderator volume ratio (F/M) of the reactor lattices were treated as independent variables. Since plutonium and U-233 are man-made substances, the entirety of the present work is restricted to recycle mode operation, which is also superior in terms of ore conservation (G-1).

1.2 Objectives

The primary objective of the present work is the determination of the effects of the use of tight-pitch PWR cores on the consumption of natural uranium and on fuel cycle cost for systems of coupled PWR's.

Two systems are studied. The first is based on the uranium cycle and is composed of two types of reactors: standard PWR cores using conventional uranium fuel (enriched to about 3.0 w/o in U-235) producing plutonium for tight-pitch Pu/UO_2-fueled PWR Cores. The second system is based on both the uranium and thorium cycles, and consists of three types of cores: again standard PWR-cores produce plutonium which is now used to fuel Pu/ThO_2 cores. The U-233 produced in the second reactor is used to feed the third type of core in this system:

U-233/ThO_2-fueled, tight-pitch, PWR cores.

The first system, U-235/UO_2:Pu/UO_2, was chosen because it is by far the leading candidate being worked on worldwide for LWR recycle and breeder use. The second system, U-235/UO_2:Pu/ThO_2:U-233/ThO_2, was chosen because of practical industrial considerations: uranium reprocessing will become available before thorium reprocessing, hence Pu/ThO_2 cores can be deployed sooner; also by not going to the already well-studied U-235/ThO_2 route we avoid contaminating U-235 with U-232 and other uranium isotopes which would make its re-enrichment and re-fabrication more expensive.

Because the fuel management characteristics for the standard PWR Cores are already very near their optimum values (in terms of fuel cycle cost and ore utilization (G-1)), only the characteristics of the consumer cores (Pu/UO_2 and U-233/ThO_2-fueled cores) are varied. The fuel management parameters (N, B and F/M) for the Pu/ThO_2 cores are taken (except where otherwise noted) to be the same as for the standard PWR Cores. The effects of the number of core-zones (N), discharged fuel burnup (B) and fuel-to-moderator volume ratio (F/M) of these consumer cores on the consumption of natural uranium (CNU) and on the fuel cycle costs of their respective systems are studied. The moderator-void and fuel-temperature reactivity coefficients for these cores are also estimated.

In addition, other ways to improve fuel utilization (other than by increasing F/M), for example by hardening the neutron spectrum through the use of D_2O as moderator or metallic thorium as fuel are briefly discussed.

1.3 Previous Work

1.3.1 Fuel Cycle and Core Design

The recent NASAP and INFCE efforts have greatly simplified the task of reviewing prior work. In view of the large number of studies and assessments being published under these auspices, we can confine ourselves here to two main areas: a review of the previous MIT work used as a foundation for much of the current effort, and a recapitulation of selected thorium-cycle studies which can serve as a background for the present work in that field.

Over the past two years work has been done at MIT for DOE on improving PWR's as part of their NASAP/INFCE efforts. One major subtask (F-1) has dealt with different design and fuel management strategies to optimize the once-through fuel cycle. The other major subtask (G-1, A-2) covered the use of drier lattices in PWR's.

K. Garel (G-1) studied the use of several types of fuel compositions in PWR's for a wide range of fuel-to-moderator volume ratios ($0.34 \leq F/M \leq 1.50$) both with and without recycle. The discharge burnup and the number of reactor zones were kept fixed (B = 33 MWD/KgHM and N = 3, respectively). In terms of ore conservation he found that for the uranium cycle (with or without fuel recycle) the optimum F/M is near the actual value for today's PWR's ($F/M \approx 0.5$) and is insensitive to the system growth rate. For the U-235/ThO_2 cycle (with recycle) he found that as the system growth rate increases, the optimum F/M moves progressively closer to 0.5, while for slowly-growing systems the optimum F/M is near or above 1.5. In addition to being of a survey nature, the exclusive use of the LEOPARD

program in Garel's work to calculate mass flows for the cores containing plutonium is open to criticism since this code does not properly treat the low-lying resonances for plutonium isotopes. Also the weight given to Pu-239 and Pu-241, 0.8, to account for isotopic degradation in ore consumption calculations appears to be too low.

A. Abbaspour (A-2) analyzed in economic terms the data from Garel's work. He basically found that cost-optimum thorium lattices are drier than current PWR lattices, but are not economically competitive with cost-optimum uranium lattices, which are essentially those in use today.

Edlund's work (E-1, E-2) on the physics of tight-pitch PWR-lattices using Pu/UO_2 as fuel indicates that breeding (CR $\sim$ 1.08) is feasible for F/M > 2.0. He explains that breeding is possible due to an increase in the "fast fission effect" in U-238 and Pu-240 (about 17% of the fissions occur in these isotopes at F/M $\sim$ 2.0).

The core of the Light Water Breeder Reactor (LWBR) at Shippingport (L-1) uses fuel modules, each composed of a central movable seed region (F/M = 1.7) surrounded by a stationary blanket region (F/M = 3.0). It uses a $U\text{-}233/ThO_2$ mixture in these modules and ThO_2 in the blanket. This core is designed to achieve a breeding ratio slightly greater than unity for low discharged fuel burnup.

Combustion Engineering's work on the use of thorium in PWR's (S-1) includes a brief analysis of tight-pitch lattices in the range $0.5 \leq F/M \leq 1.0$, and concludes that improved fuel utilization by tightening the lattices is partially offset by the higher fissile inventory needed. The Spectrum Shift Control Reactor (SSCR) is also reviewed and it is concluded that this concept can not only save (at least) 20% in the consumption of natural uranium for both uranium and thorium fueled reactors (with fuel recycling)

but also needs less fissile inventory ($\sim$7 %) than the respective standard versions using light water and controlled by soluble boron.

The work by Oosterkamp and Correa (O-1, C-1) on thorium utilization in PWR's looked briefly at optimizing the fuel-to-moderator volume ratio. Their results show an optimum for the fuel cycles analyzed in the F/M range of 0.67 to 1.0.

General Electric's study on the utilization of thorium in BWR's (W-1) concluded that increased coolant boiling (this is equivalent to increased F/M) for U-233/ThO_2 fuel compositions would provide slightly better uranium utilization than the standard void-fraction case (CR = 0.72 at 40% core averaged voids and CR = 0.76 at 70% voids).

References (K-1) and (D-1) are useful because they provide an ample discussion of the potential utilization of the thorium fuel cycle in nuclear power reactors and give an extensive list of references on thorium studies.

1.3.2 Experimental Benchmarks

As part of the efforts to verify our methods of calculation, an extensive bibliographic search was made in the available literature relative to critical and exponential experiments having uniform lattices moderated by light water with F/M ratios in the range of 0.5 to 4.0. Unfortunately, most experiments fueled with U-233/ThO_2 (W-2), U-235/ThO_2 (W-3) or Pu/UO_2 (G-1) have F/M ratios less than 1.0. No experiment using Pu/ThO_2 was found.

Only for lattices fueled with enriched uranium were experiments found with F/M in the range of 0.1 to 2.3 (B-1). Also, because of the higher density of metallic uranium compared to uranium dioxide

(19.0 vs 10.96 g/cm^3 (P-1)), some light water lattices fueled with metallic uranium simulate tight-pitch lattices fueled with uranium dioxide (H-1). Similarly some thorium lattices containing D_2O simulate tight-pitch thorium lattices moderated by H_2O (W-2, W-3).

Exponential experiments using Pu-Al as fuel and moderated by D_2O (O-2) produce highly-epithermal neutron fluxes, but the absence of fertile fuel in the lattices decreases the utility of this data for the present work.

There are some highly-heterogeneous tight-pitch critical experiments using thorium fuel and light (L-1, M-1, M-2) or heavy water (H-2) as moderator done as part of the LWBR program. Reference U-1 analyzes these and other thorium benchmark experiments, using several methodologies, and compares their calculations with other published results.

1.4 Outline of Present Work

In Chapter 2 the physics characteristics of the heavy nuclides in the uranium and thorium chains are discussed, focusing on characteristics important to understand the advantages and disadvantages of the use of one fuel over another.

In Chapter 3 the thermal-reactor computer programs used in the calculations are described. Comparisons are made with experimental results and with fast reactor-physics methods.

Chapter 4 constitutes the main portion of this work. The fuel cycles and methods of calculation are detailed. Mass flows and fuel cycle costs for a number of fuel strategies are calculated for both systems of coupled reactors examined. Reactivity (moderator-void and fuel-temperature) coefficients for the tight-pitch cores are also evaluated. Thermal-hydraulics

is briefly discussed and uncertainties in the calculated results are estimated.

Chapter 5 briefly treats some alternative concepts to improve ore conservation. The use of D_2O as moderator, metallic thorium as fuel, variable fuel-to-moderator volume ratio for reactivity control, denatured uranium as fuel, and the use of stainless steel as cladding material (for tight-pitch PWR cores) are included in this chapter.

Chapter 6 summarizes the present work and gives its main conclusions and recommendations for future work.

Appendix A documents the pertinent characteristics of the Maine Yankee PWR on which the reactor core models studied in this work are based.

Appendices B and C tabulate the main parameters for the many exponential and critical experiments used to benchmark the EPRI-LEOPARD and LASER computer programs, comparing calculated with experimental results.

Appendices D, E and F present mass flow results for the U-235/UO_2 and Pu/ThO_2, U-233/ThO_2 and Pu/UO_2 fueled cores, respectively.

CHAPTER 2

BACKGROUND

2.1 Introduction

This chapter briefly reviews some of the physical characteristics of the thorium and uranium nuclide chains in a fission reactor which are important in understanding the advantages and disadvantages of a given fuel cycle. The basic parameters used to measure the neutronic performance of a fuel cycle, namely, the fissile critical mass and instantaneous conversion ratio are also discussed. References (K-1, S-1, P-2, U-2) provide a more detailed comparison between thorium and uranium-based fuel cycles.

2.2 World Reserves of Uranium and Thorium

It is well known that the only naturally-ocurring elements available in economically significant amounts that can fuel fission reactors are uranium and thorium. Natural uranium is constituted mainly by the isotopes U-235 (0.71 w/o) and U-238 (99.29 w/o) while natural thorium appears as almost pure Th-232. Although U-238 and Th-232 may be fissioned by high energy neutrons (Fig. 2.2), only the least abundant of these nuclides, U-235, can sustain a fission-chain reaction. However, U-238 and Th-232 can be transformed into the fissile nuclides Pu-239 and U-233, respectively, by the process of capturing a neutron followed by two consecutive beta decays (Fig. 2.1). A core designed such that, for each fissile nuclide (U-233, U-235, Pu-239 and Pu-241) consumed, at least one fissile nuclide is produced by neutron capture in a fertile isotope (Th-232, U-234, U-238 and Pu-240) can, theoretically, consume all fissile and fertile material

supplied as fuel.

This is not the case for a typical PWR which consumes some 6.0×10^3 ST U_3O_8/GWe during its nominal 30-year lifetime, operating on the once-through uranium cycle (Table 2.3). The neutron economy for the PWR is such that only about 2% of the uranium mined is actually consumed to produce energy. The rest of it remains as 0.2 w/o-enriched depleted uranium (as enrichment plant tails) (80%) and as burned fuel composed of a mixture of uranium and plutonium isotopes (18%). Contrary to uranium, thorium is not enriched by using an enrichment plant but instead by mixing it with fissile material. In this way no "depleted" thorium is produced and the amount of thorium mined is only about one-fifth that for uranium.

Tables 2.1 and 2.2 give the world resources of uranium and thorium, respectively. The reserves of thorium are believed to be at least as large as those for uranium, waiting only for an economic incentive to be found (N-1). Table 2.3 shows the consumption of natural uranium for a standard 3-zone PWR utilizing different fuels. It also shows the number of reactors that the known reserves of uranium could support over their assumed thirty-year lifetime. On the other hand, the LWR's which are already installed, under construction or on order total some 300 GWe (Table 2.4). These estimates support the goal of increasing the energy output from the assured reserves of uranium. With advanced cores the known reserves of uranium and thorium could eventually support this number of reactors, or more, for a long period - indeed some hundreds of years.

TABLE 2.1

NON-COMMUNIST WORLD URANIUM RESOURCES ($30/lb U_3O_8)

Reasonably Assured (Reserves)	Thousand Tonnes, U*
United States	490
Australia	330
Sweden	300
So. & SW. Africa	280
Canada	170
Other	290
Total	1860

Estimated Additional (Probable Potential)	Thousand Tonnes, U
United States	820
Canada	610
Australia	80
Other	310
Total	1820

*1.3 short tons U_3O_8 = 1 metric tonne (1000 Kg)U

Reference (N-1)

TABLE 2.2

NON-COMMUNIST WORLD THORIUM RESOURCES (MT Th)

$15/lb of ThO_2

	Reserves	Estimated Additional Resources	Annual Production Capability
Australia	5,000	10,000	500
Brazil	10,000	15,000	150
Canada	80,000	100,000	2,000
India	240,000	200,000	400
Malaysia	15,000	-------	200
United States	50,000	270,000	500
Other	15,000	340,000	500
Total (Rounded)	400,000	900,000	4,000

Reference (N-1)

TABLE 2.3

30-YR U_3O_8 REQUIREMENTS FOR PWR's *

Fuel Cycle	U_3O_8 (Short Tons/GWe)	Number of Reactors**
UO_2 (No fuel recycle)	5989	404
UO_2 (U & Pu recycle)	4089	591
ThO_2 (93% U-235 homogeneous recycling)	3483	694

*at 75% capacity factor; 0.2 w % diffusion plant tails assay

**number of reactors which could be fed with 2.42×10^6 ST of U_3O_8

Reference (S-1)

TABLE 2.4

NUCLEAR POWER PLANTS*

(Operable, Under Construction, or on Order ($\geq$ 30 MWe), as of 1/1/79

TYPE (COOL/MOD.)	UNITED STATES		WORLD	
PWR } LWR (H_2O)	131	(67.2%)	283	(54.1%)
BWR } LWR (H_2O)	61	(31.3%)	119	(22.8%)
PHWR (CANDU)			35	(7.8%)
LWCHWR			2	
HWBLWR (D_2O)			2	
GCHWR			2	
GCR			36	(13.8%)
AGR			11	
LGR (Graphite)	1		23	
HTGR	1		1	
THTR			1	
LMFBR (Na)	1		8	
TOTAL UNITS	195		523	
TOTAL GWE	190		405	
TOTAL OPERABLE	68		209	
GWE OPERABLE	50		109	

*Reference (N-2)

Table 2.4

(continued)

KEY:

PWR = Pressurized Water Reactor

BWR = Boiling Water Reactor

PHWR = Pressurized Heavy Water Moderated and Cooled Reactor

LWCHR = Light Water Cooled, Heavy Water Moderated Reactor

HWBLWR = Heavy Water Moderated Boiling Light Water Cooled Reactor

GCHWR = Gas Cooled Heavy Water Moderated Reactor

GCR = Gas Cooled Reactor

AGR = Advanced Gas-Cooled Reactor

LGR = Light Water Cooled, Graphite Moderated Reactor

HTGR = High Temperature Gas Cooled Reactor

THTR = Thorium High Temperature Reactor

LMFBR = Liquid Metal Cooled Fast Breeder Reactor

2.3 Fissile Inventory and Conversion Ratio

The two basic parameters generally used to measure the performance of a given fuel cycle, in terms of ore economy, are the initial fissile inventory and the conversion ratio (CR). The smaller the fissile inventory and the greater the conversion ratio the better the performance.

Both of these parameters depend on the reactor type and its fuel management characteristics, such as: core geometry, fuel composition, fuel-to-moderator volume ratio (F/M), power density, number of staggered fuel batches, discharge burnup, etc. An inclusive conversion ratio may be defined as an average over the fuel cycle, including fabrication and reprocessing (and all out-of-core) fuel losses.

The neutron balance in a reactor may be expressed as:

$$P^f + P^F + P^p + P^L = \frac{1}{k}\left[\eta^f P^f + \eta^F P^F + \eta^p P^p\right] = 1 \qquad (2.1)$$

where:

P = average probability of a neutron being absorbed or leaking from the system

η = average number of neutrons produced per neutron absorbed

k = effective multiplication factor.

Superscripts:

f = fissile nuclides

F = fertile nuclides

p = all other nuclides

L = leakage

k may be written as:

$$k = \varepsilon \eta^f P^f = 1 \tag{2.2}$$

where:

$$\varepsilon = \frac{\eta^f P^f + \eta^F P^F + \eta^p P^p}{\eta^f P^f} = \frac{\eta^f P^f + \eta^F P^F}{\eta^f P^f} = \tag{2.3}$$

"fast fission factor" for the system: the ratio of the total rate of neutron production to that produced only by fissile nuclides.

The amount of heavy nuclides other than fissile or fertile nuclides, and their respective η's, are in general so small that the product $\eta^p P^p$ can be neglected in the definition of ε.

2.3.1 Critical Mass

The critical fissile mass for the system is proportional to N^f, the average atomic concentration of the fissile nuclide. N^f is related to P^f by:

$$P^f = \frac{N^f \sigma^f}{N^f \sigma^f + N^F \sigma^F + N^p \sigma^p + DB^2} \tag{2.4}$$

where: N = atomic concentration

σ = (averaged one-group) absorption cross section

D = (averaged one-group) diffusion coefficient

B = geometric buckling

Combining Eqs. (2.2) and (2.4), we obtain:

$$N^f = \frac{1}{\sigma^f(\varepsilon \eta^f - 1)} \left[N^F \sigma^F + N^p \sigma^p + DB^2\right] \tag{2.5}$$

This last expression shows the obvious fact that the higher the absorption cross section of the fissile nuclide the smaller the critical mass. The opposite is true for the fertile and parasitic materials (and for neutron losses due to leakage). Because the product $\varepsilon\ \eta^f$, for thermal and epithermal reactors is on the order of 2.0, we see the importance of ε and η^f, since a 10% increase in either one will decrease the fissile critical mass by about 20%.

2.3.2 Conversion Ratio

The instantaneous conversion ratio is defined as the ratio between the rate of neutron captures by the fertile material and the rate of neutron absorptions by the fissile material:

$$CR = \xi \frac{P^F}{P^f} \tag{2.6}$$

in which

$$\xi = \frac{\sigma c^F}{\sigma^F} \tag{2.7}$$

where

ξ = average capture-to-absorption ratio for the fertile material.

Using Eqs. (2.1), (2.2) and (2.6), CR can also be written:

$$CR = \xi\varepsilon\ \eta^f\ P^F = \xi[\varepsilon\ \eta^f\ (1 - P^P - P^L) - 1] \tag{2.8}$$

We see that the higher the product $\varepsilon\ \eta^f$ and the smaller the neutron losses to the non-fissionable materials (and losses due to leakage) the higher the conversion ratio. The fact that an increase in ε helps to increase CR is not obvious since the factor ξ is simultaneously decreased. An increase in ε allows P^f to be decreased in order to keep the reactor just

critical (Eq.(2.2)) by decreasing the critical fissile mass (Eq. (2.5)). More neutrons become available to be absorbed by the fertile material, thereby increasing P^F. Because while P^f decreases, P^F increases, any increment in ϵ is double-counted in CR (Eq. (2.6)) and this effect is only partially offset by the smaller ξ.

An increased absorption cross section for the fertile material will require a higher fissile critical mass to maintain criticality (Eqs. (2.2) and (2.5)). In this way, both P^f and P^F are increased (Eq. (2.1)), reducing neutron losses to parasitic absorbers and to leakage (P^P and P^L are reduced). The net result is a higher conversion ratio (Eq. (2.8)).

With fuel depletion, the conversion ratio stays fairly constant, depending mainly on η^f which can vary if the bred fuel is different from the original fuel. The factors ϵ and ξ, which depend on the fertile material, remain almost unchanged. Leakage losses (P^L) are also small and relatively constant. Neutron losses to control absorbers have to be decreased to compensate for the fissile burnup (if CR < 1) and also for increased losses to fission products and to heavy parasitic absorbers. This increases P^F by a small amount, causing CR to increase somewhat with fuel depletion (Eq. (2.8)).

It is interesting to note that in the SSCR concept (S-1) criticality is maintained by hardening the neutron spectrum at beginning-of-cycle (BOC) and by softening it towards the end-of-cycle (EOC). Control is achieved mainly by exploiting the much higher absorption cross sections for the fissile nuclides at thermal compared to epithermal energies (relative to fertile materials). Losses to control absorbers are drastically reduced allowing a higher CR to be achieved (compared to poison-controlled

reactors); this in turn lowers the initial fissile inventory (S-1).

2.4 Nuclear Properties of Major Heavy Nuclides

This section presents the nuclear properties of the main heavy nuclides in the thorium and uranium chains (Fig. 2.1) which affect the critical mass and/or the conversion ratio. When comparing fissile to fissile (or fertile to fertile) nuclides, it is assumed that the environment where the comparison is being made remains the same. Only thermal and epithermal spectra are discussed. Predominantly thermal spectra will be those designated where more than half of the fissions occur below some specified energy cutoff (1 eV, for example).

Figure 2.1 shows the main components in the nuclide chains following from Th-232 and U-238. Both chains are very similar: a neutron capture by the original fertile nuclide (Th-232 or U-238) followed by two consecutive beta decays produces the primary fissile nuclide in the chain (U-233 or Pu-239). Subsequent neutron captures produce the intermediate fertile nuclides (U-234 or Pu-240), the secondary fissile nuclides (U-235 or Pu-241) and the parasitic absorbers (U-236 or Pu-242).

Table 2.5 presents the main nuclear reactor-related properties for these isotopes. The relatively low cross section of Np-239 combined with its short half-life leads to a negligible effect on the critical mass and conversion ratio. The precursor of U-233, Pa-233, on the other hand although also having small cross section (compared to the fissile nuclides) has a long half-life (27 days). Neutron losses to Pa-233 are, however, rather small: less than 2% of the Pa-233 formed is lost by neutron absorption, decreasing somewhat the conversion ratio. For long periods of reactor shutdown, the slow increase in reactivity due to Pa-233 decay must

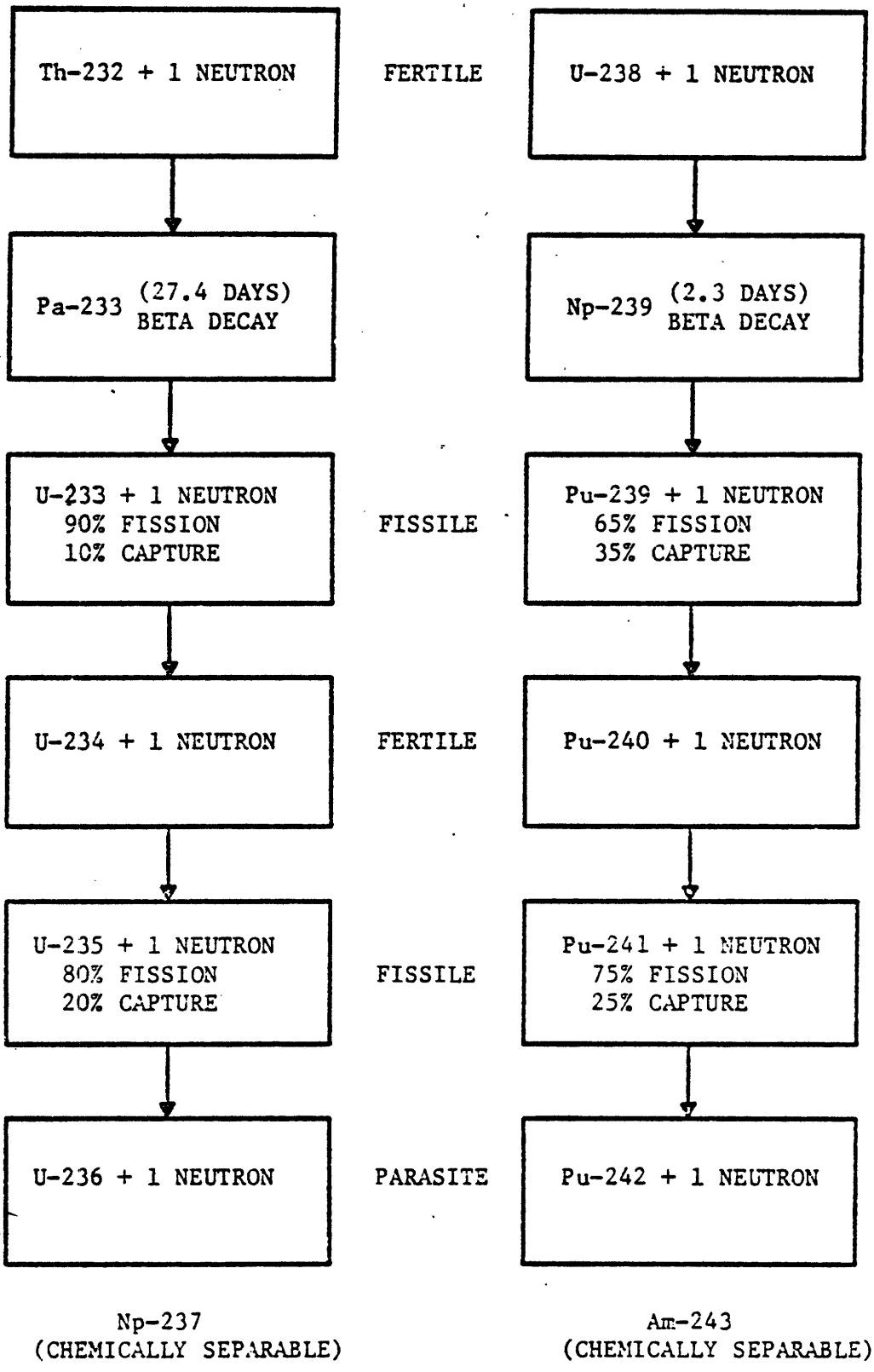

Figure 2.1 THE ISOTOPIC BUILDUP IN THORIUM AND URANIUM REFERENCE (S-1)

TABLE 2.5

CROSS SECTIONS FOR PRINCIPAL NUCLIDES IN THE THORIUM AND URANIUM CHAINS*

	ISOTOPE											
	Th-232	Pa-233	U-233	U-234	U-235	U-236	U-238	Np-239	Pu-239	Pu-240	Pu-241	Pu-242
THERMAL DATA												
σ_a(0.025 eV)	7.40	41.46	571.01	95.77	678.40	6.00	2.73	80.00	1013.04	290.08	1375.37	30.00
σ_c(0.025 eV)	7.40	41.46	45.99	95.77	101.30	6.00	2.73	80.00	271.19	290.02	367.81	30.00
σ_f(0.025 eV)	0.00	0.00	525.11	0.00	577.10	0.00	0.00	0.00	741.85	0.06	1007.56	0.00
α	--	--	0.0874	--	0.1755	--	--	--	0.3656	--	0.3651	--
ν	--	--	2.498	--	2.442	--	--	--	2.880	--	2.936	--
η	--	--	2.300	--	2.077	--	--	--	2.109	--	2.151	--
INFINITELY DILUTE RI (barns) 0.625 eV-10 MeV												
ABSORPTION	85.78	858.83	883.73	632.16	380.13	348.82	273.57	0.00	445.15	8494.02	686.76	1118.65
CAPTURE	85.20	857.00	135.10	627.96	130.22	346.55	272.37	0.00	168.58	8486.17	112.41	1115.00
FISSION	0.58	1.83	748.63	4.20	249.91	2.27	1.20	0.00	276.57	7.85	574.35	3.65
α	--	--	0.1805	--	0.5210	--	--	--	0.6096	--	0.1957	--

* Reference (S-1)

be considered.

Because of its high α (capture-to-fission ratio) Pu-239 will always be produced mixed with considerable amounts of Pu-240. The value of Pu-239 is then decreased, although fuel depletion is partially compensated by the subsequent production of the high-worth secondary fissile nuclide Pu-241 (see Section 4.3.4). Due to its small α, the same effect is not so important for U-233 (although it worsens in epithermal spectra).

2.4.1 Thermal Spectra

In a thermal spectrum, because of their much higher thermal cross sections, the fissile plutonium isotopes require less critical mass than the fissile uranium nuclides (Table 2.5). In the case of Pu-239, the difference would be small compared to U-233 because its averaged η would be much smaller than that of U-233 (Table 2.6). Furthermore, the isotopic degradation of plutonium (typical composition: Pu-239, 54%; Pu-240, 26%; Pu-241, 14% and Pu-242, 6%) may require a higher critical mass than U-233 or even U-235. The conversion ratio is highest for U-233 due to its superior thermal eta, (Eq. (2.8)).

The use of Th-232 requires more fissile material than U-238 because its thermal cross section is almost three times that for U-238 (Table 2.5). Furthermore, because U-238 has a lower fission threshold and larger fission cross section than Th-232 (Fig. 2.2) it produces a higher fast fission factor (typical values: 1.09 for U-238 and 1.02 for Th-232 (C-1)), further decreasing the fissile inventory needed (Eq. (2.5)). The superiority of U-238 is to some extent decreased because its shielded resonance integral is about 20% higher than that for Th-232 (Section 2.4.2). The higher absorption in Th-232 and its inferior ε have opposite effects on the

TABLE 2.6

AVERAGED VALUES OF ETA (η) FOR FISSILE AND FERTILE FUELS FOR A TYPICAL PWR (F/M = 0.5)*

Energy Range	0 eV → 0.625 eV	0.625 eV → 5530 eV	5.53 KeV → 821 KeV	0.821 MeV → 10 MeV
U-233	2.28	2.13	2.38	2.68
U-235	2.07	1.58	1.92	2.48
Pu-239	1.86	1.75	2.42	3.19
Pu-241	2.18	2.44	2.56	3.10
U-238	0	0	∿0	2.45
Th-232	0	0	0	1.60
Pu-240	∿0	∿0	1.30	3.01

* EPRI - LEOPARD Calculations using ENDF/B-IV Cross sections

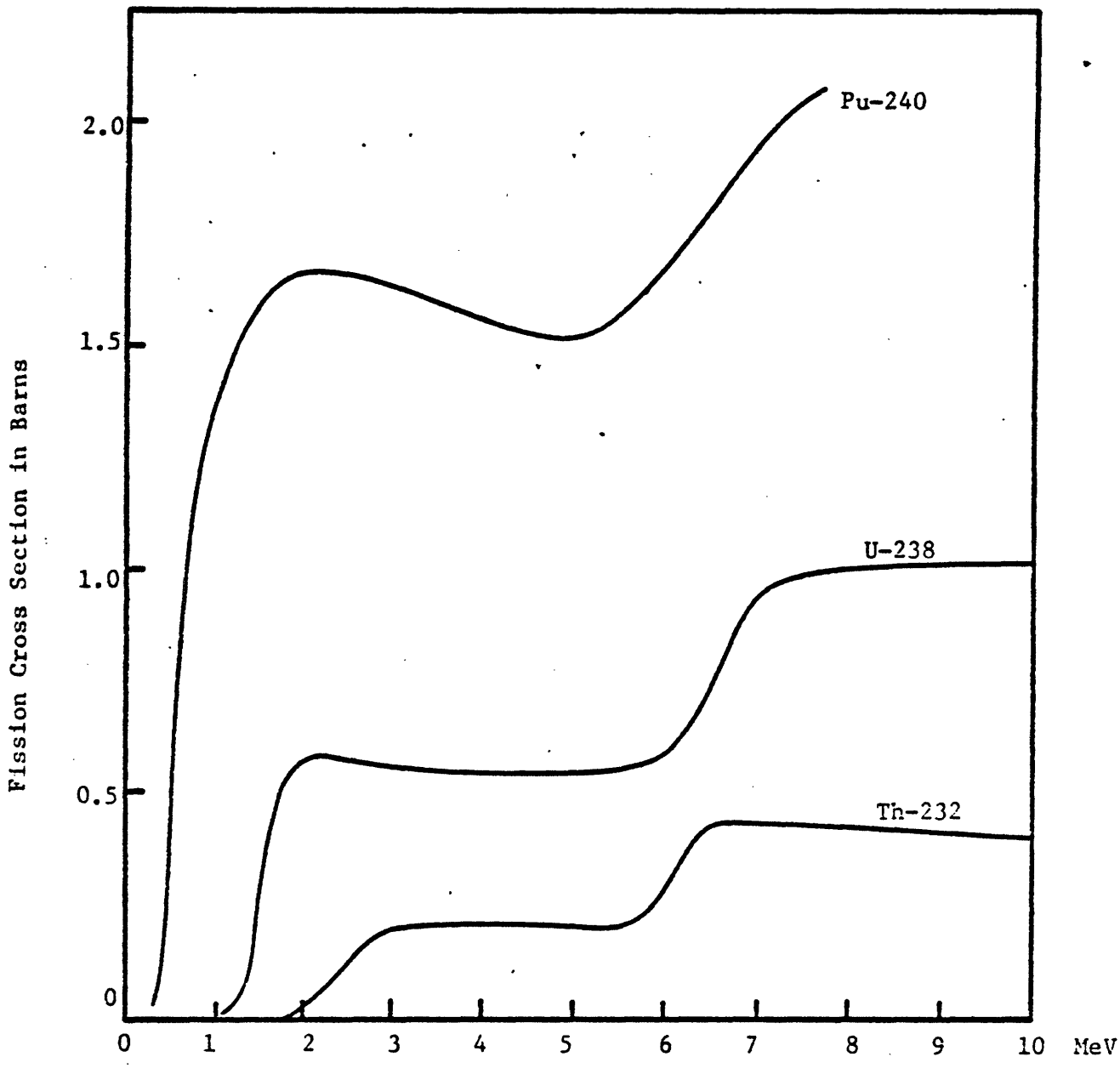

Figure 2.2 FISSION CROSS SECTIONS OF FERTILE ISOTOPES
REFERENCE (C-1)

conversion ratio; in the net it is relatively unmodified compared to U-238.

2.4.2 Epithermal Spectra

In an epithermal spectrum, the advantages of U-233 over the other fissile nuclides in terms of fissile inventory and conversion ratio are definitive, since it has the highest resonance integral and eta except for Pu-241. The higher eta of Pu-241 compared to U-233 helps plutonium-bearing fuels to recuperate to some degree their performance.

Although the infinitely-dilute resonance integral of U-238 is about three times that for Th-232 the heavy self-shielding due to the high fertile concentrations in typical fuels causes the effective resonance integral of U-238 to be comparable to that for Th-232 (S-1, U-2). In an epithermal spectrum this difference is balanced by the larger fast fission contribution from U-238, and both nuclides require about the same fissile inventory and produce similar conversion ratios. Nevertheless, as the fuel is depleted, Th-232 produces U-233, while U-238 produces Pu-239, which leads to an improvement in the conversion ratio for the thorium-bearing fuels relative to their uranium counterparts.

2.5 Fission Products

The net yield of Xe-135 and Sm-149 and the average absorption cross section for the plutonium fission products are larger than for uranium fission products (K-1, G-2). However, the higher cross section of plutonium in thermal spectra decreases the worth of its fission products. In general, hardening of the neutron spectrum tends to decrease the cross sections of the fission products relative to the fertile nuclides (C-2).

Neutron losses to fission products can also be decreased by reducing discharge fuel burnup, which helps to increase the conversion ratio and bring down fissile inventory. However decreased fuel exposure will increase fuel reprocessing and fabrication losses.

2.6 Fuel Contamination

During fuel irradiation, some minor heavy nuclides are produced which are not important as neutron absorbers, but may later on require remote fuel refabrication (A-1). Reference A-1 concludes that radiation levels for both plutonium and U-233 would demand remote fuel fabrication. Radiation from plutonium comes mainly from Pu-238, Pu-240 and Pu-241 in the form of low energy gamma rays and neutrons from spontaneous fissions and (α-n) reactions with oxygen. The main radiation associated with U-233 fuels is gamma radiation from daughter products of U-232.

Because of the higher radiation doses "from" U-232, thorium-based fuels are projected to be 15% more expensive to fabricate (A-1). On the other hand, the toxicity of Pu-bearing fuels, although similar to that of U-233-bearing fuels in water, is higher in air. The short-term decay heating, which is important for the design of waste shipping, storage and disposal facilities is similar for both types of fuel (Pu and U-233).

2.7 Physical Properties of Uranium and Thorium Fuels

Some of the important physical properties, from a reactor-physics and thermal-hydraulics point of view; of U, Th, UO_2 and ThO_2 are displayed in Table 2.7.

The lower density of ThO_2 compared to UO_2 helps to reduce its higher

TABLE 2.7

PHYSICAL PROPERTIES OF METALLIC URANIUM

AND THORIUM AND THEIR DIOXIDE COMPOUNDS

	U	Th	UO_2	ThO_2
Theoretical Density (g/cm^3)	19.0	11.7	10.96	10.00
Melting Point (°C)	1130	1750	2760	3300
Thermal Conductivity at 600°C (w/cm°C)	0.41	0.44	0.0452	0.044
Heat Capacity at 600°C (Joule/g_m°C)	0.18	0.14	0.30	0.28

Reference (P-1)

fissile inventory requirements,increasing at the same time the specific power. Thermal conductivities for both fuels are about the same (also true for their metallic forms) but the higher melting temperature for ThO_2 is an advantage. Irradiation behavior of ThO_2 and $(Th,U)O_2$ appear to be good at burnups up to 80 MWD/KgHM (O-3) at relatively high average linear heat rates (9.1 to 10.7 KW/ft).

Thorium metal behaves better than uranium in terms of metal-water reactions and dimensional instability (Z-1). The corrosion rate by water for metallic thorium is about two orders of magnitude smaller than for uranium. Alloys of these metals generally have more favorable characteristics than pure metallic uranium. Compared to the oxides of uranium and thorium, metallic thorium stores considerably less energy (because of its much higher conductivity), which is important in Loss of Coolant Accident (LOCA) considerations. Because of the higher density of metallic thorium compared to its oxide form, it will require higher fissile inventories and produce higher conversion ratios.

2.8 Conclusions

This chapter has summarized the important physical characteristics of the thorium and uranium fuel cycles in a fission reactor. Based only on this summary it is not possible to decide what type of fuel cycle is best for tight-pitch PWR cores.

Reserves of thorium were found to potentially be comparable to those for uranium and do not constitute a constraint. Physical properties and hazards associated with these fuels are also similar. The advantage of U-233/ThO_2 over Pu/UO_2 fuel in terms of the conversion ratio in epithermal spectra is not clear because, although U-233 has a higher eta than Pu-239,

U-238 provides a much larger fast fission effect. The advantage of U-233 over other fissile nuclides in an epithermal spectrum derives from its very high resonance integral, which reduces fissile inventory needs.

CHAPTER 3

COMPUTATIONAL METHODS

3.1 Introduction

The verification of methods and data in the range of present interest, 0.5 (current lattices) < F/M < 4 is limited by the scarcity of experiments with F/M > 1.0. Nevertheless, the EPRI-LEOPARD (B-2) and LASER (P-3) programs used for the ($U\text{-}235/UO_2$, $U\text{-}233/ThO_2$ and Pu/ThO_2) and (Pu/UO_2) calculations, respectively, were benchmarked against several of the more useful experiments. In this chapter, we describe these two programs, discuss a modification made on LEOPARD, and assess their limitations by comparing calculated results with critical and exponential benchmark experiments and with fast reactor-physics methods (ANISN (E-3) + SPHINX (D-2)). The SIMMOD (A-2) program used to calculate fuel cycle costs is also described.

3.2 The LEOPARD Program

3.2.1 Description

The LEOPARD (B-2) program calculates the neutron multiplication factor and few-group (2 or 4) constants for water moderated reactors using only basic geometry and temperature data. In addition the code can make a point-depletion calculation, recomputing the spectrum before each discrete burnup step.

LEOPARD utilizes the programs MUFT(B-3) and SOFOCATE (A-3) to calculate the nonthermal and thermal neutron fluxes, respectively. MUFT solves the one-dimensional steady-state transport equation assuming only

linearly anisotropic scattering, approximating the spatial dependence by a single spatial mode expressed in terms of an equivalent bare core buckling B^2 (the B1-approximation) and treating elastic scattering by a continuous slowing down model (Greuling-Goertzel model) and inelastic scattering by means of a multigroup transfer matrix. Cross sections for the heavy nuclides at resonance energies are treated by assuming only hydrogen moderation, with no Doppler correction.

SOFOCATE determines the thermal-group constants based on the Proton Gas (Wigner-Wilkins) Model to describe neutron thermalization. This model yields the correct 1/E behavior at high energies caused by a slowing down source and accounts for absorption heating and leakage cooling effects and also for flux depression at thermal resonances.

The cross section sets used by MUFT and SOFOCATE have 54 and 172 groups, respectively. The cross section sets for the EPRI-LEOPARD version are based on the Evaluated Nuclear Data File-Version B-IV (ENDF/B-IV). The thermal cutoff energy is 0.625 eV, and few group constants are prepared for use in diffusion codes in three or one epithermal groups (10 MeV → 0.821 Mev, 821 KeV → 5.53 KeV and 5530 eV → 0.625 eV or 10 MeV → 0.625 eV) and one thermal group (0.625 eV → 0 eV).

Because MUFT and SOFOCATE perform homogeneous calculations, LEOPARD has to correct their results for cell heterogeneities. In the thermal spectrum, disadvantage factors calculated for each thermal group are used based on the integral method proposed by Amouyal and Benoist (ABH - Method) as modified by Strawbridge (S-2) to include cladding effects. In the fast spectrum advantage factors are calculated for the first ten fast groups based on the method of successive generations (S-2).

At resonance energies, only the most abundant fertile nuclide (U-238 or Th-232) present in the fuel is spatially shielded. This correction includes Doppler broadening, fuel lumping and rod shadowing effects but does not include resonance interference effects with the other heavy nuclides (note the opposing effects between the Doppler correction, which tends to increase resonance absorption, and the other corrections which tend to decrease resonance absorption). The concentrations for the other heavy nuclides are assumed to be low enough (true for typical PWR's) that spatial self-shielding for them can be neglected. This latter assumption and the neglection of resonance interference effects for the fertile material may become large enough, at high fuel enrichments ($\varepsilon > 3.0$ w/o) and/or high F/M ratios, to decrease k by one per cent (or more) since resonance absorption is overestimated (section 3.2.3). This effect is particularly strong for U-233-bearing fuels since U-233 has the highest resonance integral among the more prominent fissile nuclides. Problems also arise for plutonium fuels due to the large low-lying resonances of Pu-239 and Pu-240.

The spatial self-shielding factor (L-factor) for U-238 (or Th-232) is found by an iterative process on the ratio (ω) of nonthermal neutrons captured in U-238 (Th-232) to those thermalized. Special MUFT runs are made, where zero leakage and no captures except in U-238 (Th-232) are assumed, and ω is found. This ω is compared to another ω obtained for the unit cell in question using an experimental resonance (metal-oxide) correlation for U-238 (Th-232). The L-factor (which multiplies the resonance integral for each resonance of U-238(Th-232)) is changed until the MUFT-ω matches the correlated-ω. We should mention here that whenever the ω-search does

not converge, LEOPARD uses an L-factor for U-238 (Th-232) based on Zernik's unpublished formulation. Zernik's L-factor is also always used to self-shield Pu-240 in EPRI-LEOPARD as a first approximation. The merit of this procedure was not evaluated in the present work.

LEOPARD calculates few-group cross sections for all types of fissile and fertile materials and for any combination of H_2O and D_2O. The concentration of boron, or the percentage of D_2O, in the moderator (H_2O) can be input as functions of the fuel burnup. In this way, PWR's and SSCR's can be simulated by LEOPARD.

The burnup equations are solved for the Th-232 and U-238 chains of nuclides and for the fission products: Pr-149, Sm-149, I-135, Xe-135 and one pseudo-element which accounts for all other fission products (one lumped fission product is assumed to be produced per fission event). For each time step the total rate of neutron absorption is assumed constant.

The absorption cross section for the lumped fission product is represented as a function of fuel exposure (Section 3.3.1) and assumed to be zero from 5.53 KeV to 10 MeV, constant from 0.625 to 5530 eV and vary with 1/v from 0. to 0.625 eV. An option is provided in LEOPARD to input a scaling factor to adjust these cross sections for each fuel type. This factor was found to be $\sim$0.84 for typical PWR fuels (M-3) and about 50% higher (than 0.84) for plutonium fuels (S-4). The value 0.84 was used for all U-235/UO_2 and U-233/ThO_2 depletion calculations, although perhaps a smaller value should be used for U-233/ThO_2 (G-2). The value 1.26 was used for all Pu/ThO_2 depletion calculations. No dependence on the F/M ratio was assumed because the epithermal cross section (which is the important part for F/M $\gtrsim$ 0.5) for the lumped fission product is much less sensitive to the F/M ratio than its thermal cross section (C-2).

For more elaborate studies depletion programs, such as CINDER (E-4) and ORIGEN (B-4), which can handle hundreds of fission products should be used to generate proper fission-product cross-section correlations for LEOPARD (and LASER) for each fuel type and at each F/M ratio. Programs similar to, but more advanced than LEOPARD treat each major fission product chain individually: CEPAK (S-1); EPRI-CELL (C-3).

LEOPARD also allows the inclusion of an extra region in the "supercell" calculations which represents control guides, structural material components and inter-assembly water. The thermal flux in this region can be adjusted by an input factor.

3.2.2 Modifications

The replacement of the metal-oxide resonance-integral correlation for thorium by a new one based on the resonance integral correlation reported by Steen (S-3) was the only major modification made to EPRI-LEOPARD.

The resonance integral correlation for thorium (for isolated rods) reported by Steen, based on experimental data, for the energy range 0.5 eV to 10 MeV is given by:

$$I(S/M) = 5.66 + 15.64 \sqrt{S/M} \text{ @ } 300°K \qquad (3.1)$$

$$I(S/M) = 4.56 + 22.69 \sqrt{S/M} \text{ @ } 1200°K \qquad (3.2)$$

where

I = resonance integral (barns)

S/M = fuel pellet surface-to-mass ratio (cm^2/g)

Shapiro (S-1) adjusted this correlation to a 0.625 eV cutoff energy, which amounted to a 0.25 barn reduction in the unshielded or constant term in the correlation. Assuming that the capture integral varies linearly with $\sqrt{T°K}$, and correcting for rod shadowing effects, he obtained,

$$RI^{02} = 6.51 + 8.59\ \sqrt{SD/M} + [-0.06351 + 0.40703\ \sqrt{SD/M}]\ \sqrt{T} \qquad (3.3)$$

for

$$0.4 < \sqrt{SD/M} < 1.0$$

and

$$300°K < T < 1200\ °K$$

where

D = Fukai Dancoff factor.

The old metal-oxide correlation for thorium used in LEOPARD was:

$$RI^{02}_{old} = 1.285X + 2.72 + (0.0249X + 0.0237)\ T^{1/2}_{eff} \qquad (3.4)$$

where (B-2, S-2)

T_{eff} = effective fuel temperature (°K)

$$X = \left[\frac{\Sigma_{so}}{N^{02}_{o}} P_o + \frac{D}{2R_o N^{02}_{o}}\right]^{1/2} \qquad (3.5)$$

Σ_{so} = scattering cross section of the fuel. The microscopic scattering cross sections used were 12.0 and 3.8 barns for thorium and oxygen, respectively.

N^{02}_{o} = Th-232 number density in the fuel region

R_o = fuel radius

$$P_o = \left\{1 - \left[1 + \frac{R_o \Sigma_{so}}{2.29}\right]^{-4.58}\right\} / (2R_o\Sigma_{so}) \qquad (3.6)$$

D = effective shielding factor for the lattice (Dancoff factor)

In order to transform Eq. (3.3) to the format of Eq. (3.4) we have:

$$\frac{S}{M} = \frac{2\pi R_o}{\pi R_o^2 \rho^{02}} = \frac{2}{R_o \rho^{02}} = \frac{2}{R_o \frac{N_o^{02} M^{02}}{A_{vo}}}$$

$$\frac{S}{M} = \frac{2}{R_o N_o^{02}} \times \frac{0.6022}{232}$$

$$\therefore R_o N_o^{02} = \frac{0.00519052}{S/M} \qquad (3.7)$$

and

$$R_o \Sigma_{so} = (\sigma_s^{02} + 2\sigma_s^{oxygen}) \quad R_o N_o^{02}$$

$$R_o \Sigma_{so} = \frac{0.101734}{S/M} \qquad (3.8)$$

$$P_o = \left\{1 - \left[1 + \frac{0.0444254}{S/M}\right]^{-4.58}\right\} / \left[\frac{0.203469}{S/M}\right] \qquad (3.9)$$

$$X = [19.60\ P_o + 96.3294\ S/M]^{1/2} \qquad (3.10)$$

Fitting $\sqrt{SD/M}$ as a function of X we get:

$$\sqrt{SD/M} = 0.108246X - 0.155683 \rightarrow (r^2 = 0.9999) \qquad (3.11)$$

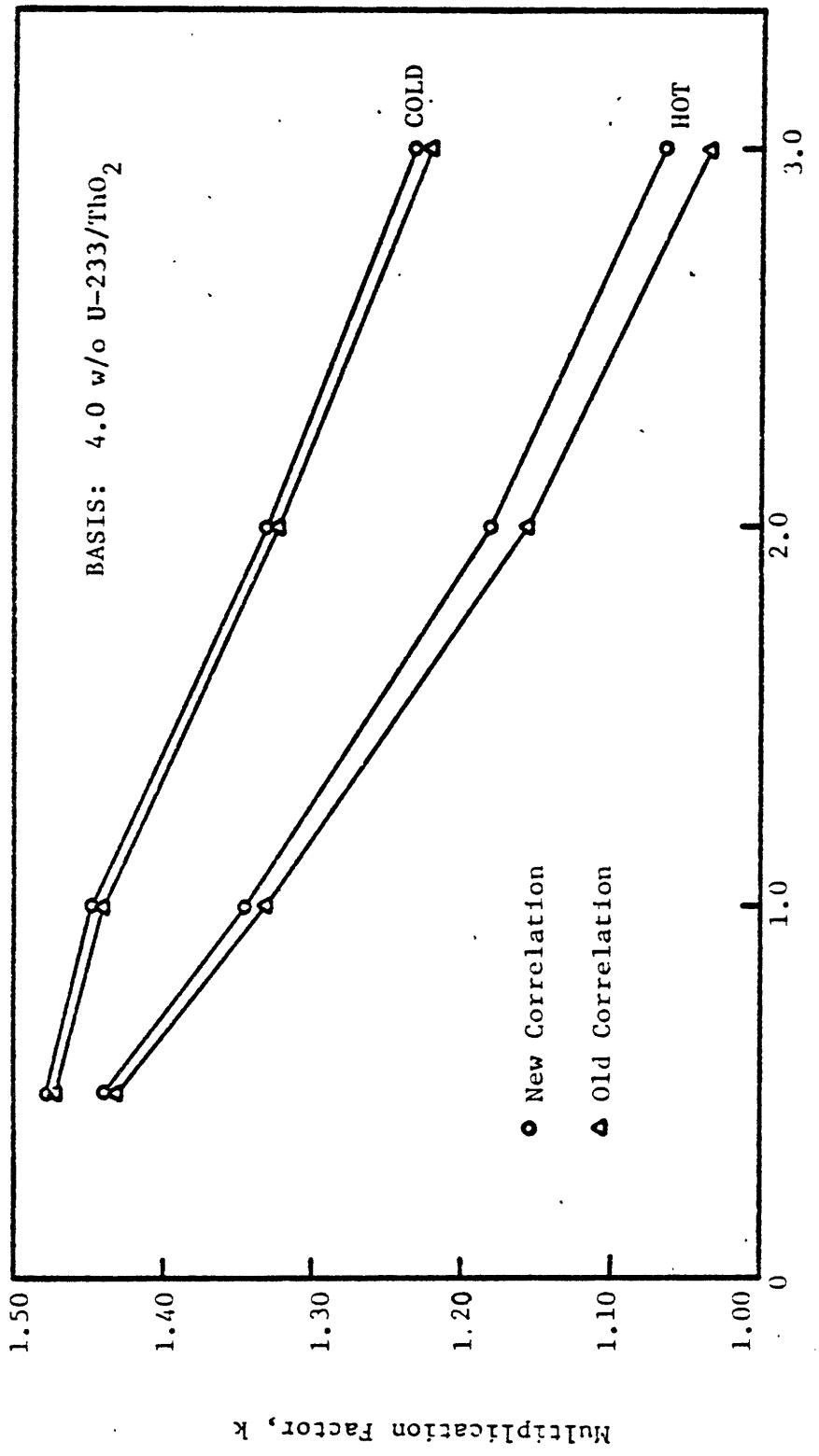

Figure 3.1 EFFECT OF THE NEW (STEEN) RESONANCE-INTEGRAL CORRELATION FOR THORIUM ON k CALCULATION WITH LEOPARD

for $0.4 < \sqrt{SD/M} < 1.0$

Substituting Eq. (3.11) into Eq. (3.3), we have:

$$RI^{02}_{STEEN} = 0.9298X + 5.1727 + [0.04406X - 0.12688] \cdot T^{1/2}_{eff} \qquad (3.12)$$

for $5 \lesssim X \lesssim 11$

Figure 3.1 shows the effect of this new (Steen) correlation on the values of k calculated using LEOPARD. It can be seen that k increases by 0.5% for regular lattices (F/M = 0.5) and by as much as 3% for tight lattices (F/M = 3.0) at operating temperatures. At cold temperatures (68°F) the effect is smaller.

In the rest of this work, all LEOPARD calculations include the new (Steen) correlation for thorium (unless otherwise stated).

3.2.3 Evaluation

3.2.3.1 Comparison of LEOPARD with Benchmark Experiments

As a part of our efforts to verify the validity of using EPRI-LEOPARD (with its ENDF/B-IV based cross sections) to generate few group cross sections for tight-pitch lattices, we made an extensive literature search on critical and exponential experiments. We were mainly interested in uniform lattices fueled with U-233/ThO_2, U-235/ThO_2, Pu/ThO_2 or Pu/UO_2, and moderated by light water with the fuel-to-moderator volume ratio (F/M) in the range: 0.5 (current lattices) < F/M < 4.0.

Unfortunately, most lattice experiments using these types of fuel have F/M ratios less than 1.0. No experiment using Pu/ThO_2 as fuel

was found.

Table 3.1 summarizes the main characteristics of the experiments analyzed with LEOPARD, and compares calculated with experimental results for quantities of interest. Several lattices fueled with U-235/UO_2 (or U-235/U-Metal) are included in this table for completeness. Appendix B and Reference (G-1) give detailed data on these benchmark comparisons.

In terms of average k, reasonably good results are obtained for all types of fuel analyzed, the worse case being for plutonium-fueled lattices, where a positive (average) bias of 2% is found. The use of the program LASER, which treats plutonium-bearing fuels in a more appropriate manner decreases this bias and also the standard deviation of $\bar{k}$ (see Section 3.3 and Appendix C).

When particular experiments are analyzed (see Appendix B and Reference (G-1)) we note that there is a trend for k to decrease with F/M (for F/M > 0.5) for both thorium and plutonium lattices. The use of the new metal-oxide resonance-integral correlation for thorium (based on Steen's correlation (S-3)), when compared to results based on the old correlation, decreases this trend, giving better values for k for very epithermal lattices (case 16 in Table B-1 and cases 15 and 16 in Table B-3). Better agreement with experimental results for calculated ρ_c^{02} (the epithermal-to-thermal capture ratio in Th-232) is also achieved for these epithermal lattices. The use of the new Th-correlation increases the $\bar{k}$'s by about 0.3%, however, and decreases the average $\rho_c^{02}/\rho_{c\,exp.}^{02}$ ratio by 2%, leading to poorer average results (see Tables B-1 to B-4).

TABLE 3.1

SUMMARY OF BENCHMARK COMPARISONS

Fuel:	$U\text{-}233/ThO_2$	$U\text{-}235/ThO_2$	$U\text{-}235/UO_2$	U-235/U	$U\text{-}235/UO_2$	Pu/UO_2
ϵ (w/o)	3.00	3.78 - 6.33	3.00 - 4.02	0.7 - 1.5	1.3 - 4.1	1.5 - 6.6
F/M	0.01 - 1.00	0.11 - 0.78	0.23 - 2.32	0.15 - 1.69	0.1 - 1.3	0.1 - 0.9
(H+D)/U-238 (or/Th-232)	3.4 - 403.	4.7 - 36.	1.31 - 14.6	0.8 - 5.7	2.9 - 15.	3.5 - 39.
ϕ_1/ϕ_2***	0.3 - 21.	1.7 - 23.	2.4 - 50.	1.3 - 12.	1.6 - 12.	1.2 - 20.
D_2O (%)	0. - 99.34	0. - 81.96	0. - 89.14	-	-	-
Boron (PPM)	-	-	-	-	0. - 3400.	-
$\bar{k}$	1.003 $\pm$ 0.012	1.009 $\pm$ 0.016	0.998 $\pm$ 0.006	1.006 $\pm$ 0.011	1.003 $\pm$ 0.012	1.018 $\pm$ 0.014
# of cases	16	16	26	82	63	42
Table*	B-1	B-3	B-5	B-6	A-1 (G-1)	A-2 (G-1)

(cont'd)

TABLE 3.1 - SUMMARY OF BENCHMARK COMPARISONS (cont'd)

Fuel:	$U\text{-}233/ThO_2$	$U\text{-}235/ThO_2$
$\rho_c^{02}/\rho_{c\ exp.}^{02}$	0.94 ± 0.08	0.98 ± 0.06
# of cases	15	4
Table*	B-2	B-4
$\rho_f^{25}/\rho_{f\ exp.}^{25}$**	-	1.07 ± 0.11
	-	13
	-	B-4
$\delta_{02}^{23}/\delta_{02\ exp.}^{23}$***	0.58 ± 0.19	-
# of cases	3	-
Table*	B-2	-

* See Appendices A and B for Tables B-1 to B-6 and Reference (G-1) for Tables A-1 and A-2

** ρ_f^{25} : epithermal-to-thermal fission rate in U-235 (as defined in Ref. (H-1))

*** Epithermal-to-thermal flux ratio (0.625 eV - thermal energy cutoff)

Ullo et. al. (U-1), using sophisticated Monte Carlo techniques to analyze thorium lattices, also found that calculated k values decrease with F/M (for F/M $\geq$ 0.5) if the measured buckling is used to correct for leakage. However, they also found that, in general, if two-dimensional Monte Carlo calculations are made (correcting only for the axial leakage) good results are obtained for k (see Fig. 3.2). They pointed out that the region of interest in tight experiments is, in general, too small compared to the driver and/or blanket regions, and thus the experimental asymptotic flux may not necessarily correspond to the asymptotic flux of a larger core.

Deviations of calculated k from unity, for thorium lattices, agree, in general, with the expected trend of deviations of ρ_c^{02} from measured values, although the latter have large uncertainties (Tables B1 to B4). In other words, when k is less than unity, ρ_c^{02} is larger than the corresponding experimental value and vice-versa.

Finally, we should note in Table 3.1 that good agreement is found between calculated and experimental values for the epithermal-to-thermal fission rate in U-235 (ρ_f^{25} often denoted δ^{25} elsewhere in the literature) for the lattices in Table B-4. It appears that fast fission in Th-232 is underestimated in LEOPARD by about 40% for some epithermal lattices (Table B-2). Although the latter value is large, its effect on k is negligible because fast fission in Th-232 is very small in any event (less than 2% of total fissions for these lattices).

Due to the absence of thorium benchmark experiments in the range of interest and the large uncertainties and difficulties associated with the measurement and interpretation of bucklings and microscopic parameters

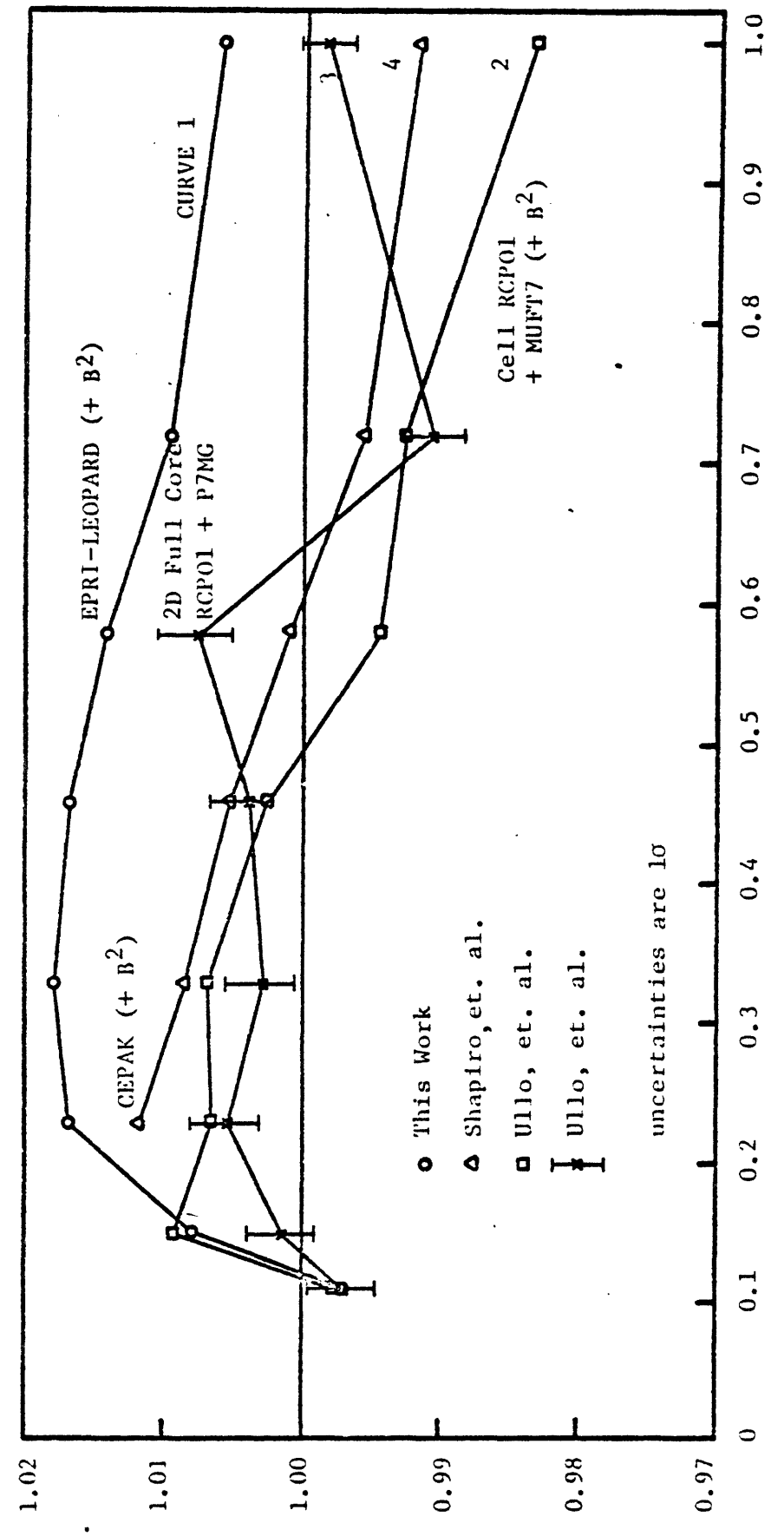

Figure 3.2 COMPARISON OF k CALCULATIONS BASED ON ENDF/B-IV FOR BNL U-233/ThO_2(H_2O) EXPONENTIAL LATTICES

for the few experiments analyzed, no other modification in LEOPARD was attempted besides that described in Section 3.2.2.

As a final note, LEOPARD results are in good accord with experimental values, in terms of k, for uranium lattices. In general, no trend of k with the F/M ratio (for F/M > 0.5) is noticed and excellent results are found even for very undermoderated lattices (Table B-5). Nevertheless, k is underpredicted by a large amount on some overmoderated and/or low-enriched uranium-metal lattices (cases 2, 3 and 11 in Table B-6). In one case (case 34, Table B-6), the thermal spectrum calculation failed to converge.

3.2.3.2 Comparison of LEOPARD with Fast Reactor-Physics Methods

From the previous section we have found that LEOPARD tends to underpredict k for tight-pitch thorium-fueled lattices. This effect may be caused by overprediction of resonance absorption in the fertile and fissile nuclides and/or overprediction of leakage stemming from use of the experimental buckling.

To further examine this question a procedure was devised combining thermal and fast reactor-physics methods, which calculates k for very epithermal lattices better than LEOPARD. This new methodology, however, contrary to LEOPARD, appears to overshield the resonance absorption for both the fissile and fertile isotopes.

The analysis was made using a simple two-group (more are possible) diffusion calculation with the thermal and epithermal cross sections taken from LEOPARD and ANISN (E-3), respectively. ANISN was used to do a k-calculation based on a (transport-corrected) P_o/S4/50-group/1-dimensional transport approximation. (Results based on a P3/S8 approximation were

essentially the same as those based on a P_0/S4 approximation). The cross sections input to ANISN were first shielded by the program SPHINX (D-2), which uses the Bondarenko shielding methodology (B-5). The 49 epithermal groups (from ANISN) were then collapsed to yield the desired one-group epithermal cross sections with a thermal cutoff of 0.683 eV. The small difference in the thermal cutoff of the two schemes (0.625 eV for LEOPARD) can be neglected. Both libraries are based on the ENDF/B-IV cross section library; the particular 50-group cross section set used in SPHINX/ANISN calculations was LIB-IV (K-2).

Table 3.2 compares the k's (and k_∞'s) calculated by LEOPARD (L) and by the combination of LEOPARD and SPHINX-ANISN (L/SA) for a series of benchmark experiments. In the calculation of the k's we used the diffusion coefficients determined by LEOPARD, since ANISN uses σ-total instead of σ-transport to calculate the diffusion coefficients.

We see that the L/SA method decreases by more than a factor of two the standard deviation of the k error for the thorium lattices compared to the LEOPARD results. Not only that, the L/SA method gives much better results for the highly epithermal lattices (cases 14, 15 and 23 in Table 3.2). For the uranium lattices, both methods give good results.

Table 3.3 compares ρ_c^{02} calculated by both methods with the experimental values for the U-233/ThO_2 (D_2O) lattices of Reference (W-2). Although more comparisons should be made, the L/SA method, as good as it otherwise seems to be, badly underpredicts ρ_c^{02} for these cases.

Although SPHINX tends to overshield both the fertile and fissile isotopes, the errors appear to cancel each other better than in the LEOPARD treatment when k is calculated. It is interesting to note that the leakage correction sometimes overshadows differences in k_∞'s between

TABLE 3.2

BENCHMARK COMPARISONS

Case #	Ref*	F/M**	% D_2O	k- ∞		k	
				L	L/SA	L	L/SA
1	B-1	0.59		1.262	1.269	1.003	1.007
2		0.73		1.372	1.374	1.000	0.996
3		0.78		1.231	1.241	1.003	1.008
4		1.04		1.186	1.200	1.001	1.009
5		1.04		1.313	1.318	0.999	0.996
6		1.32		1.261	1.269	0.999	0.998
7		1.55		1.224	1.233	0.989	0.989
8		1.90		1.177	1.187	0.990	0.991
9		2.13		1.152	1.160	0.992	0.993
10		2.29		1.135	1.140	1.000	0.999
11		2.32		1.132	1.137	0.990	0.988
				Average k		0.997 ±0.006	0.998 ±0.008
12	W-3	0.70	55.38	1.308	1.334	1.002	1.006
13		0.70	60.40	1.287	1.317	1.009	1.018
14		0.70	71.94	1.226	1.264	0.982	0.999
15		0.70	81.96	1.154	1.202	0.961	0.989
16	W-2	0.33		1.327	1.322	1.018	1.013
17		0.46		1.367	1.366	1.017	1.013
18		0.58		1.382	1.379	1.014	1.010
19		0.72		1.385	1.383	1.010	1.006
20		1.00		1.372	1.373	1.006	1.003
21		0.06	99.30	1.480	1.496	1.004	1.010
22		0.09	99.26	1.449	1.470	1.000	1.009
23		0.33	99.30	1.187	1.256	0.972	1.018
				Average k		1.000 ±0.018	1.008 ±0.008

* Ref (B-1) 3.04 w/o U-235/UO_2
Ref (W-3) 6.33 w/o U-235/ThO_2
Ref (W-2) 3.00 w/o U-233/ThO_2

** F/M = Fuel-to-Moderator Volume Ratio

TABLE 3.3

EPITHERMAL-TO-THERMAL CAPTURE RATIO IN Th-232

	Measured ρ_c^{02} *		Calculated ρ_c^{02}	
** Case #	Cd Ratio Method	Thermal Activation Method	L (0.625 eV-cutoff)	L/S-A (0.683 eV-cutoff)
21	0.559 ± 0.018	0.634 ± 0.060	0.574	0.451
22	0.780 ± 0.032	0.840 ± 0.058	0.818	0.652
23	5.190 ± 0.540	4.660 ± 0.19	5.29	3.79

* Reference (W-2)

** Refer to Table 3.2

both methods, giving similar answers for k's (cases 12 and 13 in Table 3.2).

In view of these results, this option was abandoned but further comparisons with experiments should be made to determine its value as a possible benchmarking method.

3.3 The LASER Program

3.3.1 Description

LASER (P-3) is a one-dimensional (cylindrical) multi-energy (85 groups) lattice-cell program which is based on the MUFT (B-3) and THERMOS (H-3) codes. The thermal cutoff is 1.855 eV and a burnup option is provided which can, at option, account for the non-linear effects in the burnup equations. The spatial burnup distribution within the fuel rods is explicitily calculated.

Like LEOPARD, LASER makes a homogeneous calculation in the epithermal energy range based on the MUFT program. Spatial self-shielding for U-238 may also be calculated by Strawbridge's procedure (S-2). In addition an L-factor, to account for fuel lumping, Dancoff and Doppler corrections, can be input into the code for each heavy nuclide (LASER does not include the thorium chain of nuclides). Interference between U-238 and U-235 resonances can also be treated. The spatial distribution of the epithermal resonance capture rate in U-238 is input to the code to account for the non-uniform buildup of Pu-239 in the fuel rod. The lowest 4 of the 54 groups in the regular MUFT code are dropped to permit a higher thermal energy cutoff (1.855 eV).

In the thermal energy range ($0 \leq E \leq 1.855$ eV), LASER uses the THERMOS code, which solves the integral neutron transport equation, subject to isotropic scattering, numerically by dividing the energy and the geometric space into subintervals. The energy mesh has 35 thermal groups which permits an accurate representation of the 0.3 eV Pu-239 and the 1.0 eV Pu-240 resonances. Rim and Momsen (M-3), inserted additional data into LASER to account for the Doppler broadening effect on the Pu-239 resonance at 0.296 eV (because the original version of LASER Doppler-broadened only the Pu-240 resonance at 1.056 eV). Thermal cross sections for the plutonium isotopes and thermal resonance parameters for the 1.0eV Pu-240 resonance were changed based on the ENDF/B-II cross section library. Thermal cross sections for U-235 were normalized to the 2200 m/sec parameters reported by Sher (M-3).

An isotropic scattering ring surrounding the cell is automatically provided in LASER, which eliminates to a large extent the errors introduced by cylindricizing the lattice cell (Wigner-Seitz Cell). The scattering kernel for light water may be based on the free gas scattering (Wigner-Wilkins) kernel or on the bound scattering kernel of Nelkin. For heavy water, Honeck's extension of the Nelkin kernel to D_2O is used.

Non-linearities in the system of burnup equations can be accounted for, but in general, to save computer time, the simpler linear approximation is preferred.

The fission products are divided into three components: Xe-135, Sm-149 and a lumped pseudo-fission-product, the latter being produced at a rate of one per fission. Chains for Xe-135 and Sm-149 are not included in the code. Instead, after the first and second burnup steps, Xe-135 and Sm-149 respectively are assumed to have reached their equilibrium

concentrations.

The cross sections for the lumped fission product, as in LEOPARD, are represented by polynomials in the burnup. Although the pseudo-fission-product cross section varies with fuel enrichment and metal-to-water ratio (C-2), the simpler expressions for plutonium fuel (3.53 w/o and F/M $\sim$ 0.5) derived by Momsen (M-3) were used in all depletion calculations:

1st group: $\sigma_a^{fas} = 0$

2nd group: $\sigma_a^{epi} = 31.422 + 1.1693 \times 10^{-4} B - 2.4423 \times 10^{-8} B^2 + 4.5934 \times 10^{-13} B^3$

3rd group: $\sigma_{a_o}^{th} = 195.14 - 1.0865 \times 10^{-2} B + 3.9174 \times 10^{-7} B^2 - 5.3322 \times 10^{-12} B^3$

where

1st group: (5530 eV $\leq$ E $\leq$ 10 MeV)

2nd group: (1.855 eV $\leq$ E $\leq$ 5530 eV)

3rd group: (0 $\leq$ E $\leq$ 1.855 eV)

$\sigma_{a_o}^{th}$ = the 2200 m/sec value of á 1/v cross section,

and

σ_a^{epi} is taken to be constant with energy.

B = burnup in MWD/MTHM

3.3.2 Evaluation

Table C-1 compares k's obtained with LEOPARD and LASER for the tightest lattices of Pu/UO_2 (H_2O) examined. We see that LASER not only reduces the standard deviation but also improves the average k. Note also the tendency of k to decrease with F/M (for the same fuel enrichment)

for both codes, less for LASER because of its higher thermal cutoff. Although the cross section library for LASER is based on its original library and, in part, on the ENDF/B-II library and that for LEOPARD, on ENDF/B-IV, LASER reduces k, probably because of the Doppler correction for the low-lying plutonium resonances.

Table C-3 compares k's obtained with LEOPARD and LASER for some Pu-Al-D_2O exponential experiments. Although no thorium or uranium is present, this series of lattices is useful in demonstrating the superiority of LASER over LEOPARD when treating plutonium-fueled cells. Also, we should note that because the moderator is D_2O and the F/M ratios are high, these lattices are highly epithermal.

3.4 The SIMMOD Program

A simple model (the SIMMOD Program) was developed by Abbaspour (A-2) for the calculation of overall levelized fuel cycle costs. The model assumes only equilibrium fuel batches (those which have equal in-core residence times and equal charge and discharge enrichment) and that revenue and depreciation charges occur at the mid-point of the irradiation period.

On these bases, the Simple Model takes the form:

$$e_o = \frac{1}{1000\ E} \sum_{i=1}^{I} M_i C_i F_i G_i \qquad (3.14)$$

where

e_o = levelized fuel cycle cost (mills/kwhre)

E = total electrical energy produced by an equilibrium batch during its residence time in the core (kwhre)

M_i = transaction quantity involved in the i^{th} step (e.g. KgHM)

C_i = unit price of the i^{th} step in time-zero dollars (e.g. \$/KgHM)

F_i = "composite discounting factor" which includes the effects of the discount rate and taxes.

G_i = "composite escalation factor" which includes the effects of escalation for each transaction i (and for the price of electricity).

Discrepancies between this model and the more accurate model MITCOST-II (C-4) are not greater than 3%, as reported by Abbaspour (A-2). The difference is always biased on the low side, mainly because of the omission in the Simple Model of startup batches, which have a higher fuel cycle cost.

It was concluded that this model was flexible and accurate enough for the purposes of this work.

3.5 Limitations of Methods of Analysis

Comparisons of EPRI-LEOPARD and LASER against benchmark experiments have indicated that these programs tend to underestimate k for epithermal lattices fueled with U-233/ThO_2 or Pu/UO_2, respectively. Assuming the experimental bucklings are correct, it seems that this trend is caused mainly by an overestimation of resonance absorption due to the lack of treatment of resonance interference between the heavy nuclides and spatial self-shielding for the fissile nuclides.

Sensitivity analyses have shown that a 10% overestimation in the L factor (Sections 3.2.1 and 3.3.1) for each of the heavy nuclides (at F/M = 3.0) - which would be an upper limit on the estimated discrepancy in our judgement - could cause the fissile inventory (FI) to be

TABLE 3.4

ERRORS IN THE FISSILE INVENTORY, IN THE CONSUMPTION OF FISSILE MATERIAL AND IN k_o DUE TO ERRORS IN THE TREATMENT OF RESONANCE AND FISSION PRODUCT EFFECTS

	(1) RI (± 10%)		(2) FP (± 10%)	
	(3) U-233/ThO_2	(4) Pu/UO_2	U-233/ThO_2	Pu/UO_2
(5) FI (%)	± 8	± 5	± 3	± 2
(6) CFM (%)	∓ 11	∓ 16	± 7	± 36
(7) k_o	∓ 3	∓ 2	-	-

(1) 10% error in the L factors for all heavy nuclides in the fuel

(2) 10% error in the absorption cross sections for the lumped pseudo fission product

(3) 5.5 w/o U-233/ThO_2; F/M = 3.0

(4) 9.0 w/o Pu/UO_2; F/M = 3.0

(5) FI: Fissile Inventory

(6) CFM: Consumption of Fissile Material

(7) k_o: Initial k

overestimated by less than 8% and the consumption of fissile material (CFM) to be underestimated by less than 16% for both U-233/ThO_2 and Pu/UO_2-fueled cores (Table 3.4). The effect on system ore consumption is considerably less (see Chapter 4).

Another possible major source of errors comes from the treatment of the fission products. A 10% underestimation in the absorption cross section for the lumped (pseudo) fission product could lead to an underestimation of less than 3% in the fissile inventories (FI's, (Table 3.4). The underestimation in the CFM would be less than 7% for the U-233/ThO_2 core but as large as 36% for a Pu/UO_2 core because the conversion ratio for this core is very close to 1.0. If fissile fuel losses due to re-processing and re-fabrication are included the error in CFM due to fission product σ drops to less than 13%.

3.6 Conclusions

Methods and data verification in the range of present interest, 0.5 (current lattices) < F/M < 4.0, are limited by the scarcity of experiments with F/M $\geq$ 1.0. Nevertheless, benchmarking of the EPRI-LEOPARD and LASER programs against several experiments indicated that they tend to underpredict k as F/M increases, probably due to the lack of proper treatment of resonance effects. Better agreement with experimental results were obtained with a new thorium resonance integral based on Steen's correlation (S-3). The analyses were made more difficult by the lack of confidence in the experimentally measured critical bucklings for tight lattice experiments (U-1).

The combination of fast reactor-physics methods with thermal methods should be further explored, since good agreement with benchmark experiments, in terms of k, was obtained although resonance absorption seems to be underestimated.

Based on sensitivity analyses we have concluded that a 10% error in the L-factors for the heavy nuclides can cause errors of less than 8 and 16% in the fissile inventory and in the consumption of fissile material respectively, for tight lattices (F/M = 3.0) of U-233/ThO_2 or Pu/UO_2. Similar errors can arise from a 10% error in the absorption cross sections for the lumped fission product (when fuel losses due to re-fabrication and re-processing are included).

Abbaspour's "Simple Model" for calculating fuel cycle costs (SIMMOD) was judged to be accurate enough for the purposes of the present work, based on the author's comparisons with more sophisticated schemes (MITCOST-II).

CHAPTER 4

FUEL CYCLE CALCULATIONS

4.1 Introduction

In this chapter, we describe the fuel cycles analyzed, the methods of calculation employed and the assumptions made; and present and analyze the results. The basic objective is to find the effect of tight pitch cores fueled with U-233/ThO_2 or Pu/UO_2 on the consumption of natural uranium ore when the subject reactors are operated in complete systems, namely the thorium system U-235/UO_2:Pu/ThO_2:U-233/ThO_2 and the uranium system U-235/UO_2:Pu/UO_2. Fuel cycle costs for equilibrium fuel batches are also calculated, and consideration is given to reactivity coefficients and to thermal-hydraulic effects. Finally, uncertainties inherent in the calculations are discussed.

4.2 Fuel Cycles Analyzed

The two systems of coupled reactors analyzed, namely the thorium system, U-235/UO_2:Pu/ThO_2:U-233/ThO_2, and the uranium system, U-235/UO_2: Pu/UO_2, are sketched in Fig. 4.1. All cores use 3-batch fuel management and (except for the final core in each sequence) have F/M = 0.5 and discharge fuel at 33 MWD/KgHM. Parameters varied for the final core in each sequence include the fuel-to-moderator volume ratio (F/M ratio), discharged fuel burnup (B) and the number of core zones (N).

The first system, U-235/UO_2:Pu/ThO_2:U-233/ThO_2, was chosen instead of the more common U-235/ThO_2 option because of the judgement, on practical grounds, that reprocessing of uranium fuel will precede reprocessing of

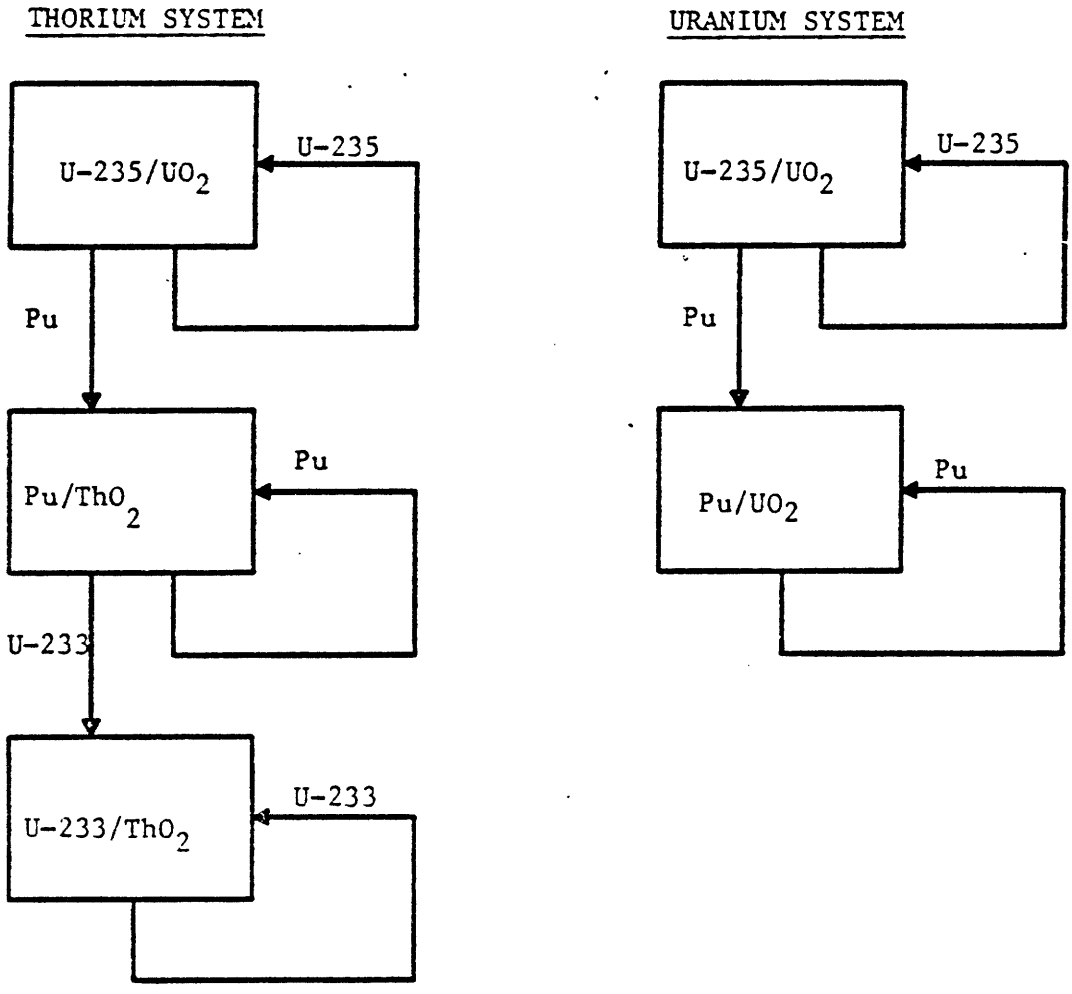

Figure 4.1 THE U-235/UO_2 : Pu/ThO_2 : U-233/ThO_2 and U-235/UO_2 : Pu/UO_2 SYSTEMS OF COUPLED REACTORS

thorium fuel, and that it is highly desirable to avoid contamination of U-235 with U-232 and other uranium isotopes, which would increase the complexity and cost of U-235 re-enrichment and re-fabrication. The second system, U-235/UO_2:Pu/UO_2, was chosen because it is by far the leading candidate being worked on worldwide for LWR recycle and breeder use.

Because the fuel management characteristics of standard PWR cores are already very near their optimum values (F/M = 0.5; B = 33 MWD/KgHM; N = 3) in terms of uranium ore utilization (G-1) and fuel cycle cost (A-2), only the characteristics of the final core in each sequence were varied. The fuel management parameters (F/M, B and N) for the Pu/ThO_2 cores were taken to be the same as for the standard PWR cores (for comparison, the effect of a tight pitch core fueled with Pu/ThO_2 is briefly discussed).

To reiterate, the basic objective is to study the effects of each of the fuel management parameters varied (F/M, B and N) for the last core in each sequence on the consumption of natural uranium ore (CNU) and on the fuel cycle cost (FCC) (calculated at the indifference value of bred fissile species) for the system.

4.3 Method of Calculation

4.3.1 Reactor Model

The reactor cores studied are based on the preliminary design parameters for the Maine Yankee PWR (M-5) listed in Appendix A. Table 4.1 gives the core characteristics kept constant, which include the fuel pin diameter, core area, total reactor coolant flow, average linear heat rate

TABLE 4.1

CORE CHARACTERISTICS KEPT CONSTANT*

Pellet Diameter, inch	0.382
Fuel Density, Stacked, % Theoretical	92
Clad Material	Zircaloy-2
Clad OD, inch	0.440
Clad Thickness, inch	0.026
Fuel Array Geometry	Hexagonal (Triangular)
Core Cross Sectional Area, ft^2	101
Total Energy Output, Mwt	2,440
Thermal Efficiency, %	33
Average Pressure, Psi Absolute	2,250
Coolant Inlet Temperature, °F	550
Average Coolant Temperature, °F	576.4
Average Clad Temperature, °F	610
Average Fuel Temperature, °F	ThO_2/1100, UO_2/1200
Total Reactor Coolant Flow, lb/hr	122×10^6
Average Linear Heat Rate of Fuel Rod, KW/ft	5.6

*control guides and inter-assembly water were not included in the calculations

(5.6 Kw/ft) and the total core heat output (2,400 Mwt). Core characteristics which depend on the F/M ratio, which was the basic geometry-dependent parameter varied, are given in Table 4.2. To facilitate comparisons, no allowance for control guides or inter-assembly water were included in the cell calculations. Also, all lattices were assumed hexagonal (≡ triangular), since this arrangement is required to reach high F/M ratios. Thus, the F/M ratio is given by:

$$F/M = \frac{\pi R_f^2}{\alpha p^2 - \pi R_{OC}^2} \qquad (4.1)$$

where

F/M = fuel-to-moderator volume ratio

R_f = fuel pellet radius

R_{OC} = outside clad radius

p = lattice pitch (pin-to-pin centerline spacing)

$\alpha = \sqrt{3/2}$

In our work F/M was <u>defined</u> using cold lattice parameters; (however, hot lattice parameters were used in LEOPARD calculations, while for LASER, cold parameters were used; differences are very small).

We should mention that the neutron balance is not too sensitive to the presence or absence of extra structural material, especially in tight-pitch cores (requiring, at most 10% in additional fuel inventory, and reducing the conversion ratio by less than 2%). While the neutron balance <u>is</u> sensitive to non-cell water, we have not explicitly included this extra water. In designing tight pitch cores it will be particularly important to minimize the amount of such extra moderator. Finally, if one wishes to evaluate systems in which non-cell H_2O <u>is</u> included this can

TABLE 4.2

CORE CHARACTERISTICS WHICH DEPEND ON THE F/M RATIO

F/M Ratio		0.5	1.0	1.5	2.0	2.5	3.0
Pitch (Hexagonal)	(in)	0.6635	0.5549	0.5136	0.4917	0.4780	0.4687
Rod-to-rod spacing	(mil)	223.5	114.9	73.6	51.7	38.0	28.7
Core height	(ft)	11.44	7.998	6.852	6.279	5.936	5.707
Power density	(w/cm^3)	74.69	106.8	124.7	136.0	143.9	149.7
Geometric Buckling	(m^{-2})	2.29	2.97	3.44	3.76	4.00	4.18

readily be done merely by using the present results at the same total F/M ratios.

Core cross-sectional area was kept constant and core height was varied to minimize pressure drop in the core, thus the cores are not optimized in terms of neutron leakage. Average moderator, clad and fuel temperatures were calculated for each cell and found to be rather insensitive to the F/M ratio since the total reactor coolant flow and the inlet coolant temperature were kept fixed. The average fuel temperature for UO_2 is about 100°F higher than for ThO_2-bearing fuels, reflecting a smaller thermal conductivity for UO_2 at these fuel temperatures and at 92% of theoretical density.

In order to maintain the average linear heat rate (5.6 Kw/ft), high core volumetric power densities are required for the tightest lattices. To achieve high F/M ratios, rod-to-rod spacing must be decreased to very low values: 30 mils for F/M = 3.0, which is considered by some to be feasible (E - 1). In practice, to achieve high F/M ratios, control guides (if used) should be filled with empty rods or rods containing fertile or inert materials, On the other hand, fuel spacers (grids or wire-wrap) remove some coolant, thereby increasing F/M. In view of these qualifying considerations we did not allow for the presence of non-cell water or structural material in our calculations, as previously noted.

The geometric bucklings, which are important to represent neutron leakage out of the core, were calculated as an average of the bucklings calculated with and without reflector (a 19-inch reflector was assumed). Comparisons with R-Z PDQ-7 (C-5) calculations showed that this procedure would adequately represent neutron leakage, with an error no larger than 10% in the small leakage component of the neutron balance (at BOC).

4.3.2 Depletion Model

Fuel depletion calculations for all types of fuel were done using EPRI-LEOPARD, except for Pu/UO_2-fueled cores, for which the LASER program was used. As noted in Chapter 3, the treatment of plutonium-bearing fuels is superior in LASER, and we would have also used this code to calculate fuel depletion for the Pu/ThO_2 types of cores if the chain of nuclides deriving from Th-232 was available in this program.

All depletion calculations were made with depletion steps of 3 MWD/KgHM, with two or three shorter steps at the beginning of depletion to allow Xe-135 and Sm-149 to saturate. Smaller time steps (1 MWD/KgHM) change the calculated k's and discharged fissile masses by no more than a tenth of a percentage point and 0.4%, respectively, up to fuel burnups of 40 MWD/KgHM. The effects of these errors were considered to be negligible for all practical purposes.

Neutron leakage from the core was represented by using the geometric bucklings of Table 4.2. The fission product scaling factor in LEOPARD was 0.84 for both $U-235/UO_2$ and $U-233/ThO_2$ cores and 1.26 for Pu/ThO_2 cores, as explained in Section 3.2.1. Absorption cross sections for the lumped fission product in LASER were taken from Momsen's work (M-3) (See Section 3.3.1). Strawbridge's procedure was the option selected to calculate the L-factor for the dominant fertile nuclide in both LASER and LEOPARD. Effective fuel temperatures were assumed equal to the average fuel temperatures since differences between these two parameters are generally smaller than the errors involved in calculating each of them (M-3, S-4). Neither soluble nor fixed control poisons

were explicitly included, however the programs employed simulate neutron losses to these materials through use of a (control-searched) material buckling in the neutron balance. Although the absorption of neutrons in control materials occurs mainly at thermal energies and neutron leakage is more important at non-thermal energies, differences can be neglected (calculated CR differences are less than 1%).

4.3.3 Fuel Management Model

To find the discharged fuel burnup for a given fuel type, fuel enrichment (ε) and F/M ratio as a function of the number of core zones (N), we have used the so-called "linear reactivity model" (G-3). This model assumes that curves of k (or ρ) versus B are linear and power density is time and space independent. Although in some cases ρ (reactivity) vs. B is more linear than k vs. B, this was not found to be a useful distinction in the present work, and hence k was used throughout The following relation between the discharged fuel burnup for an N-zone and 1-zone core is obtained (when other characteristics are kept the same):

$$B_N = \frac{2N}{N+1} B_1 \qquad (4.2)$$

where

N = number of core zones (staggered-reload fuel batches)

B_N = discharged fuel burnup for an N-zone core

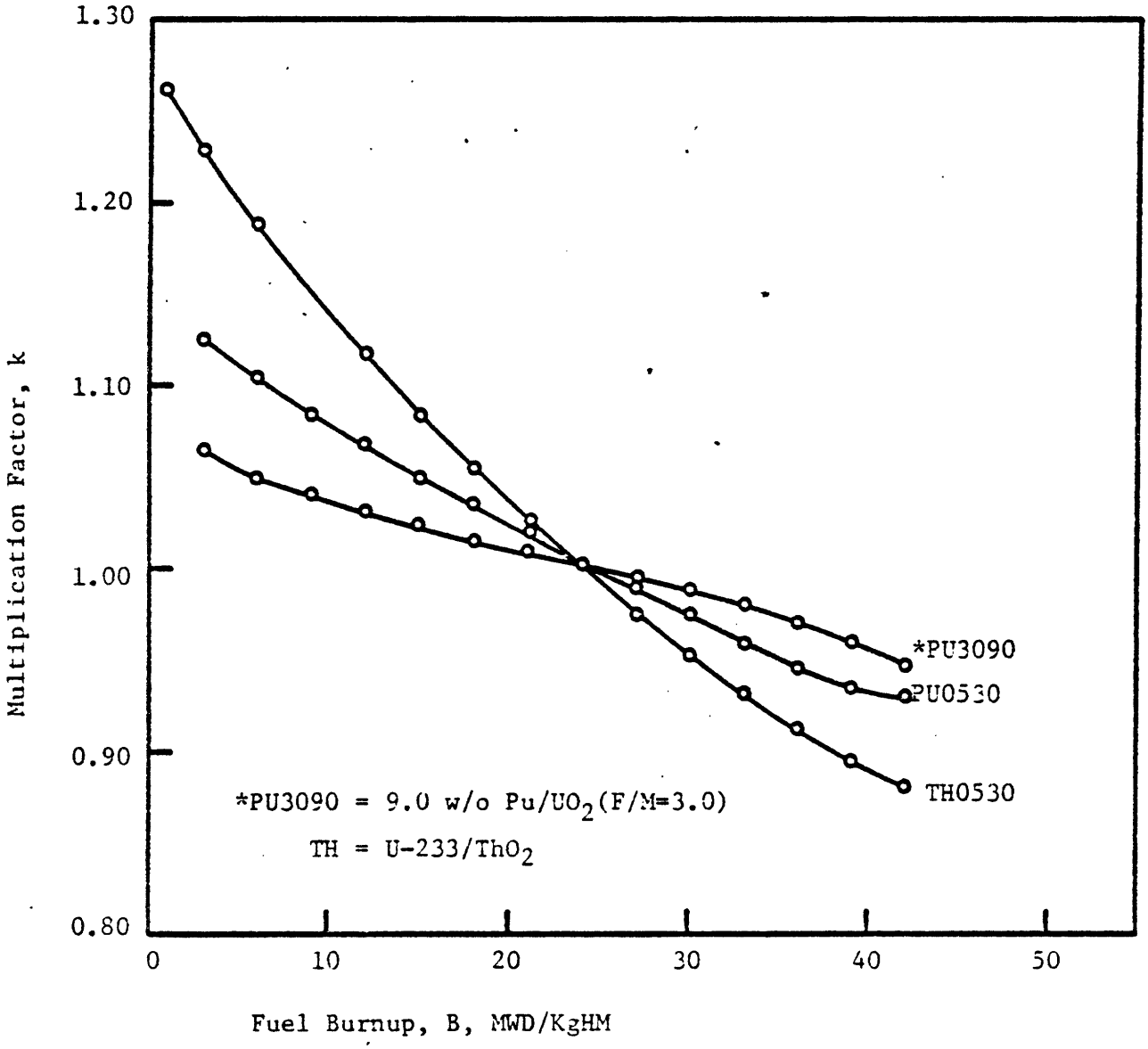

Figure 4.2 MULTIPLICATION FACTOR AS A FUNCTION OF THE FUEL BURNUP

Figure 4.2 shows some curves of k vs B. Because these curves are only roughly linear, the point B_1 where the linearized curves cut the abscissa may depend on the number of points used in the linearization. To be consistent, for a given N we have found B_N for each curve by linearizing (least-square fit) from B = 1 MWD/MTHM (to allow Xe-135 and Sm-149 to reach equilibrium concentrations) to the closest point to the B_N found using Eq. (4.2) and the (linearized) B_1.

Basically, the discharged fuel burnup increases with N (Eq. (4.2)) because less neutrons are lost to control materials, since fuel batches with negative reactivity absorb much of the available excess of neutrons from the fuel batches with excess reactivity.

4.3.4 Relative Isotopic Weights

Since the calculations of the consumption of fissile material were based on non-equilibrium fuel compositions (to save on computer expenses, and because first recycle effects are most important), recycle to extinction was simulated by appropriately worth-weighting each isotope in discharged fuel mixtures. Several types of weighting factors have been defined, mainly for breeder reactor fuels (B-6, M-4). The "standard" definition weights the fissile and non-fissile isotopes by 1.0 and 0.0, respectively. The British critical-mass-worth weight factors are calculated by:

$$\frac{w_j}{w_i} = \frac{\sigma_j(\eta_j - 1)}{\sigma_i(\eta_i - 1)} \qquad (4.3)$$

where:

w_j = relative weight factor of isotope j

σ = average absorption cross section

η = average eta

Equation (4.3) gives the correct effect in terms of k. In other words, adding w_j units of isotope i or w_i units of isotope j to the fuel will change k by the same amount. If the slope of the curve of k vs B was independent of the initial fuel composition, this definition would also be adequate for our purposes. References (B-6) and (M-4) give another, more elaborate, way to calculate weighting factors.

We have derived, as a part of this work, a simple way to estimate fuel isotopic-weight factors based on sensitivity analysis of the discharged fuel burnup to the isotopic fuel composition. For a given fuel composition, cell geometry and discharged fuel burnup, we successively change the atomic concentration of each isotope j (by the same small amount) and determine the net burnup increment ΔB_j. The relative weight factors are then defined by:

$$\frac{w_j}{w_i} = \frac{\Delta B_j}{\Delta B_i} \qquad (4.4)$$

where

w_j = weight factor of isotope j

ΔB_j = net burnup increment for isotope j

TABLE 4.3

RELATIVE ISOTOPIC - WEIGHT FACTORS

Fuel	$U\text{-}235/UO_2$*	$U\text{-}233/ThO_2$*		Pu/ThO_2*	Pu/UO_2**	
F/M	0.5	0.5	3.0	0.5	0.5	3.0
ε(w/o)	2.75	3.0	5.5	3.71	3.0	9.0
B_3(MWD/KgHM)	33.1	38.1	34.4	33.5	38.1	37.3
U-233	-	1.00	1.00	-	-	-
U-234	-	- 0.10	- 0.58	-	-	-
U-235	1.00	0.79	0.41	-	-	-
U-236	- 0.24	- 0.23	- 0.52	-	-	-
Pu-239	-	-	-	1.00	1.00	1.00
Pu-240	-	-	-	- 0.36	- 0.24	- 0.30
Pu-241	-	-	-	1.54	1.34	1.58
Pu-242	-	-	-	- 0.61	- 0.58	- 0.41

* Based on EPRI-LEOPARD

** Based on LASER

This method is essentially an extension of the British definition of weight factors since not just the instantaneous effects of isotope j on the neutron balance are considered but also the effects of all nuclides derived directly (by neutron capture) or indirectly (fission products) from it.

Table 4.3 gives the relative isotopic-weight factors calculated using this method for some cases of interest. Results were interpolated for other F/M ratios and assumed independent of the fuel enrichment and discharged fuel burnup (for the same fuel composition, the weight factors are not very sensitive to B). We note in this table that the value of Pu-241 compared to Pu-239 increases with F/M, which basically reflects the larger η of Pu-241 in epithermal spectra (Table 2.6). The opposite occurs for U-235 compared to U-233; the η effect is further enhanced by the much larger resonance integral of U-233. In general, the value of a plutonium mixture increases with F/M and the contrary is true for uranium mixtures.

4.3.5 Economic Model

To calculate the fuel cycle costs (FCC's) we have used the SIMMOD (Simple Model) program developed by Abbaspour (A-2). Fuel cycle costs were calculated for equilibrium batches (those batches which have the same initial and final fuel compositions and produce the same amount of energy).

Table 4.4 gives the unit prices assumed for each fuel cycle transaction. Lead and lag times for the transactions are given in Table 4.5. The availability-based capacity factor was held constant

TABLE 4.4

UNIT PRICES* FOR FUEL CYCLE TRANSACTIONS

Yellowcake, U_3O_8, $/lb	40/100
Enrichment, $/SWU	94
UF_6 Conversion, $/KgHM	4
Clean Fuel Transportation, $/KgHM	4
Spent Fuel Transportation, $/KgHM	17
Fuel Fabrication, $/KgHM	
U-235/UO_2	150
Pu/ThO_2	510**
U-233/ThO_2	570
Pu/UO_2	500
Reprocessing, $/KgHM	
U-235/UO_2	221
Pu/ThO_2	260**
U-233/ThO_2	278
Pu/UO_2	221
Waste Disposal, $/KgHM	
U-235/UO_2	71
Pu/ThO_2	92
U-233/ThO_2	92
Pu/UO_2	71
Thorium, $/lb Th	15
Depleted Uranium, $/lb U	15

* Unit prices from Ref. (A-2)
** Ref. (D-1)

TABLE 4.5

DATA FOR FUEL CYCLE CALCULATIONS

Transaction	Lead or Lag Time* (yr)
Pay for Fuel	-1.0
Pay for Conversion	-0.5
Pay for Separative Work**	-0.5
Pay for Fabrication	-0.2
Pay for Transportation	-0.1
Pay for Transportation	0.5
Pay for Reprocessing	0.75
Pay for Waste Disposal	0.75
Credit for Fuel	1.0
Fuel Cycle Parameters	
Refueling Downtime, yr	0.125
Availability - Based Capacity Factor	0.83
Economic Parameters	
Bond-holder Fraction	0.5
Stock-holder Fraction	0.5
Return to Bond-holder, % yr^{-1}	11
Return to Stock-holder, % yr^{-1}	15
Tax Rate, %	50
Discount Rate, % yr^{-1}	10.25
Escalation Rate, % yr^{-1}	0

*Lead Time = time before start of irradiation

Lag Time = time after end of irradiation

**Tails assay enrichment = 0.2 w %

equal to 0.83, and the refueling downtime kept equal to 0.125 yr for all cases. The high discount rate (10.25% yr^{-1}) was chosen to reflect an inflationary environment.

Fuel cycle costs for each system were evaluated with the cost for bred fissile species at their indifference values (in other words, the FCC is the same for all types of cores in the system).

4.4 Fissile Inventory and Conversion Ratio

This section compares the U-233/ThO_2 and Pu/UO_2 fueled cores in terms of reload fissile enrichment (ε or RFE) and cycle-average fuel conversion ratio (CR) as a function of the fuel-to-moderator volume ratio (F/M), the discharged fuel burnup (B) and the number of cores zones (N). Specific results are tabulated in Appendices E and F.

Figures 4.3 and 4.4 show the RFE for the U-233/ThO_2 and Pu/UO_2 cores as a function of B for several F/M ratios and for N = 3. (Appendices E and F include results for N = 1 and N = 6). Figure 4.5 compares CR for both types of fuel. The RFE increases with F/M for both fuels, reflecting the consequences of decreased fissile cross sections in epithermal spectra. The CR also increases with F/M because the average absorption cross section for U-238 and Th-232 decrease less with F/M than for other elements. Increased fast fission in the fertile elements also contributes to the increase in CR. To reach higher discharged fuel burnups, higher enrichments are required, which decreases CR since more neutrons are lost to the fissile, control and fission product materials.

For current lattices (F/M = 0.5) Pu/UO_2 requires slightly less enrichment than U-233/ThO_2 because of the higher thermal cross sections of the

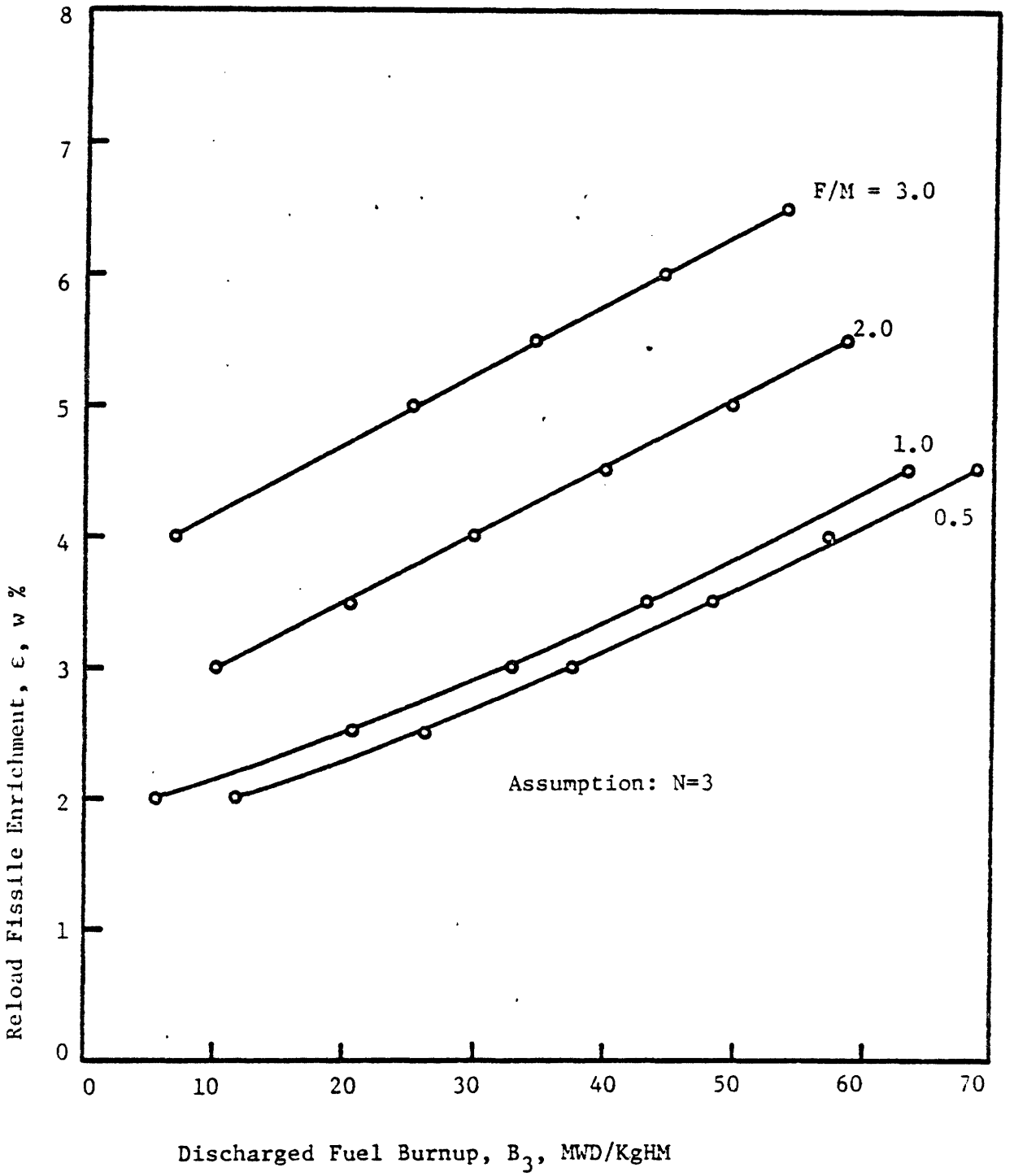

Figure 4.3 RELOAD FISSILE ENRICHMENT FOR THE U-233/ThO_2 CORE VERSUS THE DISCHARGED FUEL BURNUP

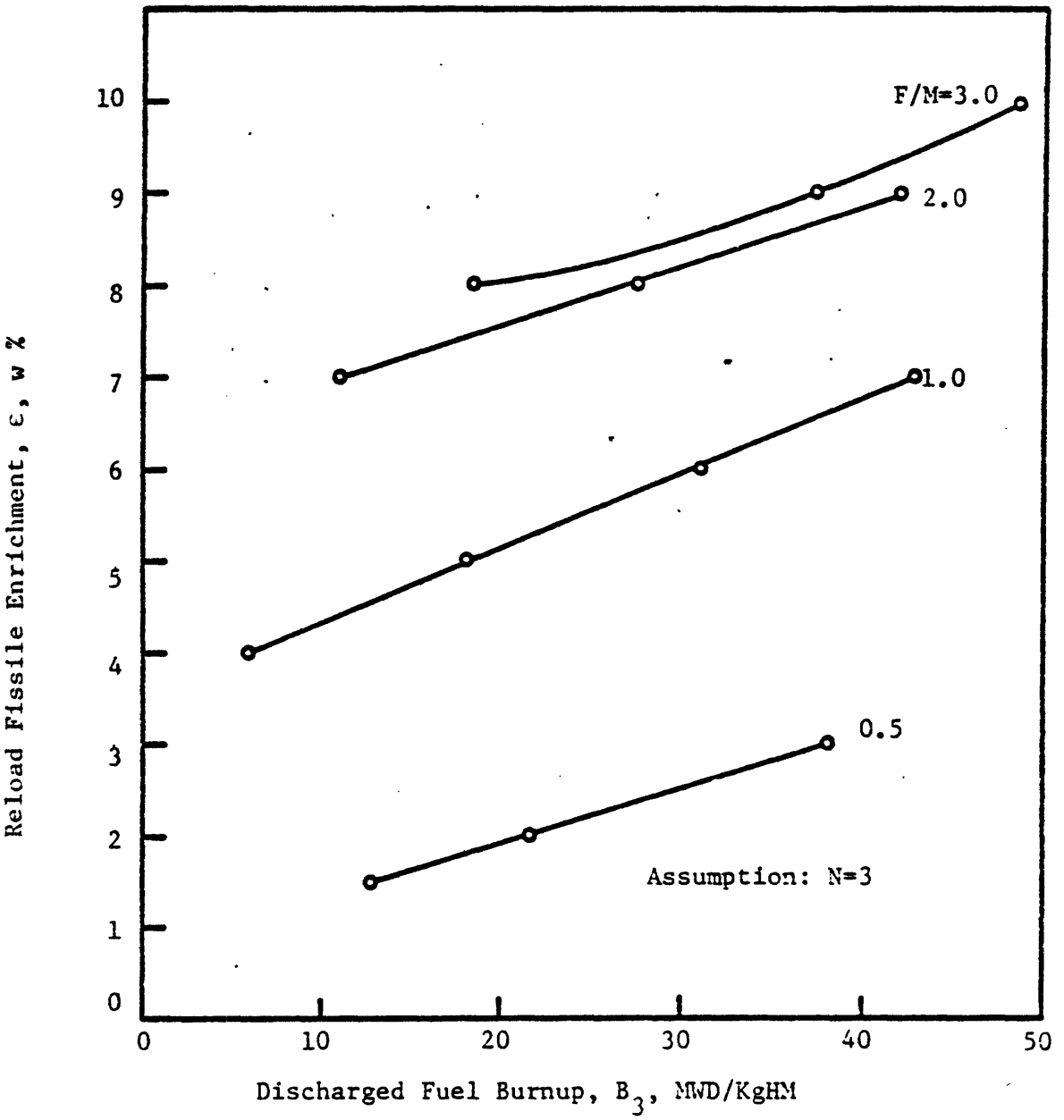

Figure 4.4 RELOAD FISSILE ENRICHMENT FOR THE Pu/UO_2 CORE VERSUS THE DISCHARGED FUEL BURNUP

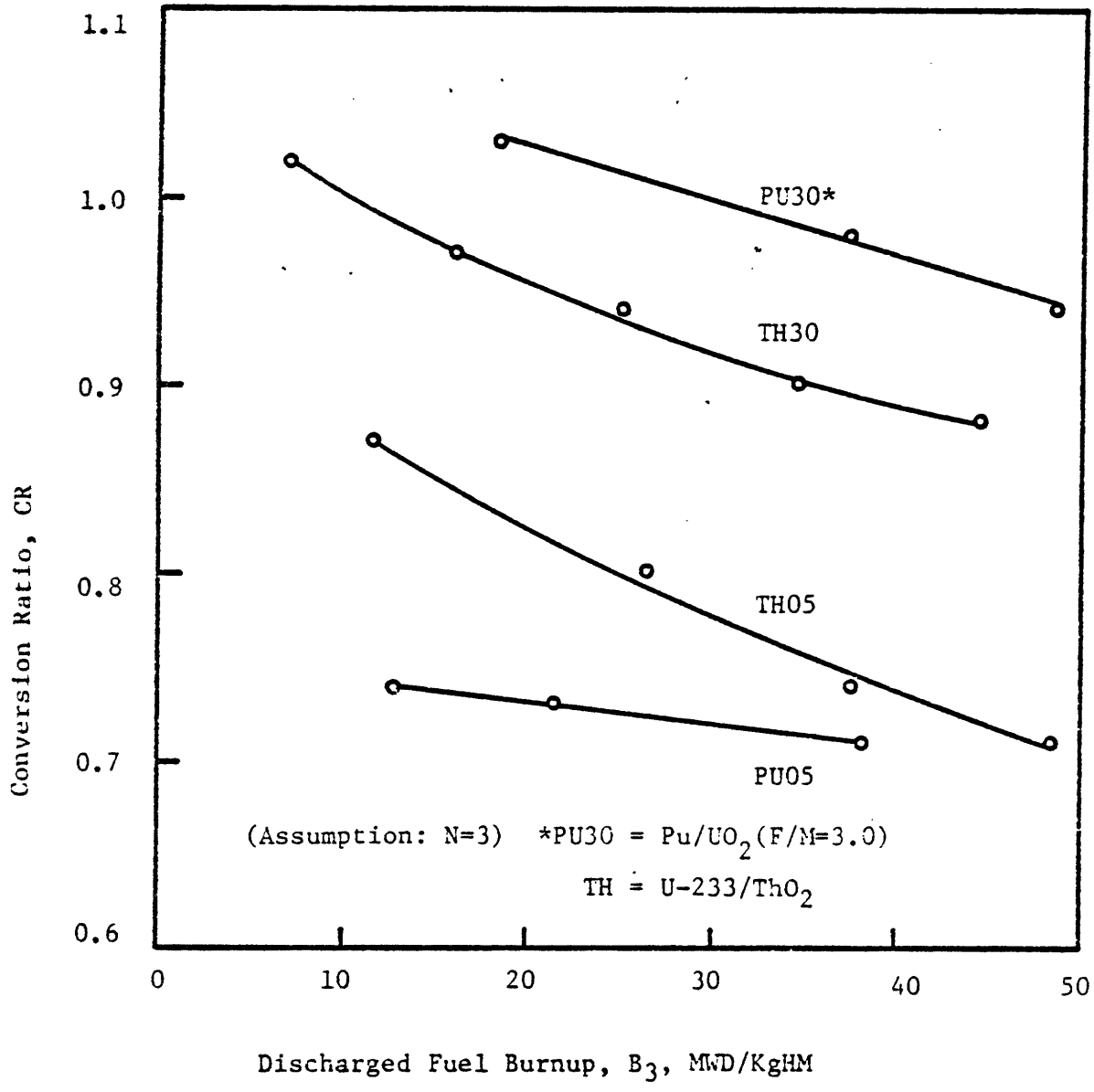

Figure 4.5 AVERAGED CONVERSION RATIO OVER THE CYCLE FOR THE U-233/ThO_2 AND Pu/UO_2-FUELED CORES

plutonium fissile isotopes compared to U-233, the smaller thermal cross section of U-238 compared to Th-232, and the larger fast fission (1.09 vs. 1.02) effect for U-238 compared to Th-232. The difference is not larger because the plutonium used contains large amounts of Pu-240 and Pu-242 (Pu-239: 54 w%; Pu-240: 26w%; Pu-241: 14 w% and Pu-242: 6w%) while the U-233 fuel contains fewer of the corresponding higher mass isotopes (U-233: 91 w%. U-234: 8 w% and U-235: 1 w%). Both fuel compositions degrade further with fuel burnup. The higher thermal η of U-233 relative to Pu-239 provides a higher CR for U-233/ThO_2 fuel, since this outweighs the fast fission differential.

For epithermal spectra, on the other hand, Pu/UO_2 requires considerably higher enrichments than U-233/ThO_2 (for the same discharged fuel burnup) because of the much smaller resonance integral of the fissile plutonium isotopes compared to U-233 (Table 2.5). The very large fast fission effect in U-238 (plus Pu-240) compared to Th-232 (1.20 vs. 1.04 at F/M = 3), helps keep the RFE for Pu/UO_2 from rising even higher, and provides larger CR values than for U-233/ThO_2 despite the higher eta of U-233. Differences in the shielded cross section for Th-232 and U-238 are less than 20% and do not change the general picture for epithermal spectra.

4.5 Consumption of Natural Uranium Ore

In this section we compare the consumption of natural uranium for both systems as a function of the fuel-to-moderator volume ratio, discharged fuel burnup and number of core zones for the last reactor in each sequence.

Charged and discharged masses for the U-235/UO_2 and Pu/ThO_2 cores are given in Table D.2 in Appendix D. Charged and discharged masses for the U-233/ThO_2 and Pu/UO_2 cores are given in Appendices E and F, respectively.

To calculate the consumption of natural uranium for each system we have extended the simple method developed by Garel (G-1) to include burnup effects for a zero growth-rate system:

U-235/UO_2: Pu/ThO_2 : U-233/ThO_2 System

$$CNU = C_o \left\{ 1 + \frac{B_2}{B_1} \times \frac{(1 - RL)m_{49}^{d1}}{(1 - FL)^{-1}m_{49}^{c2} - (1 - RL)m_{49}^{d2}} \right.$$

$$\left. \times \left[1 + \frac{B_3}{B_2} \times \frac{(1 - RL)m_{23}^{d2}}{(1 - FL)^{-1}m_{23}^{c3} - (1 - RL)m_{23}^{d3}} \right] \right\}^{-1} \quad (4.5)$$

U-235/UO_2 : Pu/UO_2 System

$$CNU = C_o \left\{ 1 + \frac{B_2}{B_1} \times \frac{(1 - RL)m_{49}^{d1}}{(1 - FL)^{-1}m_{49}^{c2} - (1 - RL)m_{49}^{d2}} \right\}^{-1} \quad (4.6)$$

where:

CNU = Consumption of Natural Uranium Ore (ST U_3O_8/GWe.yr)

C_o = consumption of Natural Uranium for the standard core fueled with U-235/UO_2 <u>with uranium recycle only</u>, assuming 0.2 w% depleted uranium tails. (150 ST U_3O_8/GWe.yr)*

*the consumption of natural uranium ore for the standard U-235/UO_2-fueled core without recycle is 167 ST U_3O_8/GWe.yr

RL = reprocessing losses (1%)

FL = fabrication losses (1%)

m_j^{di} = discharged equivalent mass of isotope j from the i^{th} core in the sequence of coupled reactors.

m_j^{ci} = charged equivalent mass of isotope j in the i^{th} core in each sequence of coupled cores

B_i = discharged fuel burnup for the i^{th} core in each sequence.

Equivalent masses for U-233 and Pu-239 were obtained using the isotopic weight factors given in Table 4.3 (weight factors were interpolated in F/M). Equivalent masses for these nuclides are defined as:

$$m^*_{23} = m_{23} + m_{13} + w_{24}\, m_{24} + w_{25}\, m_{25} + w_{26}\, m_{26} \qquad (4.7)$$

and

$$m^*_{49} = m_{49} + w_{40}\, m_{40} + w_{41}\, m_{41} + w_{42}\, m_{42} \qquad (4.8)$$

where

m^*_j = equivalent mass of isotope j

m_i = mass of isotope i in the mixture

w_i = weight of isotope i relative to isotope j ($w_j = 1$)

Equations (4.5) and (4.6) assume the capacity factors for all reactors in each chain are the same.

Figures 4.6 and 4.7 show curves of CNU versus B at several F/M ratios (and for N = 3) for the thorium and uranium systems, respectively (Appendices E and F give detailed results for these CNU calculations). We see that the consumption of uranium ore decreases with F/M and

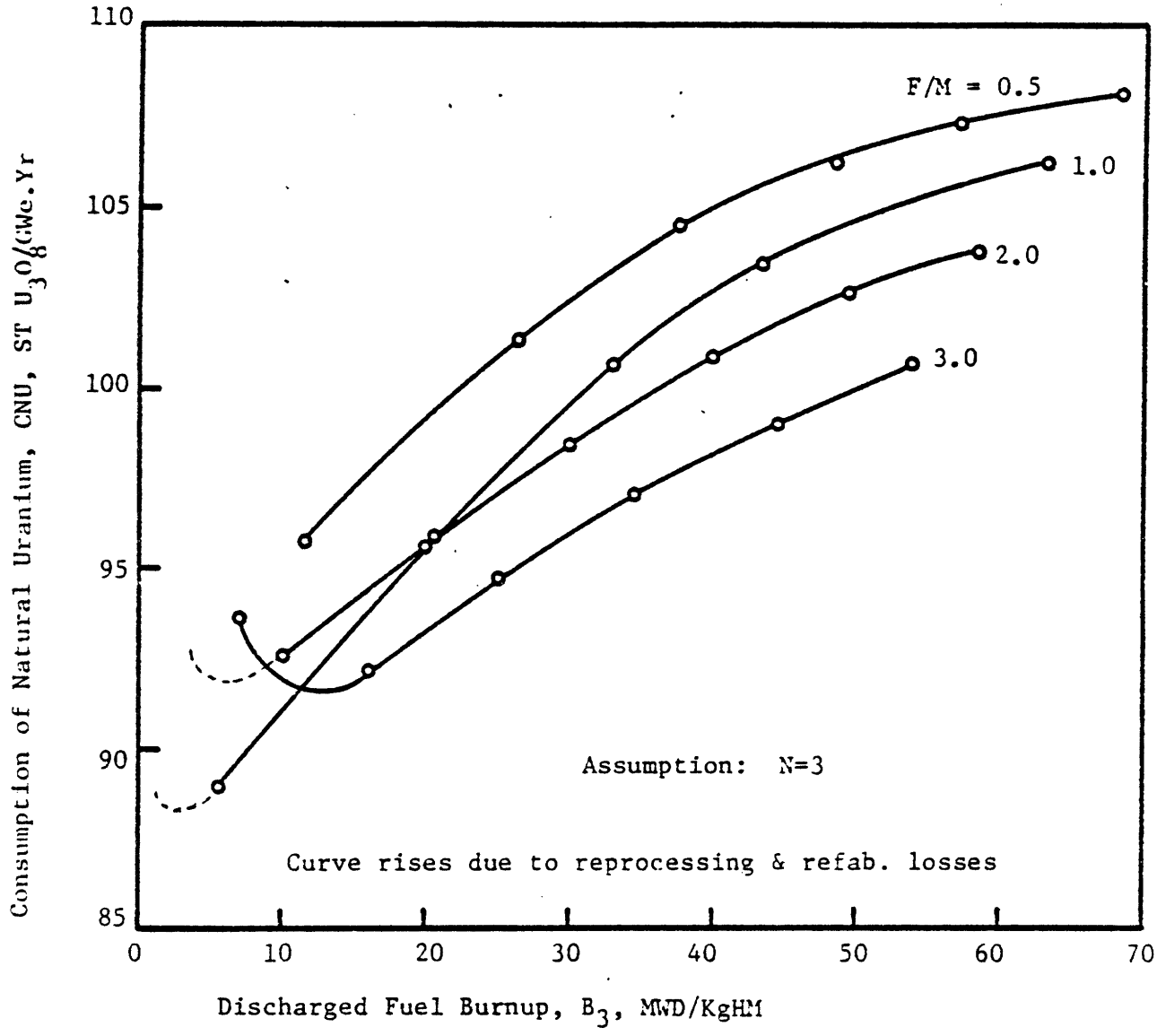

Figure 4.6 CONSUMPTION OF NATURAL URANIUM FOR THE U-235/UO_2 : Pu/ThO_2 : U-233/ThO_2 SYSTEM AS A FUNCTION OF THE DISCHARGED FUEL BURNUP FOR THE U-233/ThO_2 CORE

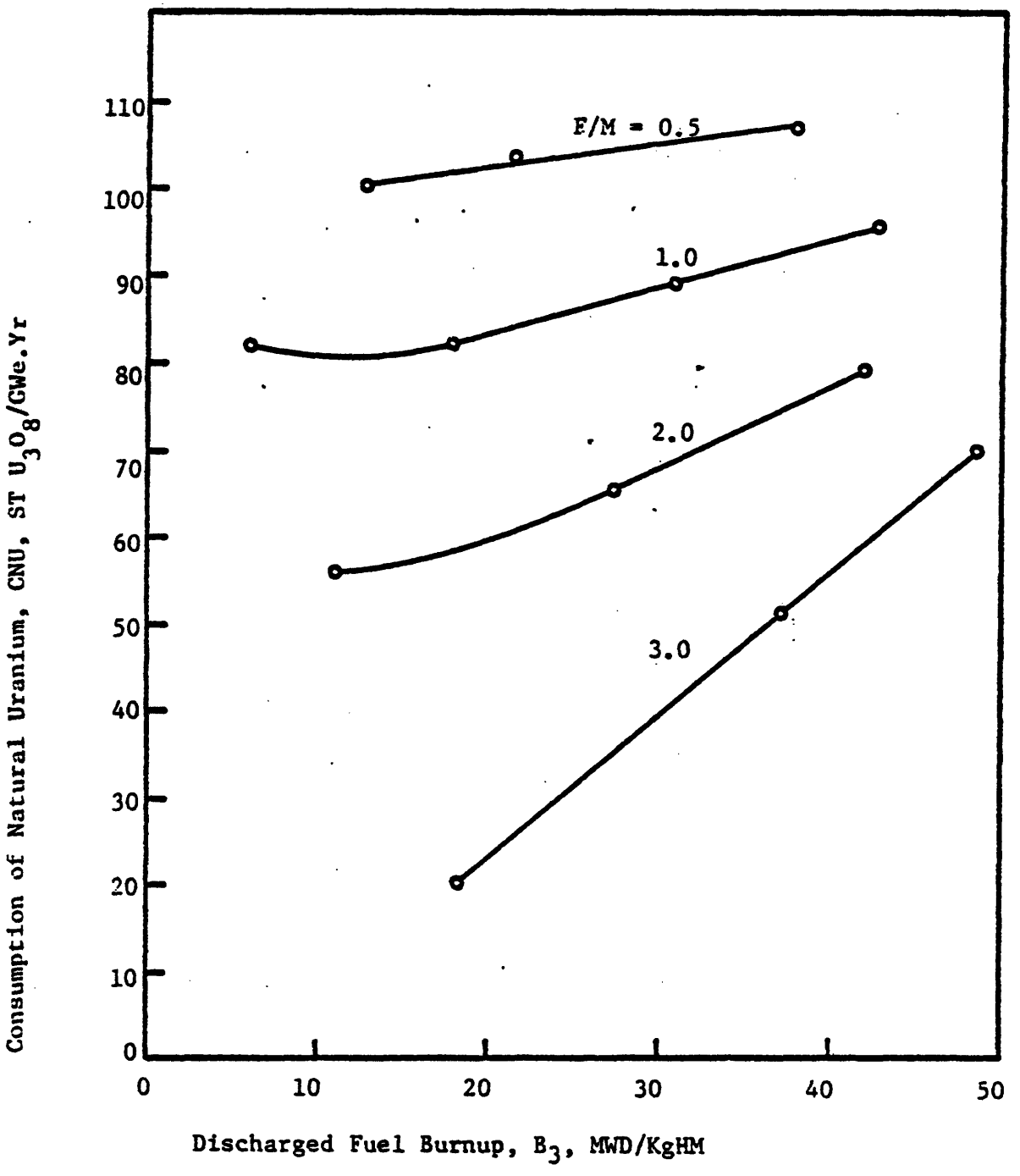

Figure 4.7 CONSUMPTION OF NATURAL URANIUM FOR THE U-235/UO_2 : Pu/UO_2 SYSTEM OF REACTORS AS A FUNCTION OF THE DISCHARGED FUEL BURNUP FOR THE Pu/UO_2 CORE

increases with B, which is consistent with the opposite behavior of CR versus F/M and B.

The CNU for B = 33 MWD/KgHM at F/M = 0.5 (and N = 3) is 103 and 106 ST U_3O_8/GWe.yr for the thorium and uranium systems, respectively. Maximum ore savings, relative to these numbers, are less than 15% for the thorium system and up to 80% for the uranium system. The disadvantage of the thorium system compared to the uranium system comes from the dominance of the Pu/ThO_2 core (with its poor performance: CR $\approx$ 0.72 - Appendix D) over the $U\text{-}233/ThO_2$ core in the thorium sequence of coupled cores. However, increasing the F/M ratio of the Pu/ThO_2 core from 0.5 to 3.0 does not significantly improve the performance of the thorium system (Fig. 4.8). We should recall however that the mass flow results for the Pu/ThO_2 cores were based on EPRI-LEOPARD calculations, which have a poorer degree of confidence for plutonium-bearing fuels. Increasing the number of core zones improves fuel performance for both systems (Figs. 4.9 and 4.10) since neutron losses to control materials are reduced.

Figures 4.11 and 4.12 show the effects of re-fabrication and reprocessing losses and fuel weighting on the consumption of natural uranium ore for the thorium and uranium systems. Curves A in these figures do not include either fuel losses or fuel isotopic weighting effects, curves B include only fuel loss effects and curves C include both fuel losses and weighting effects. We note that fuel losses and weighting effects are more important for high F/M ratios and low discharged fuel burnup since, in these cases, the CR is near unity, and discharged and charged masses are practically the same (Eqs. 4.5 and 4.6). In general, the CNU will exhibit a minimum because of fuel loss effects for very low values of discharged fuel burnup, B.

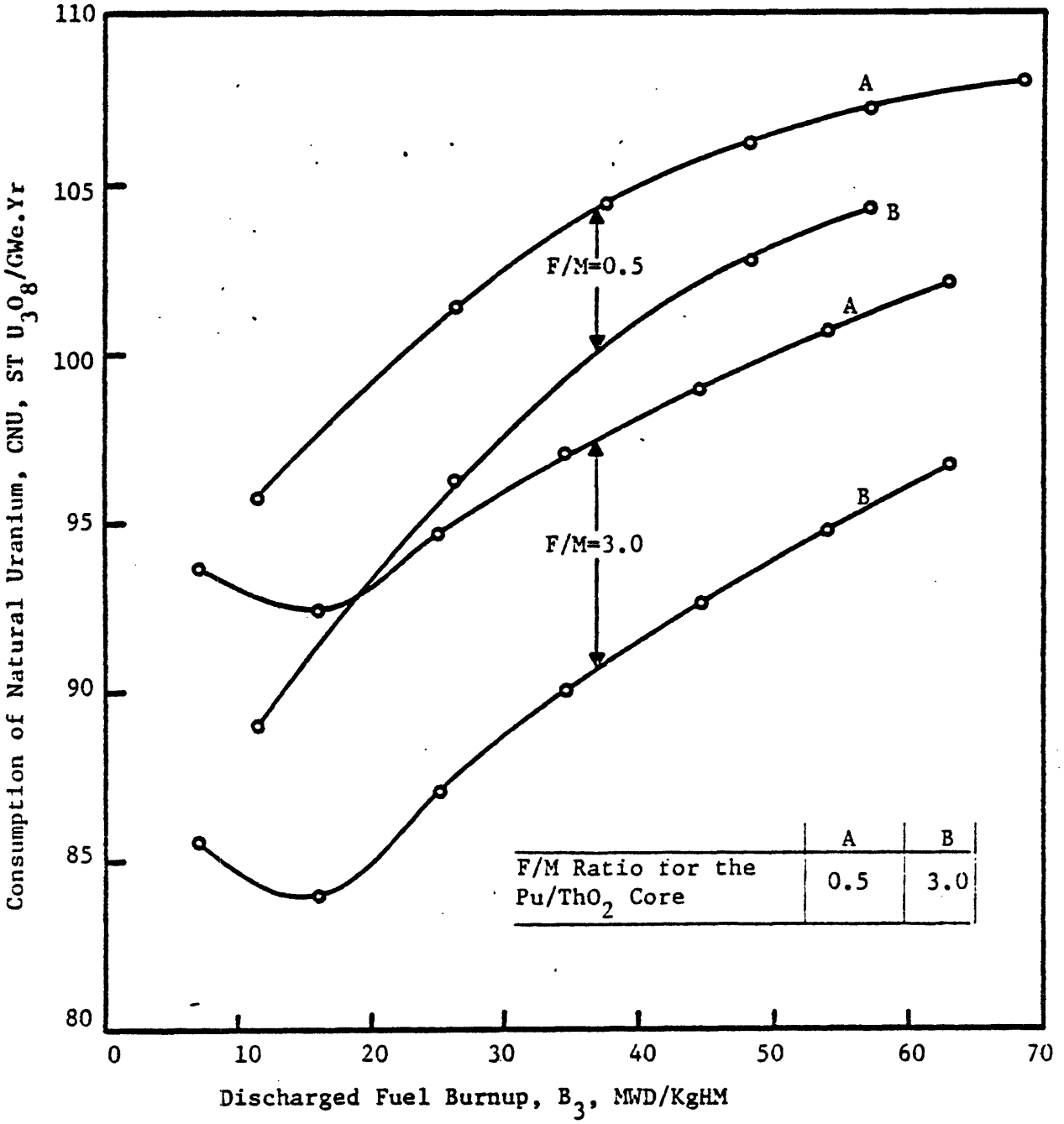

Figure 4.8 DEPENDENCE OF THE CONSUMPTION OF NATURAL URANIUM FOR THE U-235/UO_2 : Pu/ThO_2 : U-233/ThO_2 SYSTEM ON THE F/M RATIO FOR THE Pu/ThO_2 CORE

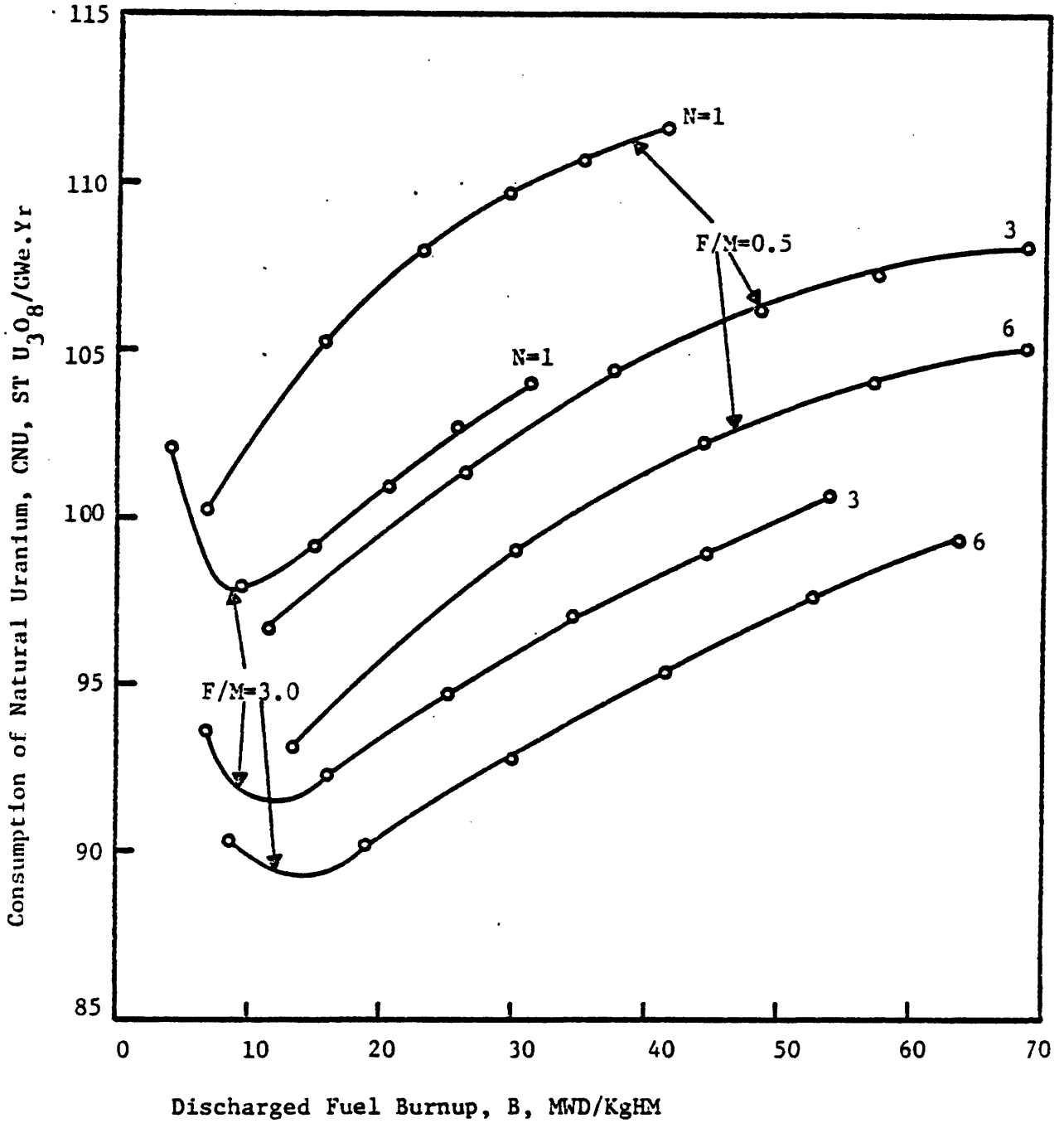

Figure 4.9 EFFECT OF THE NUMBER OF CORE BATCHES IN THE U-233/ThO_2 REACTOR ON THE CONSUMPTION OF NATURAL URANIUM FOR THE U-235/UO_2 : Pu/ThO_2 : U-233/ThO_2 SYSTEM

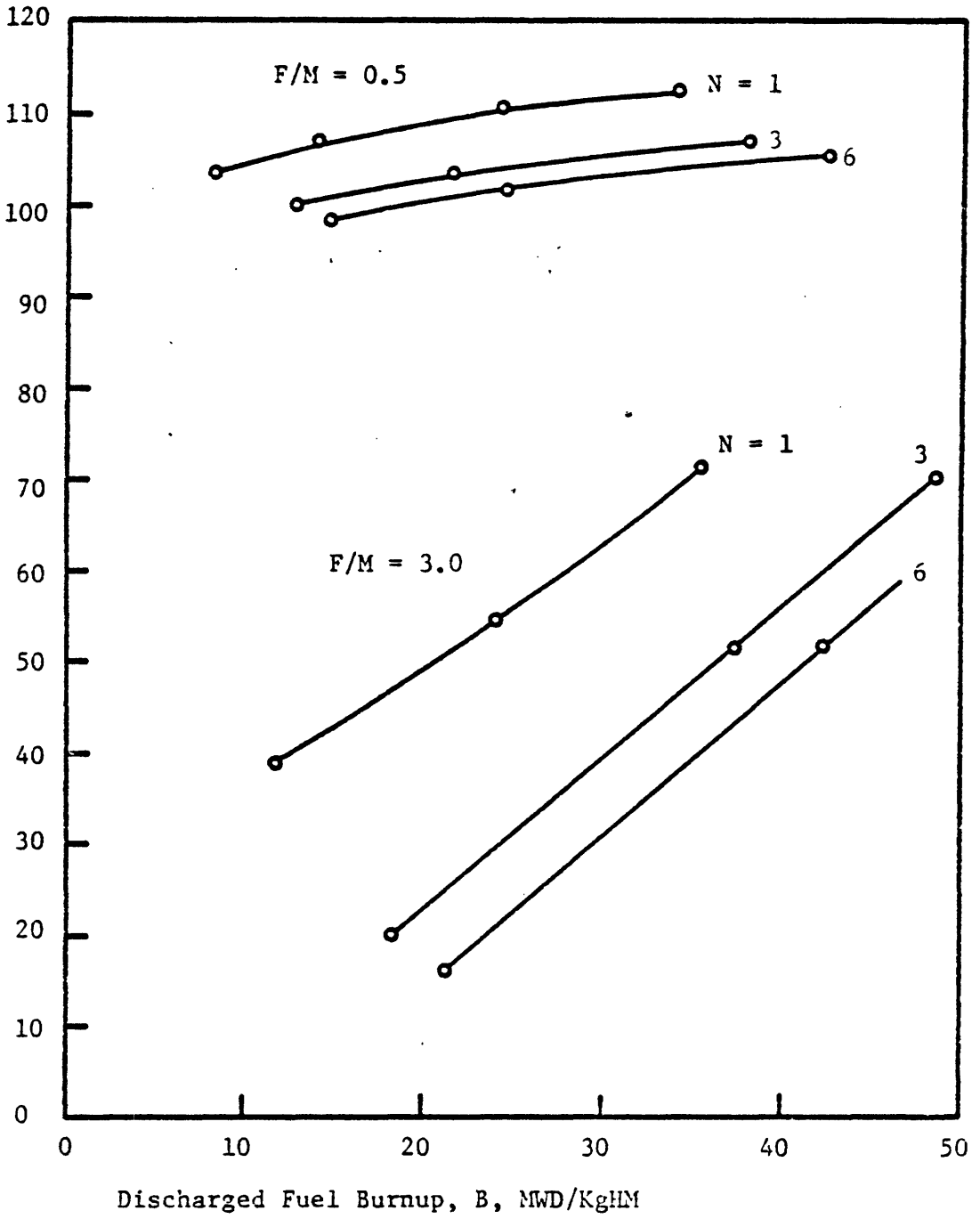

Figure 4.10 EFFECT OF THE NUMBER OF CORE ZONES FOR THE Pu/UO_2 REACTOR ON THE CONSUMPTION OF NATURAL URANIUM FOR THE U-235/UO_2 : Pu/UO_2 SYSTEM

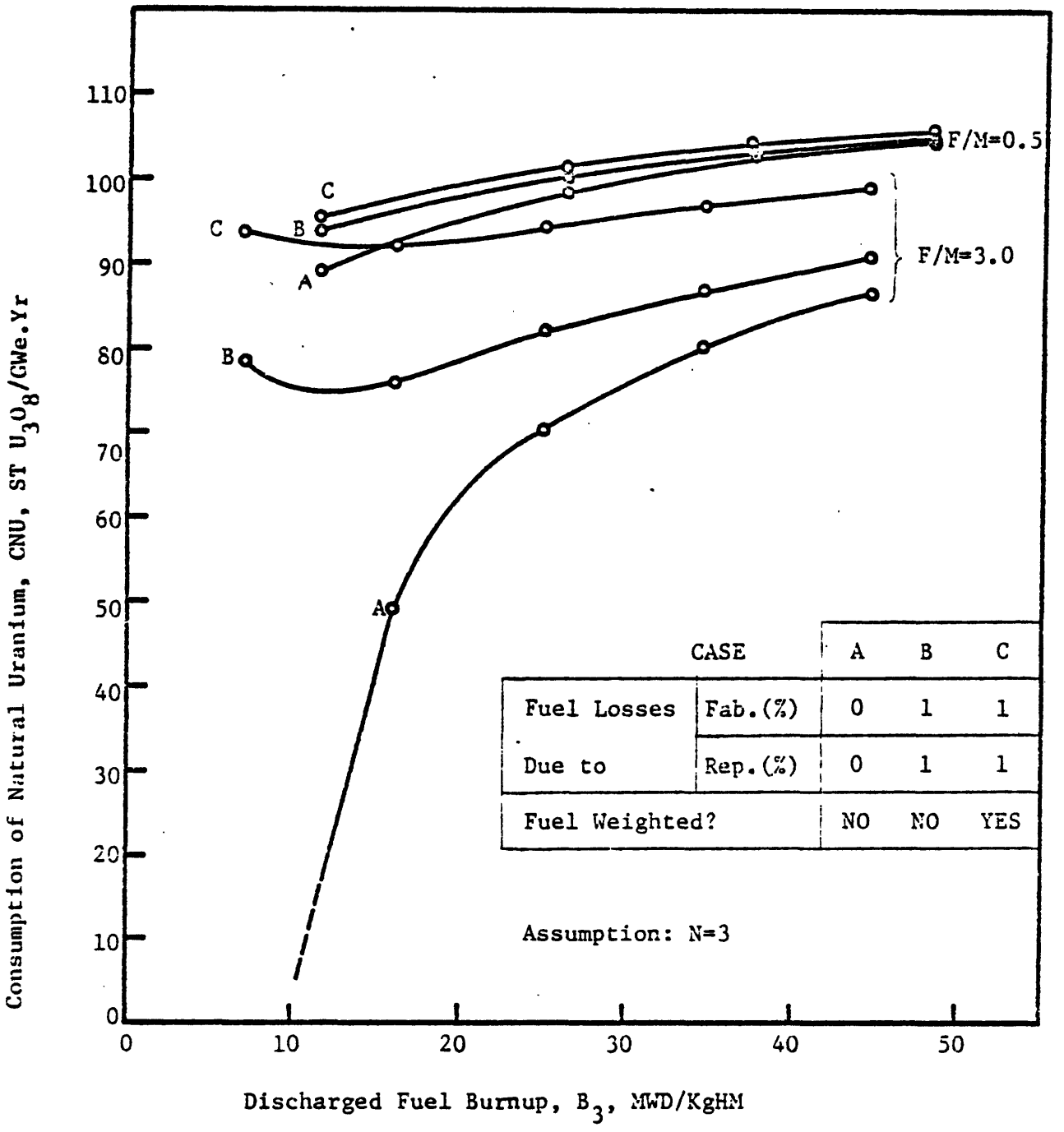

Figure 4.11 EFFECTS OF RE-FABRICATION AND REPROCESSING LOSSES AND ISOTOPIC WEIGHTING ON THE CONSUMPTION OF NATURAL URANIUM FOR THE U-235/UO_2 : Pu/ThO_2 : U-233/ThO_2 SYSTEM OF COUPLED REACTORS

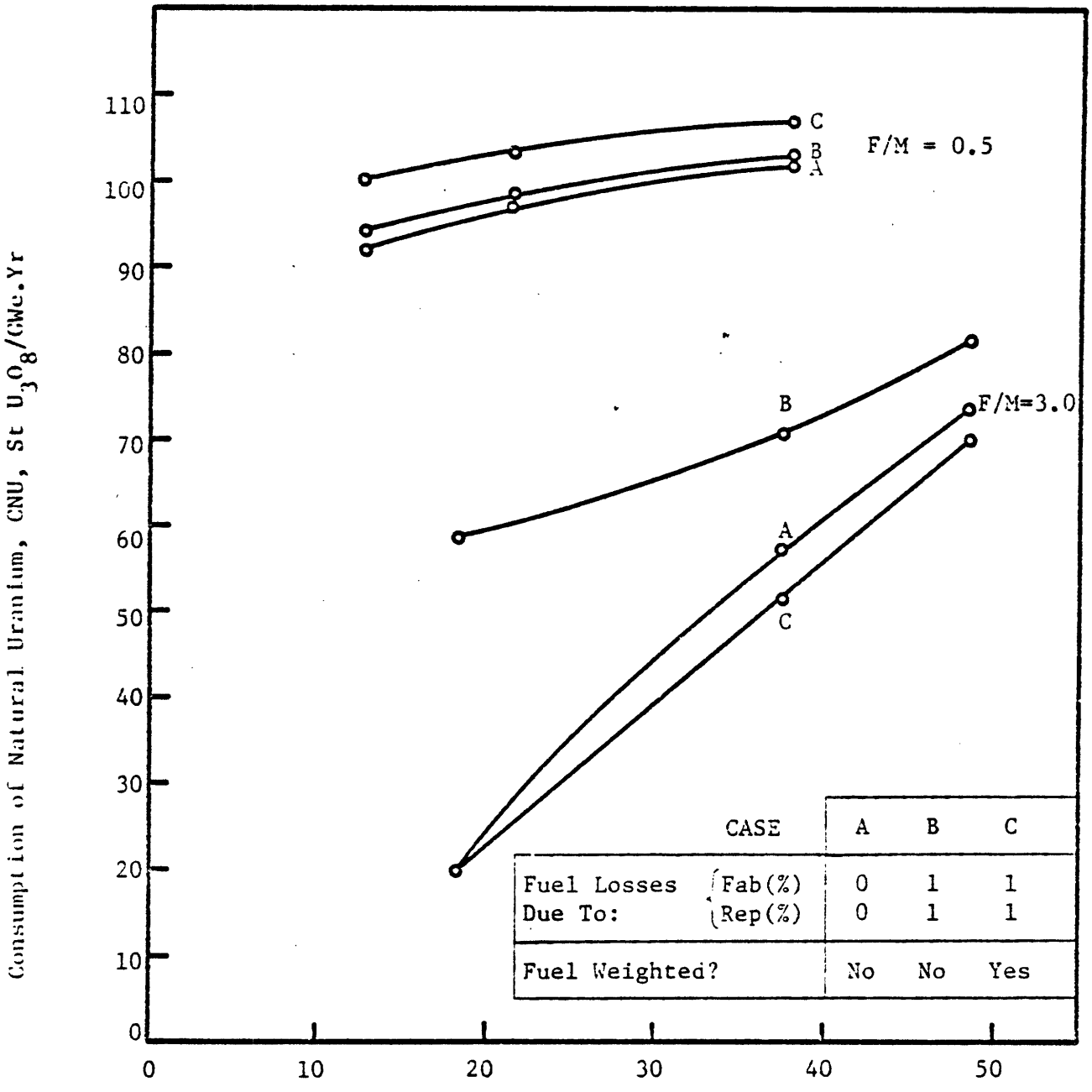

Figure 4.12 EFFECTS OF RE-FABRICATION AND REPROCESSING LOSSES ON THE CONSUMPTION OF NATURAL URANIUM FOR THE U-235/UO_2 : Pu/UO_2 SYSTEM OF COUPLED REACTORS

Fuel weighting for the uranium system may even reduce the CNU at high F/M ratios because in hard spectrum cores the isotopic percentage of fissile plutonium may increase with fuel depletion (Fig. 4.12).

4.6 Fuel Cycle Costs

Results from fuel cycle cost calculations are given in Appendices E and F for the thorium and uranium systems, respectively. Data given in these appendices include indifference values for the bred fissile species at two prices of yellowcake (40 and 100 \$/lb U_3O_8).

Figures 4.13 and 4.14 show that the indifference value of the bred fissile species decreases with burnup, B, since reprocessing and re-fabrication costs increase with B; it also decreases with the F/M ratio because higher fissile inventories are needed. For low discharged fuel burnups, the indifference values for U-233 and Pu-239 may even become negative.

The effect of this variable on the FCC is very small, however. The designations "equivalent U-233" and "equivalent Pu-239" in the captions of Figs. 4.13 and 4.14 indicate that isotopic weighting was used, as defined in Equations (4.7) and (4.8).

Although the indifference values for the bred fissile materials vary widely with F/M, B and N, the fuel cycle cost for each system is rather insensitive to these parameters, varying less than 1% for the thorium system and less than 6% for the uranium system (Table 4.6). The underlying cause for this behavior of the FCC is the small amount of plutonium produced in the standard U-235/UO_2 core (only 20% of the initial mass of

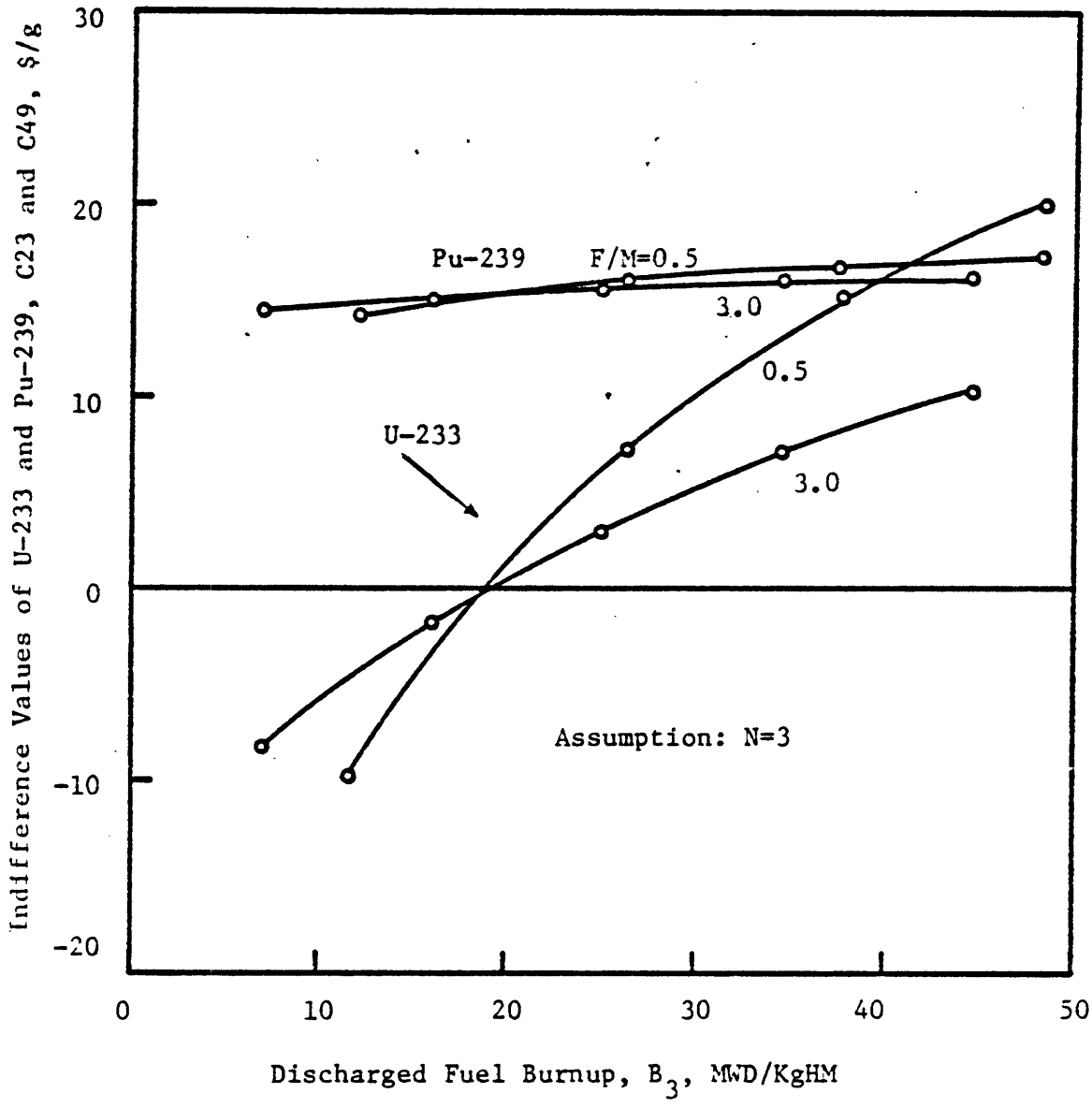

Figure 4.13 INDIFFERENCE VALUES OF EQUIVALENT U-233 AND Pu-239 FOR THE U-235/UO_2 : Pu/ThO_2 : U-233/ThO_2 SYSTEM AS A FUNCTION OF THE DISCHARGED FUEL BURNUP FOR THE U-233/ThO_2 CORE

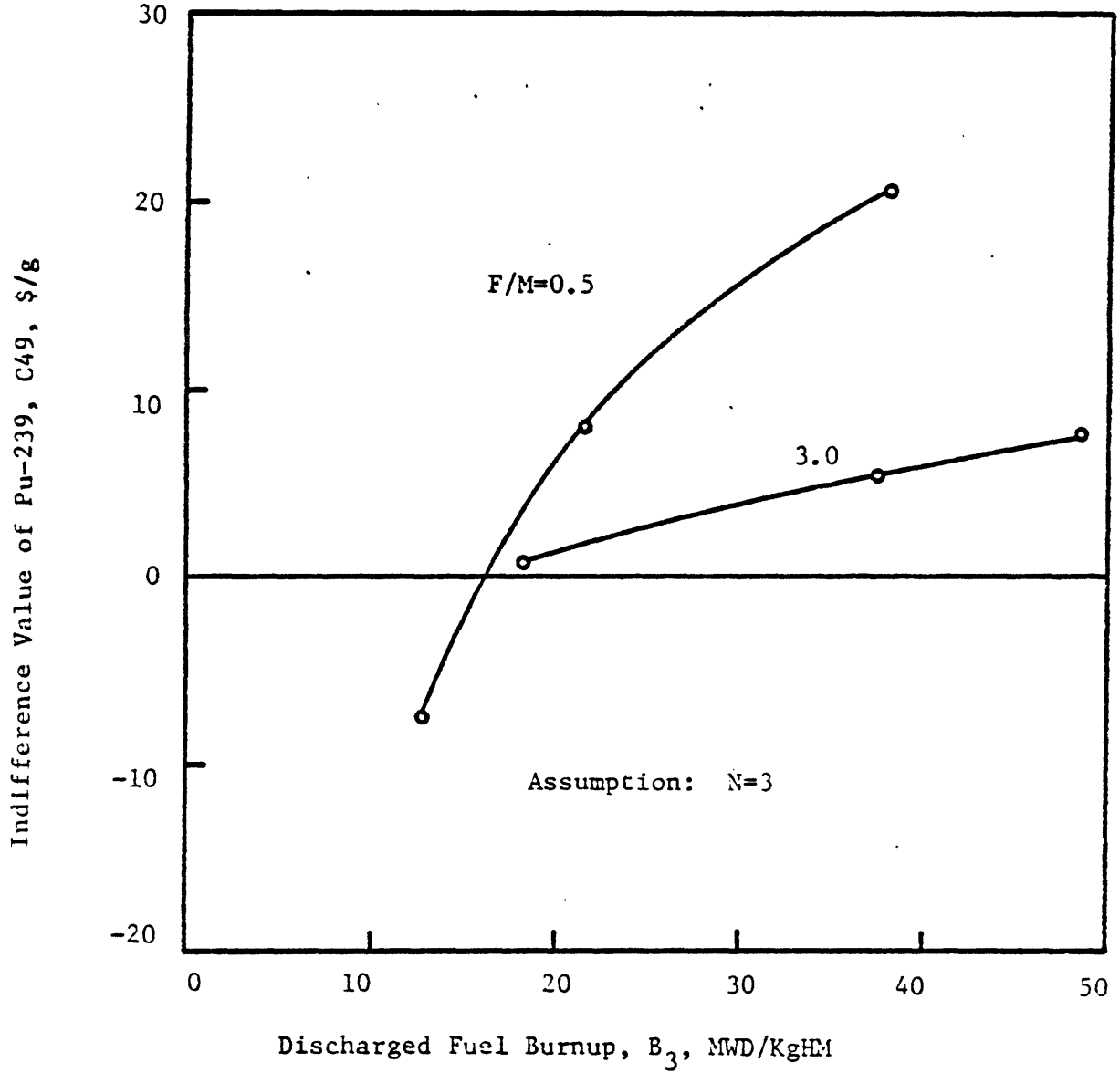

Figure 4.14 INDIFFERENCE VALUE OF EQUIVALENT Pu-239 FOR THE U-235/UO_2 : Pu/UO_2 SYSTEM AS A FUNCTION OF THE DISCHARGED FUEL BURNUP FOR THE Pu/UO_2 CORE

TABLE 4.6

FUEL CYCLE COSTS: RANGE OF VARIATION

Ore Price ($/lb U_3O_8)	Fuel Cycle Cost, mill/kwhre		
	$U\text{-}235/UO_2$ with only U - Recycle	$U\text{-}235/UO_2$: Pu/ThO_2: $U\text{-}233/ThO_2$ System	$U\text{-}235/UO_2$: Pu/UO_2 System
40	7.08	6.90 - 6.95	6.83 - 7.25
100	12.07	11.64 - 11.71	11.51 - 12.13

U-235). In addition, because of the highly inflationary environment assumed (discount rate = 10.25% yr^{-1}), the present worth factor for the discharged plutonium is very small.

The fuel cycle cost is very sensitive to the price of yellowcake (Table 4.6), since this term affects the dominant U-235/UO_2 core directly.

Although the fuel cycle cost appears to be rather insensitive to the parameters F/M, B and N and also to the type of system, it constitutes less than 50% of the generation cost of electricity. Since expenses due to fixed costs increase as the number of refuelings per calendar year increases, low discharged fuel burnups and/or high values for N can be very expensive. As an example, let us assume that:

$$e_b = \frac{C}{L} + e_f \tag{4.9}$$

$$e_s = e_b L + e_r(1 - L) \tag{4.10}$$

and:

Assume the specific numerical values $e_{bo} = 4\ e_{fo}$; $e_r = 1.5\ e_{bo}$; $e_{fo} = 7.08$ mill/KWhre, $L_o = 0.75$

where

e_f, e_b, e_s and e_r are, in turn, the fuel cycle, station busbar (or generation), system production and replacement cost of electricity (mill/KWhre)

C = fixed costs (capital plus O & M)

L = capacity factor

subscript o refers to the standard case: 2.75 w/o U-235/UO_2 (F/M = 0.5, B = 33 MWD/KgHm, N = 3).

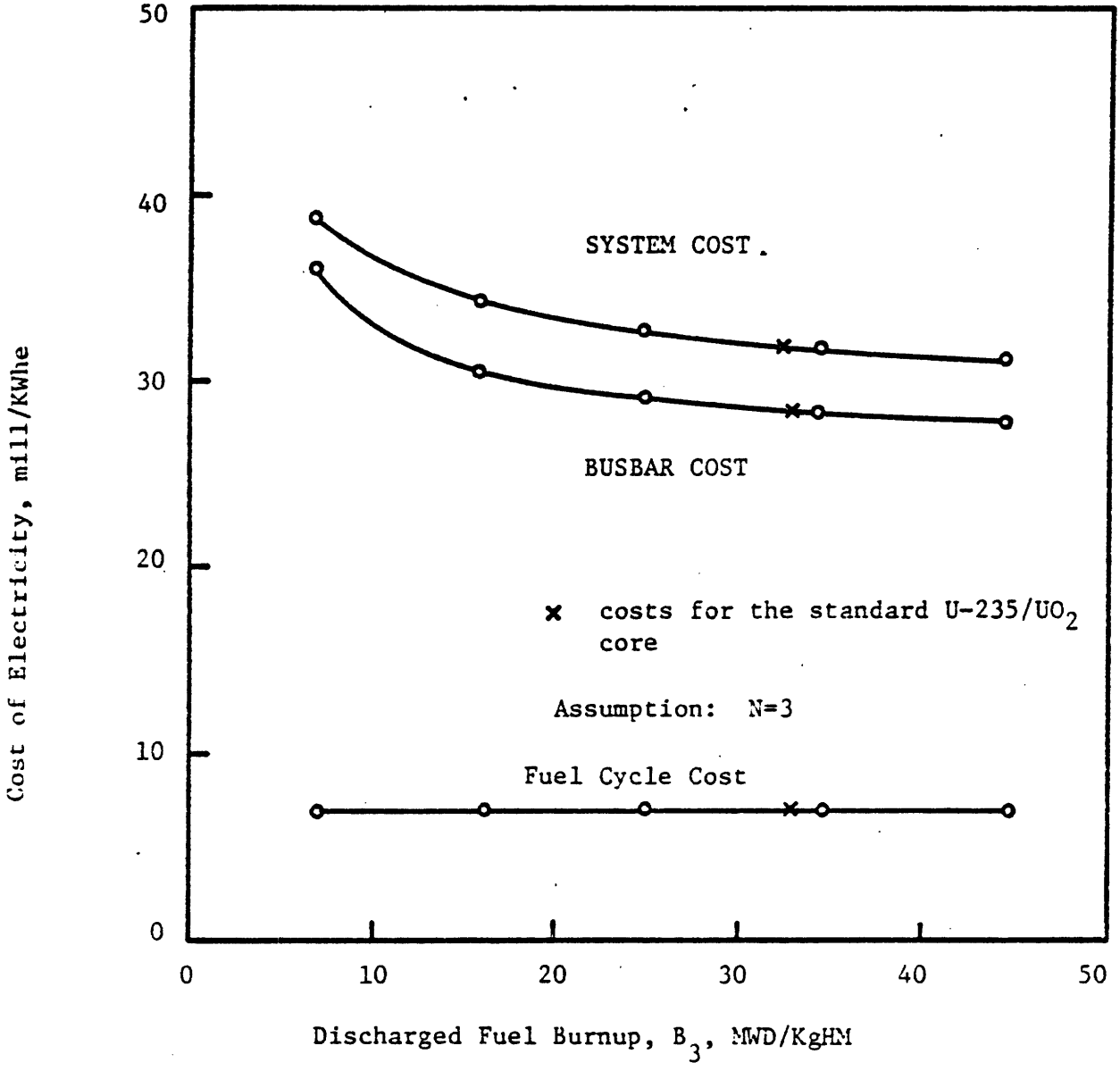

Figure 4.15 FUEL CYCLE, STATION BUSBAR AND SYSTEM PRODUCTION COST OF ELECTRICITY FOR THE U-233/ThO_2 FUELED CORE AT F/M=3.0

Figure 4.15 shows these costs as a function of B for the U-233/ThO_2-fueled core (at F/M = 3.0 and N = 3). Compared to the standard case, e_b and e_s are 17% higher at B = 10 MWD/KgHm than their respective values at B = 33 MWD/KgHm. Thus there will be no incentive for a utility to adopt short fuel cycles merely to achieve improved ore utilization. The same curves are also representative of Pu/UO_2 cores, since e_f is the same.

4.7 Reactivity Coefficients

The calculated multiplication factor decreases monotonically with the moderator void content for both U-233/ThO_2 and Pu/UO_2-fueled cores in the full range of F/M ratios studied ($0.5 \leq F/M \leq 3.0$) at beginning of cycle and with no soluble poison in the coolant (Fig. 4.16 and Table 4.7).

For **reactors** with relatively thermal spectra (F/M = 0.5) the moderator void reactivity coefficient for Pu/UO_2 is more negative than for U-233/ThO_2 (Table 4.7), consistent with the fact that the reload fissile enrichment for the latter fuel is less sensitive to the F/M ratio. The opposite is true for epithermal lattices.

Because of the Doppler effect in the fertile materials, the fuel temperature-reactivity coefficient is always negative (Table 4.7).

Although moderator void-reactivity coefficients for tight pitch cores fueled with Pu/UO_2 are calculated to be slightly negative with LASER, other computer programs may yield different results. For example, for F/M = 2.0, ε = 8.67 w/o Pu/UO_2, at BOC with no soluble poison (and without Xe-135 or Sm-149), the average void-reactivity coefficient (over the range 0 to 20% moderator void content) calculated by different codes is given in Table 4.8. We see that the result from LASER agrees in sign and in order of magnitude with fast reactor-physics methods (SPHINX + ANISN).

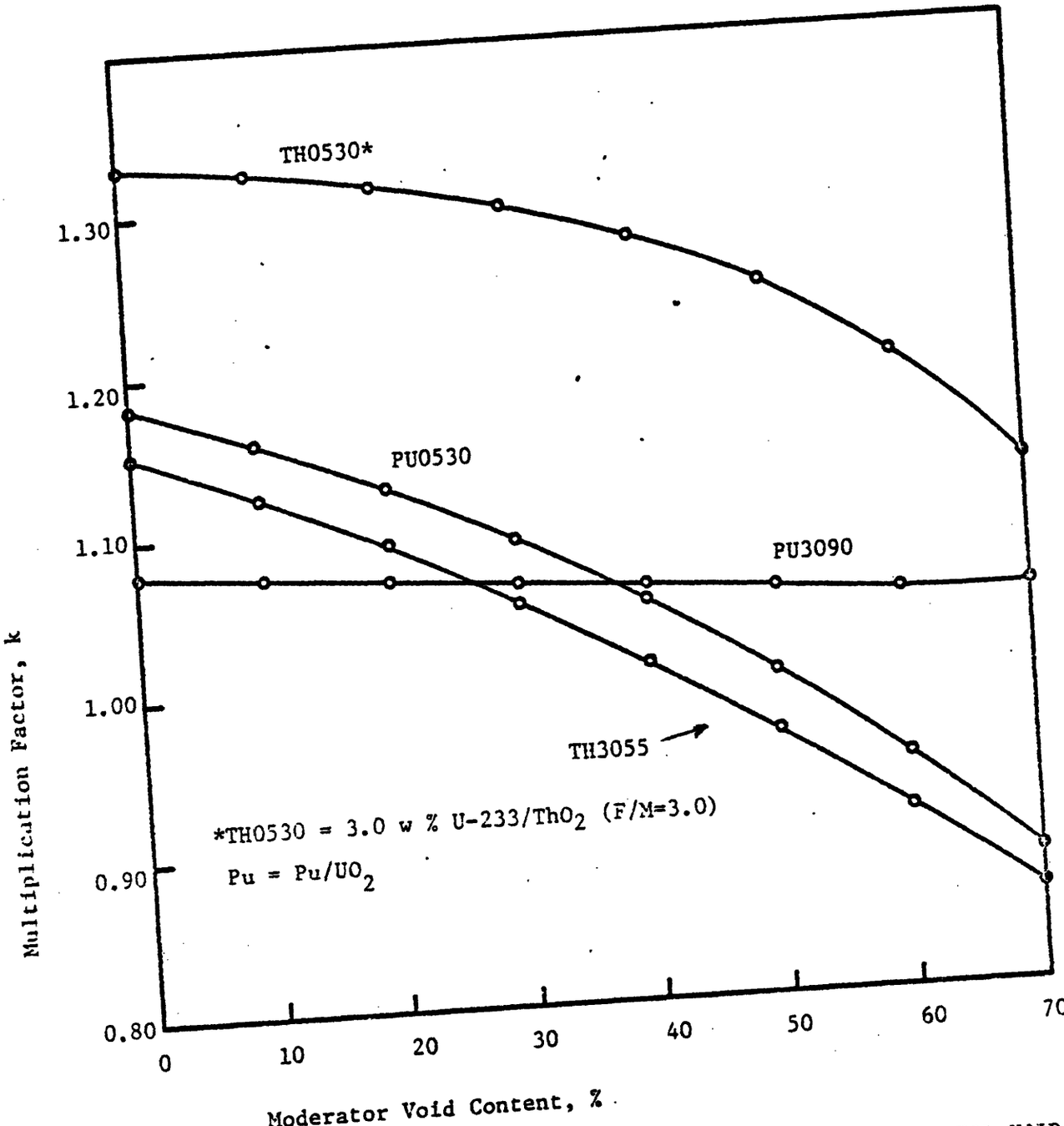

Figure 4.16 MULTIPLICATION FACTOR AS A FUNCTION OF MODERATOR VOID FRACTION (AT BEGINNING OF CYCLE WITH NO SOLUBLE POISON IN THE COOLANT)

TABLE 4.7

MODERATOR VOID AND FUEL TEMPERATURE REACTIVITY COEFFICIENTS

Fuel	MULTIPLICATION FACTOR k FOR $U\text{-}233/ThO_2$		Pu/UO_2	
F/M	0.5	3.0	0.5	3.0
ε w/o	3.0	5.5	3.0	9.0
Moderator Void (%)				
0	1.3303	1.1532	1.1837	1.0777
10	1.3229	1.1226	1.1568	1.0729
20	1.3120	1.0888	1.1258	1.0678
30	1.2965	1.0514	1.0899	1.0624
40	1.2741	1.0098	1.0486	1.0569
50	1.2422	0.9636	1.0005	1.0518
60	1.1954	0.9126	0.9445	1.0479
70	1.1233	0.8570	0.8799	1.0472
Moderator Void* Reactivity Coefficient (Δk/% Void)	-2.8×10^{-3}	-4.2×10^{-3}	-4.3×10^{-3}	-4.7×10^{-4}
Fuel Temperature (°F)				
900	1.3352	1.1627		
1000	1.3327	1.1579	1.1874	1.0801
1100	1.3303	1.1532	1.1855	1.0789
1200	1.3280	1.1488	1.1837	1.0777
1300	1.3258	1.1445	1.1819	1.0766
1400	1.3236	1.1403	1.1802	1.0755
1500	1.3215	1.1363	1.1786	1.0744
1600	1.3194	1.1323	1.1770	1.0734
1700			1.1754	1.0724
Fuel Temperature** Reactivity Coefficient (Δk/°F)	-2.2×10^{-5}	-4.3×10^{-5}	-1.7×10^{-5}	-1.1×10^{-5}

* range: 0 - 70% void
** range: 900 - 1700 °F

TABLE 4.8

MODERATOR VOID-REACTIVITY COEFFICIENT
CALCULATED BY DIFFERENT PROGRAMS*

Method	Cross Section Library Based On	$\Delta k/\% \Delta V$
LASER	ENDF/B-II**	-6.2×10^{-4}
SPHINX/ANISN	ENDF/B-IV	-2.8×10^{-4}
HAMMER	ENDF/B-III	$+ 4.4 \times 10^{-4}$
EPRI-LEOPARD	ENDF/B-IV	$+ 1.6 \times 10^{-3}$

* 8.67 w/o Pu/UO_2 at F/M = 2.0 with no soluble poison in the moderator, and neither Xe-135 nor Sm-149 in the fuel

** Based on ENDF/B-II only for the thermal cross section of plutonium, and for other nuclides based on the original LASER cross-section library (see Section 3.3.1)

As we would expect, EPRI-LEOPARD is the worst method (for Pu-bearing fuels).

The main problem seems to be the treatment of the low-lying 1.056 eV Pu-240 resonance. Using HAMMER (S-5), we investigated the isotopic effect on the void coefficient and found that only when Pu-240 is omitted does the HAMMER void coefficient become negative. Based on the adjoint flux for this cell calculated with SPHINX/ANISN we found that as moderator density is reduced neutrons otherwise captured in the lowest Pu-240 resonance increase in worth, whereas the bulk of the epithermal neutrons above 20 eV decrease in worth as the spectrum hardens. Extreme care in modeling, and calculational precision are called for in order to properly account for the difference in these counterbalancing tendencies.

4.8 Thermal-Hydraulic, Mechanical and other Practical Considerations

Rod-to-rod spacings as small as 30 mils would be required to obtain high F/M ratios. Even with the shorter cores envisioned, the primary pumping power would have to be as much as doubled to compensate for increased pressure losses in the lower plenum and in the reactor core itself, thereby decreasing the thermodynamic efficiency by as much as 0.6%. Alternatively, a higher temperature rise across the core could be employed, but for constant outlet temperature this would reduce the mean moderator temperature, and penalize the efficiency by a larger increment.

If feasible, wire wrapping (as in the LMFBR) would reduce the pressure drop in the core, as compared to the type of spacers used in the tight-pitch LWBR assemblies (L-1). As in the LWBR, half of the fuel elements in each assembly would probably have to be attached to its top and the other half to its bottom to provide passages for the coolant.

Calculations using the WABCORE program (B-7) have indicated that the MDNBR would not constitute a limiting factor for the deployment of these types of cores, in terms of their steady state performance, when the total reactor coolant flow is kept the same as for the standard Maine Yankee PWR (Table 4.1) (Although transient and accident thermal-hydraulics may still prove insurmountable).

Another potential problem for tight pitch cores is the control of reactivity. Boron, for example, while being an excellent thermal absorber, is a very poor absorber in epithermal spectra. At BOC, the concentration of boron needed for criticality is about 1,200 ppm at F/M = 0.5 and as large as 10,000 ppm at F/M = 1.68 for U-233/ThO_2-fueled cores. We should recall that at 130°F, the limiting concentration (solubility) of $H_2B\ O_3$ in water is 20,000 ppm of boron.

Conventional rod control would probably require rod followers, and all other control guide positions should be filled with rods of inert or fertile materials to avoid decreasing the lattice average F/M (for a non-lattice fraction equal to 12%, control guide and inter-assembly water would reduce the F/M ratio from 2.57 to 1.68, for example). On the other hand, control guide and inter-assembly water do not appear to constitute a major problem for tight cores as regards power peaking. Two-dimensional power-distribution studies for a hexagonal assembly (F/M = 2.5, 2.57 and 1.68 for a fuel cell, the fuel cell with wire-wrap spacers, and for the whole assembly including control guide and inter-assembly water) using PDQ-7 (C-5) have shown that the peaking power is only 1.10 (near inter-assembly positions).

As a last observation, although we have studied separate reactors, when the same pitch is involved the calculations could also refer to separate zones or even dispersed assemblies in the same core. Different pins in the same assembly, however, could give results intermediate to the all-of-one-kind systems.

4.9 Uncertainties in the Calculations

Based on the results of Table 3.4 we have estimated that given a 10% overestimation in the L-factors for each of the heavy nuclides (at F/M = 3.0) the consumption of natural uranium (CNU) would be underestimated by only 2% for the thorium system, and by less than 15% for the uranium system. A 10% underestimation in the absorption cross section of the lumped fission product (again, a conservative upper limit on the likely error) could lead to an underestimation of 1% in the CNU for the thorium system and less than 12% for the uranium system. The smaller error consequences for the thorium system stem from the small effect of the U-233/ThO_2 core on the CNU for this system.

4.10 Conclusions

Although Pu/UO_2 requires higher fissile inventories than U-233/ThO_2 for tight pitch cores, it produces higher conversion ratios, due mainly to the much larger contribution to fast fission by U-238 (and Pu-240) compared to Th-232.

At steady state, the U-235/UO_2 : Pu/UO_2 system (at F/M = 3.0) can save as much as 60% on ore use rate compared to the same system (conventional recycle) with F/M = 0.5 for the same discharged fuel burnup (33 MWD/KgHM).

On the same basis, the U-235/UO_2 : Pu/ThO_2 : U-233/ThO_2 system saves less than 10% on ore because of the poor performance of the second core in the sequence.

The calculated CNU for these systems is very sensitive to fuel losses and to fuel isotope weighting, especially for high F/M ratios and low discharged fuel burnups when CR is near unity for the tight pitch cores. Errors in the CNU due to errors in the treatment of resonance cross sections and fission products for the tight pitch cores are estimated to total less than 15%.

Many practical questions must be answered before serious consideration can be given to use of tight pitch cores: thermal-hydraulics, mechanical and economical. While moderator void-reactivity coefficients and steady state DNBR are not calculated to be limiting, plant and core redesign to accomodate higher core pressure drops appears an inevitable requirement, and transient/accident limits await a definitive assessment. Fuel cycle cost calculations show that system fuel cycle costs (at the indifference value of bred fissile species) are quite insensitive to the fuel-to-moderator ratio — resulting in low impediments or low incentives depending on one's point of view.

CHAPTER 5

ALTERNATIVE CONCEPTS

5.1 Introduction

In this chapter, we briefly discuss a few other core design concepts that could potentially reduce the consumption of natural uranium ore for LWR's and/or improve other core characteristics. The use of D_2O/H_2O mixtures to harden the neutron spectrum permits one to keep the thermal hydraulic characteristics of the core unchanged and still obtain the same uranium ore savings as for tight-pitch LWR cores (using only H_2O as the moderator). The control of core reactivity by varying the moderator density (variable-fuel-to-moderator volume-ratio reactivity control) is another version of the SSCR concept which, however, does not make use of D_2O to control reactivity. Neutron leakage is an important factor for tight pitch cores since the neutron mean free path increases with F/M; its effect on the consumption of natural uranium for the Pu/UO_2 core in the uranium system analyzed in Chapter 4 is estimated.

Due to its higher thermal conductivity and lower heat capacity, thorium metal stores less energy than UO_2 (or ThO_2), which may be a potential advantage during undercooling transients/accidents. The denatured uranium thorium cycle, compared to other fuel cycles for LWR's, has the advantage of increasing fissile material safeguards by reducing plutonium production while keeping uranium enrichment below a "safe" level. Finally, although from an economic point of view, Zircaloy is better than stainless steel (SS) for typical LWR lattices (F/M = 0.5), this advantage decreases for tight pitch cores since the microscopic cross section of SS becomes less than that of Zr.

5.2 Use of D_2O in the Moderator

Heavy water has a moderating power ($\xi\Sigma_s$) about eight times smaller than light water. This fact permits achievement of very hard neutron spectra by properly choosing the proportion of D_2O to H_2O in the moderator without having to increase the F/M ratio by spacing fuel pins closer together. Thermal-hydraulic and mechanical-design characteristics of the core can then be kept essentially the same as for today's standard LWR cores. This strategy would completely bypass questions as to the satisfactory performance of tight pitch cores.during off-normal conditions.

Figure 5.1 compares the consumption of natural uranium for the thorium system analyzed in Chapter 4, for a tight-pitch (F/M = 3.0) U-233/ThO_2-fueled core moderated by light water with the CNU for a standard-pitch (F/M = 0.5) U-233/ThO_2-fueled core moderated by D_2O. The core moderated by D_2O produces higher conversion ratios but because of the harder neutron spectrum, needs higher fuel enrichments than the core moderated by H_2O. Consequently, the D_2O-moderated core consumes less fissile material compared to the H_2O-moderated core, as reflected in the curves of Fig. 5.1. By properly choosing the right moderator composition (H_2O to D_2O ratio) and keeping F/M=0.5, the CNU could be matched to the CNU for the tight-pitch case with H_2O only. Since, for epithermal spectra, absorption in H_2O becomes essentially negligible, similar fuel enrichments and conversion ratios would be obtained for the two cases.

Even though by the use of mixtures of H_2O/D_2O as moderator the thermal-hydraulic and mechanical characteristic of the core could be kept essentially invariant, capital and operational expenses would be increased to cover purchase of the initial D_2O inventory and to replenish it due to

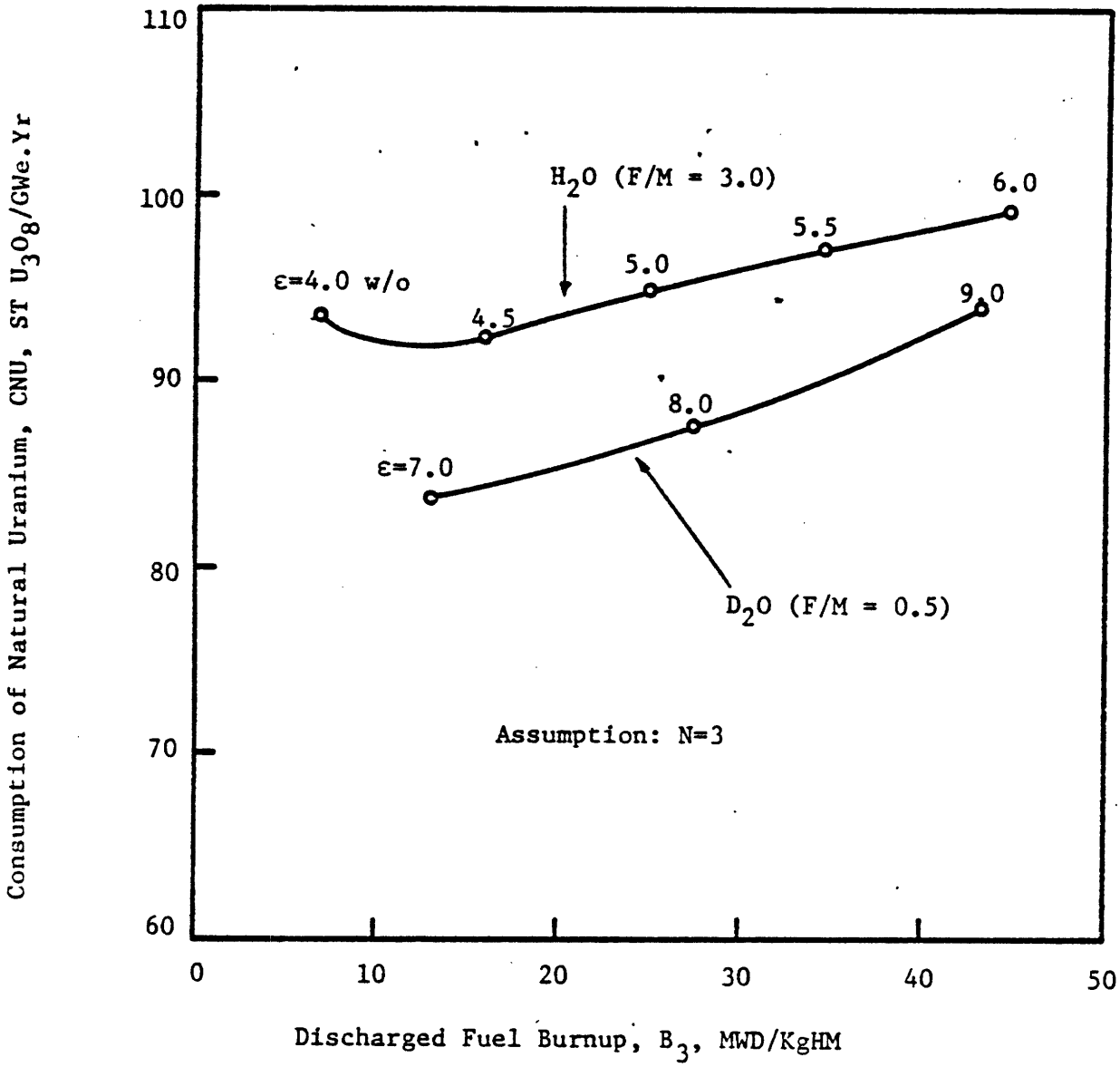

Figure 5.1 DEPENDENCE OF THE CONSUMPTION OF NATURAL URANIUM FOR THE U-235/UO_2 : Pu/ThO_2 : U-233/ThO_2 SYSTEM ON THE TYPE OF MODERATOR USED IN THE U-233/ThO_2 CORE

day-by-day losses of D_2O. Another major problem would be cooling the core during a loss-of-coolant-accident since, due to the high fuel enrichments used and low F/M ratios, pure H_2O could not be used to cool the core, otherwise a large positive-reactivity insertion would occur.

The approach discussed in this section also applies to Pu/UO_2 fueled cores.

5.3 Variable Fuel-to-Moderator Reactivity Control

In the SSCR (E-5, S-1) concept, reactivity is controlled by varying the percentage of D_2O in the coolant. At BOC when the reactivity (ρ) is maximum, the amount of D_2O is made maximum, such that a very epithermal neutron spectrum is produced which decreases k, since the spectrum-averaged absorption cross section of fissile nuclides is decreased. In addition, when the neutron spectrum is hardened the absorption cross section of fertile nuclides decreases less than for other nuclides present which contributes to increased CR. As fuel is burned, D_2O is gradually replaced by H_2O to keep the core critical by thermalizing the neutron spectrum. The majority of the neutrons that would otherwise be lost to parasitic absorptions in the control materials are then absorbed in the fertile material since the absorption in D_2O is negligible. Because CR is increased in this concept, relative to conventional LWR's, the reload fissile inventory is decreased.

Since neutron absorption in D_2O is always very small, the control of reactivity by varying the effective F/M ratio in the core is essentially equivalent to use of the SSCR concept. In a BWR, F/M could be increased by increasing the void fraction in the moderator; in a PWR, no concept

for achieving this objective which is both fail-safe and economically practicable has yet been proposed.

The potential benefits of the Variable Fuel-to-Moderator Control Reactor (VFMCR) were examined in the present study (without regard to the specific mechanism employed to effect the variation) using the EPRI-LEOPARD program.

The example studied was the 3-batch Maine-Yankee PWR (Appendix A) in which F/M was varied nearly continuously over the equilibrium cycle (actually in seven finite increments). Figure 5.2 shows that relative to the standard type of reactivity control (soluble poison) the VFMCR increases the reactivity-limited burnup from 11 to 13 MWD/KgHM per cycle (using the same reload fuel enrichment). In these runs the F/M ratio of all in-core fuel was the same and adjusted to keep core k = 1.0 at all times; at beginning-of-cycle F/M=0.796, and at end-of-cycle F/M=0.513 (standard case). Hence there is no end-of-cycle reactivity penalty due to retained voids in partially burned fuel assemblies.

Thus there is some incentive for use of variable F/M control if a practical means for its implementation can be found. For a once-through fuel cycle,ore savings of on the order of 20% or more can be realized. This type of control may be even more attractive for tight-pitch recycle-mode cores, since they otherwise require soluble boron concentrations which are probably impractically high. Also, unlike the once-through cores (where one has to be concerned with overmoderation at the wet end of the range, F/M < 0.5) the tight pitch cores are always undermoderated.

Another strategy examined was the adjustment of batch F/M after each refueling shutdown. This was found to be ineffective (it is important to note that here soluble poison is used to control reactivity). The example

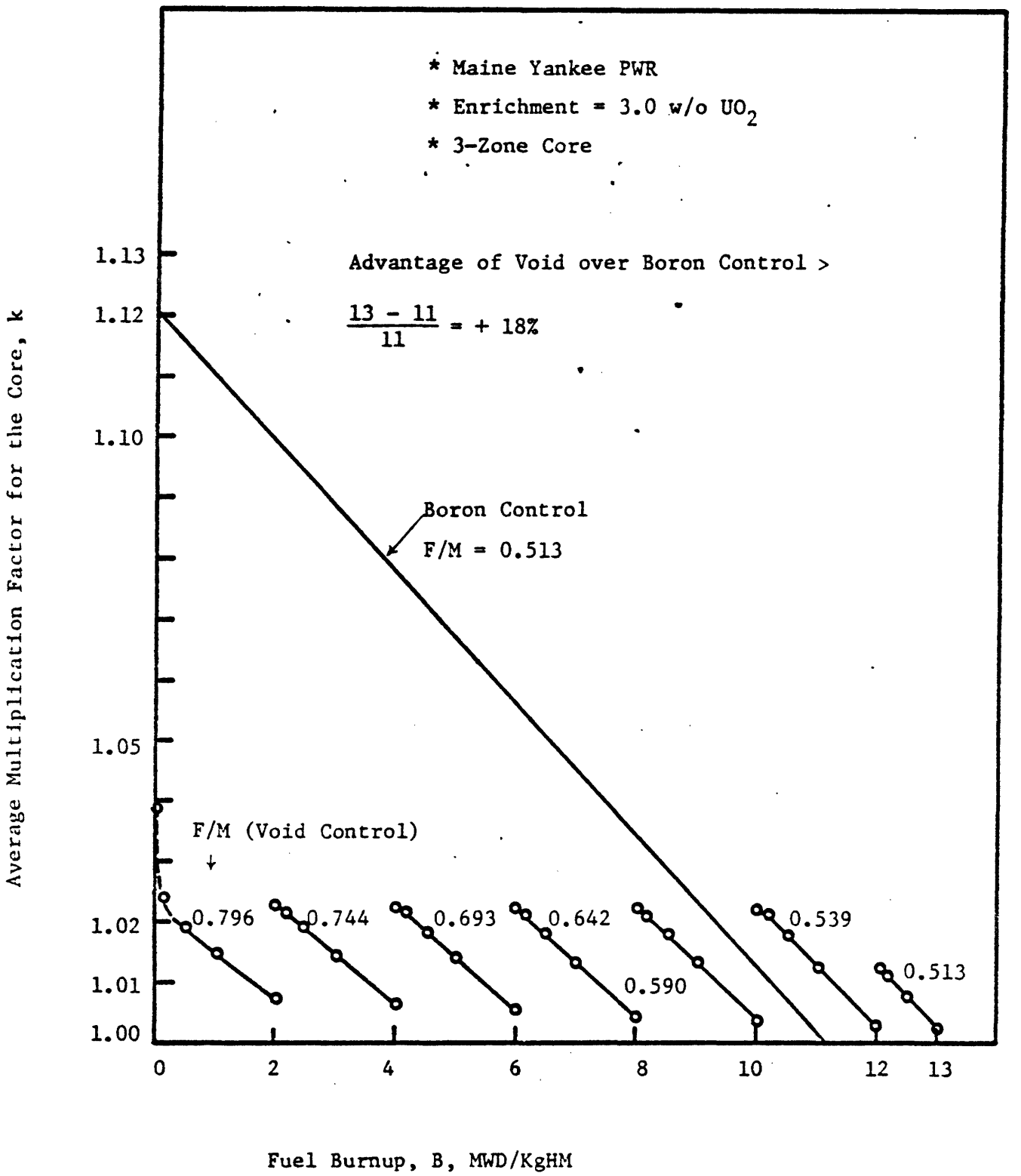

Figure 5.2 EFFECT OF VARIABLE FUEL-TO-MODERATOR REACTIVITY CONTROL ON CYCLE BURNUP

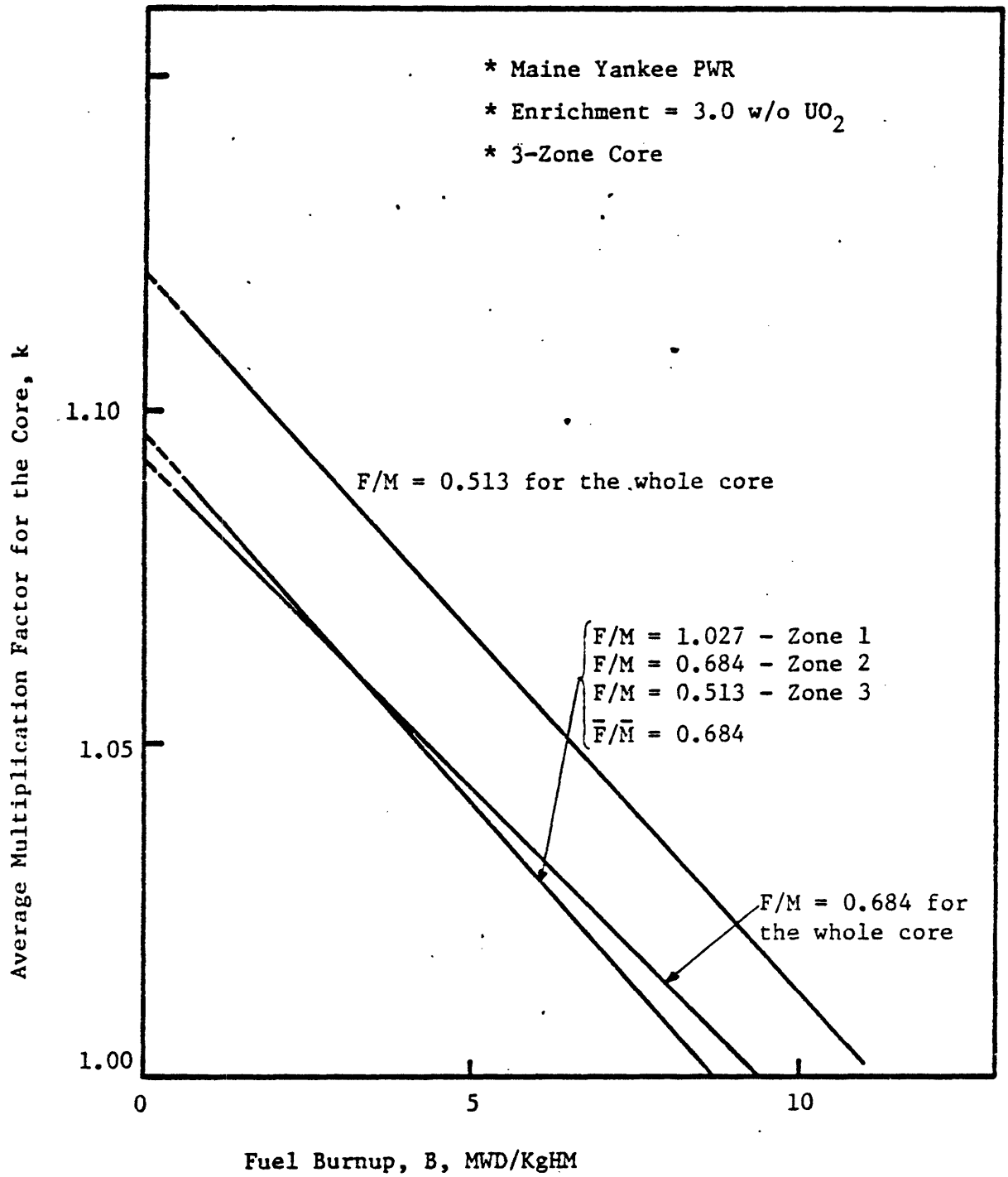

Figure 5.3 EFFECT OF ADJUSTMENT OF BATCH F/M RATIO AFTER EACH REFUELING SHUTDOWN ON THE AVERAGE CYCLE BURNUP

studied was again the 3-batch Maine Yankee core in which reload fuel had a F/M = 1.027, successively adjusted to 0.684 and 0.513 at 1/3 and 2/3 of burnup respectively. For this example and a once-through fuel cycle, the achievable reactivity-limited burnup was actually decreased relative to fuel having the same reload enrichment and burned at F/M=0.513 over its entire residence time in the core (8.7 vs. 11 MWD/KgHM (Fig. 5.3)). This is attributed in part to the fact that at the end of any equilibrium cycle the average F/M of the three batches involved is higher than 0.513 and hence a reactivity loss is sustained. If fuel having F/M=0.685 is compared to the variable F/M case, it is found that the reactivity limited burnups are closer (Fig. 5.3). Thus it is concluded that frequent F/M adjustment is needed if any major benefit is to be realized. We should note that our analysis here has not been very profound, and that a detailed evaluation of the variable F/M concept for once-through PWRs is presently underway (R-1) - preliminary results indicate an ore savings of less than 5%.

5.4 Reduced Neutron Leakage

Figure 5.4 shows how neutron leakage from the second core in the U-235/UO_2 : Pu/UO_2 system of coupled reactors analyzed in Chapter 4 affects the consumption of natural uranium for this system. Because the mean free path for the average neutron in the core increases with F/M, we see in this figure that ore savings due to reduced neutron leakage increases dramatically with F/M, diminishing the CNU to near-zero values even for high discharged fuel burnups ($\sim$33 MWD/KgHM).

We should recall here that, although the method used to estimate the effective geometric buckling for these cores, (including water reflector

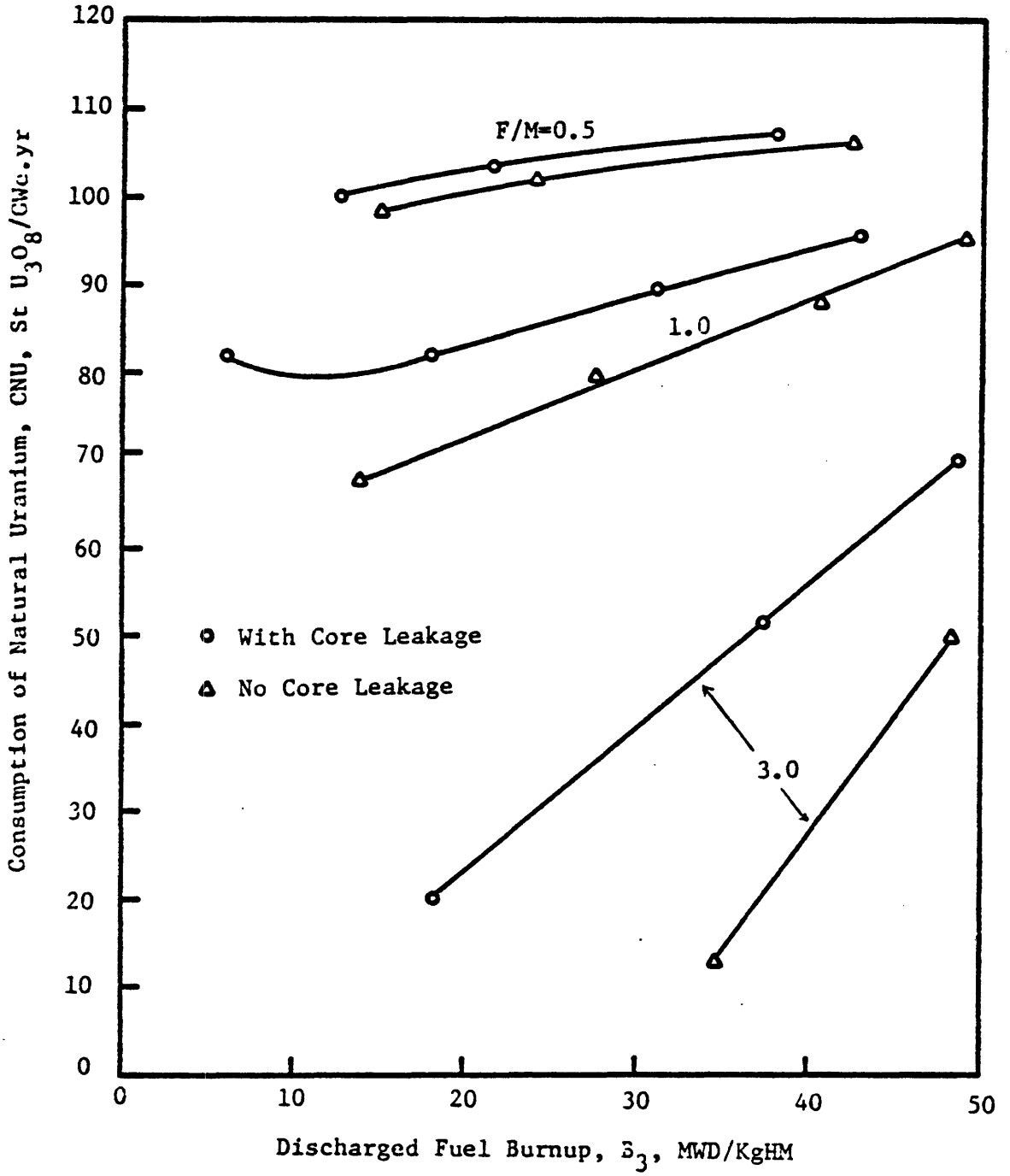

Fig. 5.4 EFFECT OF NEUTRON CORE LEAKAGE FOR THE Pu/UO_2 REACTOR ON THE CONSUMPTION OF NATURAL URANIUM FOR THE $U\text{-}235/UO_2$: Pu/UO_2 SYSTEM

effects) developed in Section 4.3.1, yielded results which agreed very well with R-Z calculations based on PDQ-7, core leakage tends to increase with fuel depletion since the axial neutron flux shape progresses from a cosine towards a flatter profile. (Thus, curves of CNU in Chapter 4 underestimate neutron leakage).

It is also worthwhile to mention here that the main goal of the LWBR project (L-1): to achieve CR > 1.0, was pursued by attacking the problem on three different fronts: 1^{st} neutron leakage was minimized by the use of radial and axial blankets of fertile material (ThO_2); 2nd neutron losses to the control elements were practically eliminated by the use of the movable-geometry seed/blanket concept (which is equivalent to the VFMCR and SSCR concepts); 3rd the low discharged fuel burnup (10 MWD/KgHM) was chosen to minimize the combined effect of neutron losses to fission product materials and fissile material losses due to fuel reprocessing and re-fabrication.

5.5 The Denatured Uranium-Thorium Cycle

The denatured uranium-thorium cycle (F-2, S-6) involves the use of mixtures of uranium-thorium as fuel, such that the maximum uranium enrichment is kept below a safe level (considered to be unsuitable for weapons purposes without further isotopic enrichment); frequently quoted guidelines are 20% U-235 in U-238 and 12% U-233 in U-238. The basic nonproliferation advantage of this cycle is the reduction in the production of chemically separable plutonium fuel.

The use of this type of cycle in LWR's at high F/M ratios could eventually also lead to higher CR's than pure U-235/UO_2 fuel. When Th-232 replaces U-238 the fast fission effect decreases, while the average η

increases (due to the production of U-233). Furthermore, the absorption of neutrons in the fertile nuclides is increased since less resonance self-shielding will occur (although interference effects will increase).

Figure 5.5 (C-6) shows the effect of the denatured U/Th cycle on the consumption of natural uranium for the Maine Yankee core (Appendix A). The CNU is given as a function of the initial fraction (f) of Th-232 in the fertile fuel (Th-232 + U-238). For f=0 we have the standard all-uranium fuel and for f $\sim$ 1.0, the "all" thorium fuel case (mixed with 93 w% enriched uranium in U-235). The discontinuity in the curves of Figure 5.5 at f = 0.5 is due to LEOPARD, which spatially shields only U-238 for f $\leq$ 0.5 and only Th-232 for f > 0.5.

We see from Figure 5.5 that the CNU decreases with f only if uranium (or uranium and plutonium) is recycled, since the larger absorption cross section of Th-232 relative to U-238 in thermal spectra (F/M > 0.5) requires higher fissile enrichments. At f = 0.85, the uranium enrichment is 20 w% (although the overall fuel enrichment is only 3.8 w %), and the production of fissile plutonium is about one third of that for the all uranium case. With uranium and plutonium recycling the CNU(at f = 0.85) would be 28% smaller than the standard case (f=0); the consumption of separative work would be 5% higher and the reload fissile inventory 32% higher.

We are not involved here with an assessment of whether or not a factor of three reduction in plutonium production is a worthwhile objective - some discount this as a substantial improvement in non-proliferability. However these results do establish that imposition of enrichment restrictions on uranium will not necessarily compromise any ore-conserving advantages

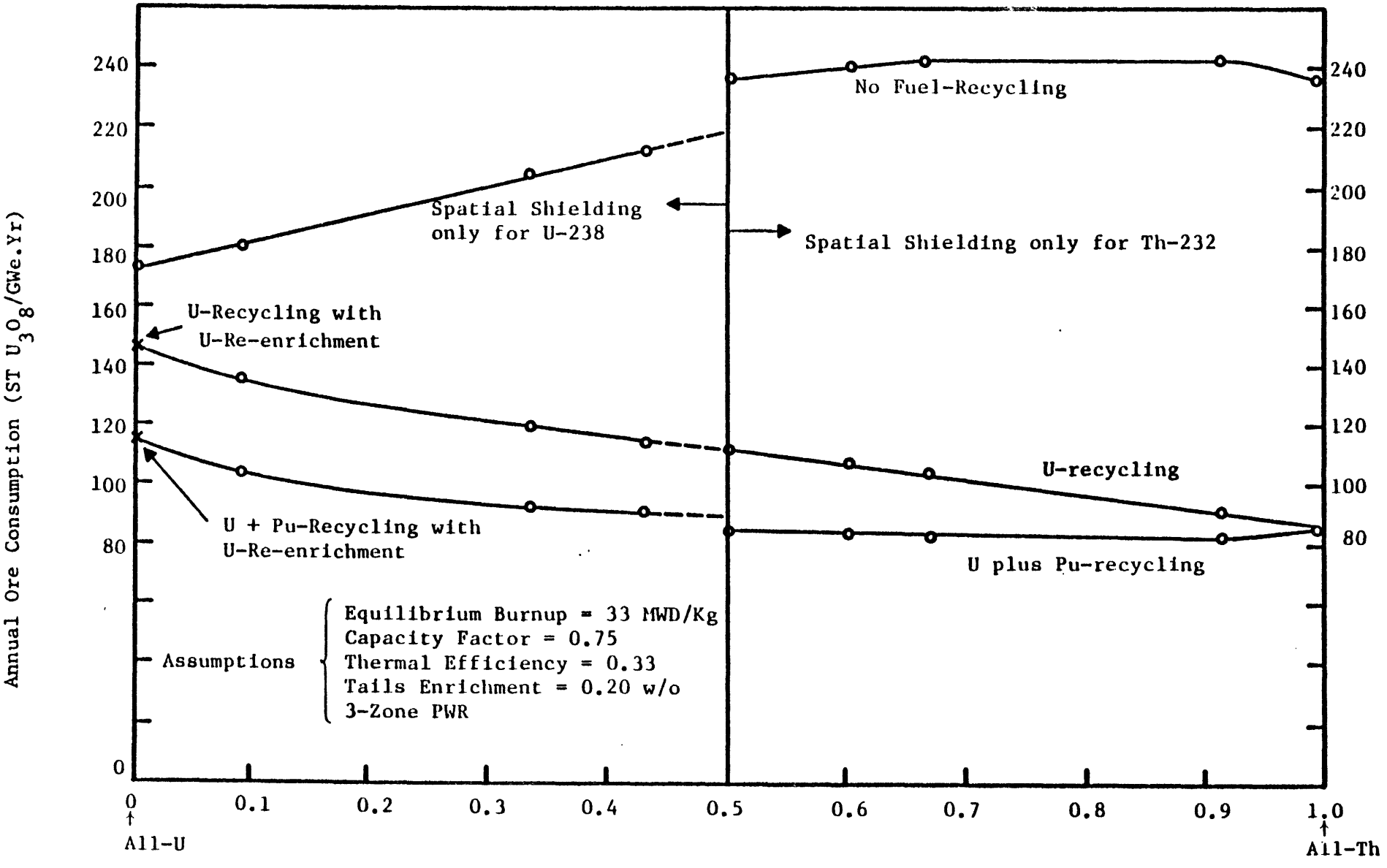

Figure 5.5 ANNUAL ORE CONSUMPTION FOR THE MAINE YANKEE PWR AS A FUNCTION OF THE FRACTION OF THORIUM IN THE FERTILE FUEL *Reference(C-6)

of the thorium cycle. We have compared cycles at normal lattice F/M; since plutonium/uranium fuel improves relative to U-233/thorium as F/M increases, one can safely conclude that denaturing would be even less onerous in tight pitch core applications.

5.6 Use of Metallic Thorium Fuel

The low heat capacity and high thermal conductivity of thorium metal compared to UO_2 and ThO_2 (Table 2.7) indicate the potential for substantially better performance during undercooling transients/accidents.

Consider the average temperature of a fuel rod relative to the average moderator temperature:

$$\overline{\Delta T} = \frac{q'}{2\pi}\left[\frac{1}{4k_f} + \frac{1}{h_g R_f} + \frac{1}{k_c}\ln\frac{R_{co}}{R_{ci}} + \frac{1}{hR_{co}}\right] \qquad (5.1)$$

where:

$\overline{\Delta T}$ = difference between the average temperatures of the fuel and moderator

q' = linear power rating

k_f = thermal conductivity of the fuel

k_c = thermal conductivity of the clad

h_g = thermal conductance of the gap

h = coefficient of heat transfer by convection between the clad and the coolant

R_f = fuel pellet radius

R_{ci} = clad inner radius

R_{co} = clad outer radius

For the standard Maine Yankee core fueled with U-235/UO_2, the first and the second terms in brackets in Eq. (5.1) correspond to 60 and 35% of $\overline{\Delta T}$, respectively. If thorium metal is used instead of UO_2 (assuming other parameters are kept the same) the first term in Eq. (5.1) is decreased by 90% and then:

$$\frac{\overline{\Delta T}_{Th}}{\overline{\Delta T}_{UO_2}} = \frac{k_{UO_2}}{k_{Th}} + \frac{0.7}{1.7} \approx 0.10 + 0.41 = 0.51$$

The stored energy in the fuel is given by:

$$E = \rho\, C_p\, \overline{\Delta T} \qquad (5.2)$$

where:

E = stored energy in the fuel

ρ = fuel density

C_p = heat capacity of the fuel

then:

$$\frac{E_{Th}}{E_{UO_2}} = \frac{(\rho\, C_p)_{Th}}{(\rho\, C_p)_{UO_2}} \times \frac{\overline{\Delta T}_{Th}}{\overline{\Delta T}_{UO_2}} = 0.26$$

Thus the stored energy in thorium metal is only 1/4 of that stored in UO_2 (if the clad/fuel gap could be eliminated for metallic thorium fuel, this number would decrease to 1/20). Consequently, in the early stages of a LOCA when the primary heat source comes from stored energy in the fuel the peak clad temperature will be much lower for Th-metal than for UO_2 fuel. Since the fuel time constant is also proportional to ($\rho\, C_p/k$), Thorium-metal should dump its energy much faster than UO_2,

which would also be an advantage during the very early stages of the blowdown phase when the departing coolant can remove energy conducted to it. A more thorough analysis of all stages of the LOCA, including reload, would be necessary to be sure of the net advantage overall. Also we must analyze other accidents, such as overpower transients, where lower heat capacity might be a disadvantage.

Another potential advantage of Th-metal over ThO_2 (C-1, Z-1) is its 17% higher density (Table 2.7), which produces a higher effective F/M ratio for the same cell geometry (alleviating thermal-hydraulic design problems). The curves of ore utilization for the U-233/ThO_2 core obtained in Chapter 4 should also apply to U-233/Th, by properly re-scaling F/M since the effect of oxygen should not constitute a major factor due to its low moderating power and absorption cross section. Fujita (F-1) has shown this practical equivalence of oxide and metal fueled systems for both uranium and thorium fuels.

5.7 Use of Stainless Steel Instead of Zircaloy as a Cladding Material

Although for typical LWR's, the economic advantages of Zircaloy over stainless steel clad have long since been proven (B-8, A-2), this seems not necessarily true for very epithermal cores, since the main advantage of zircaloy over stainless steel, its much smaller absorption cross section, diminishes with F/M.

Figure 5.6 shows that, for H_2O as moderator, the spectrum-averaged microscopic cross section of SS-316 becomes smaller than that of Zr-2 at F/M $\gtrsim$ 2.5. If D_2O is the moderator, the microscopic cross section of SS-316 is always smaller than for Zr-2 for F/M > 0.5.

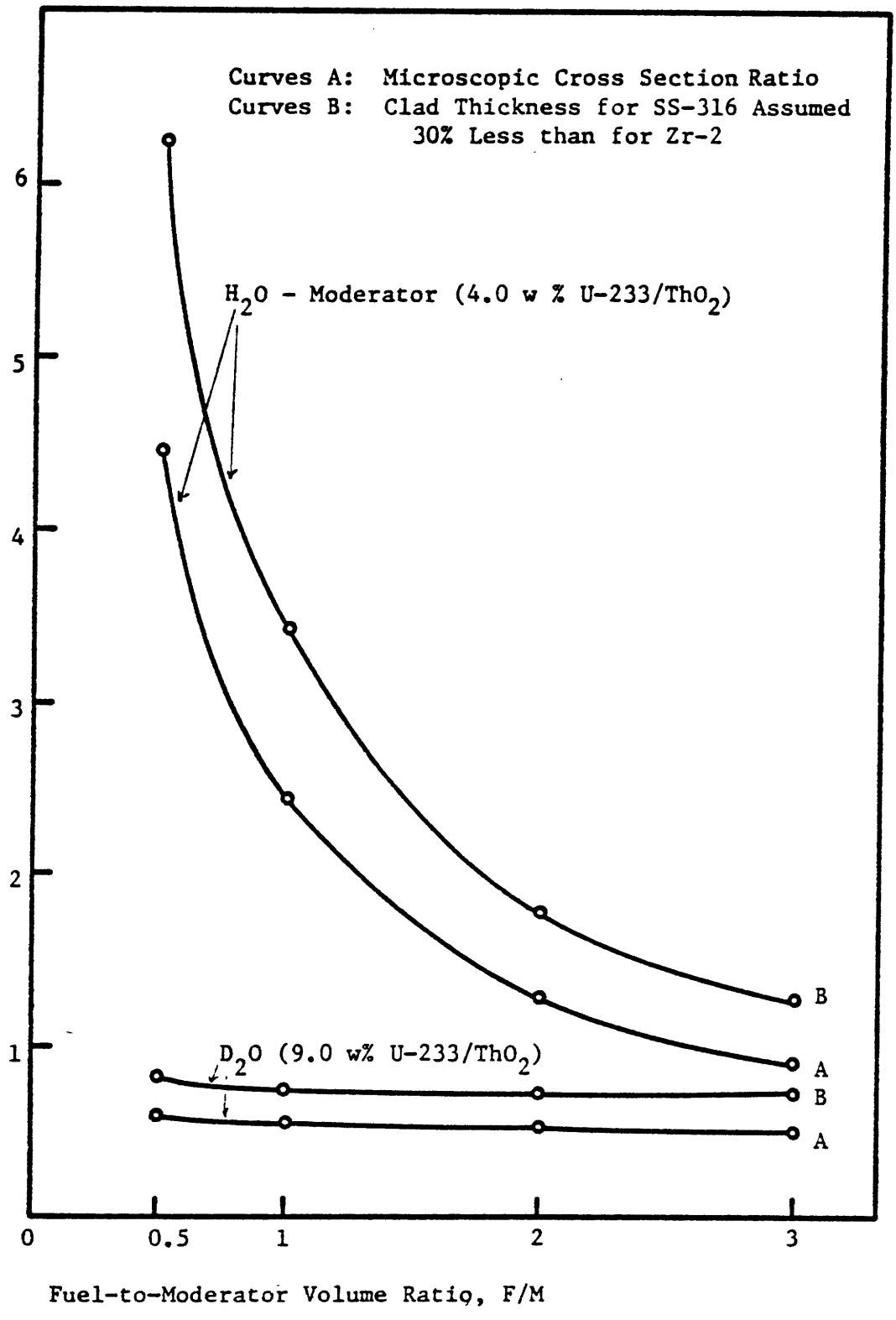

Figure 5.6 RATIO BETWEEN THE ABSORPTION OF NEUTRONS IN SS-316 AND Zr-2 AS A FUNCTION OF THE FUEL-TO-MODERATOR VOLUME RATIO

However, since the atomic density of stainless steel is twice that for Zr-2, for the same clad thickness the first would absorb more neutrons than the second. The better material and structural properties of stainless steel permits the use of a smaller clad thickness (30% less) compared to Zircaloy. Figure 5.6 indicates that under this condition SS-316 would absorb less neutrons than Zr-2 with D_2O as the moderator, for F/M $\gtrsim$ 0.5. For H_2O as the moderator, the advantage of Zr-2 would be substantially reduced, but not eliminated, for tight pitch lattices compared to the standard case (F/M = 0.5).

The better mechanical performance of stainless steel under both burnout and LOCA conditions might well help make tight lattices practicable. The above results show that this would be a neutronically tolerable design choice.

5.8 Conclusions

The core concepts discussed in this chapter are intended to improve ore savings or other core characteristics which would permit or facilitate implementation of ore-conserving options. For standard F/M ratios (F/M $\gtrsim$ 0.5), neutron spectra as hard as those in tight pitch H_2O-moderated cores can be obtained by properly choosing the D_2O to H_2O ratio and, consequently, comparable ore savings can be achieved. The variable fuel-to-moderator control reactor is completely equivalent to the SSCR, since both very nearly eliminate neutron losses to control materials; but unlike the SSCR it does not make use of D_2O. The large mean free paths characterisitc of tight pitch cores call for the use of radial and/or axial blankets of fertile material to reduce the neutron leakage.

Because metallic thorium fuel stores less energy than UO_2 (or ThO_2) it can lead to smaller clad temperatures in the early stages of a LOCA; however this might not necessarily hold true in the final stages, and disadvantages might be incurred in other types of accidents or transients. From a non-proliferation point of view, the use of the so-called denatured thorium-uranium cycle in LWR's has the advantage of producing two-thirds less plutonium than the conventional uranium cycle while still holding the uranium enrichment below a weapons-safe level. In addition, it can reduce the consumption of uranium ore (at the expense of higher fissile inventory) to very nearly the level of a highly enriched system. Finally, the advantage of zircaloy over stainless steel as a cladding material for highly epithermal spectra appears to diminish considerably since the ratio between the microscopic absorption cross sections of SS and Zr decreases sharply with F/M (even becoming smaller than unity).

Further, more elaborate studies are needed in each of these areas to assess their characteristics, advantages and practicability. However, the existence of so many promising options indicates that there should be a high probability that designers can cope with the engineering problems encountered in the attempt to realize the benefits of tight-pitch PWR cores.

CHAPTER 6

SUMMARY, CONCLUSIONS AND RECOMMENDATIONS

6.1 Introduction

The increasing dependence of world electric-energy production on fission energy and the delay in the development and deployment of advanced converter and breeder reactors have shortened the projected time-horizon for exhaustion of the known low-cost reserves of natural uranium. Since about 75% (N-2) of the committed nuclear power plants in the world are LWR's, renewed interest in the re-optimization of LWR cores in terms of ore conservation has arisen.

The present work represents one subtask of a project carried out at MIT for DOE as part of their NASAP/INFCE-related efforts involving the optimization of PWR lattices in the recycle mode. As identified in the preliminary survey by Garel (G-1), attention must inevitably be focused on designs having high fuel-to-moderator volume ratios, and consideration given to the use of thorium. We therefore have concentrated our efforts on the study of two systems of coupled reactors, namely the thorium system, U-235/UO_2 : Pu/ThO_2 : U-233/ThO_2 and the uranium system, U-235/UO_2 : Pu/UO_2. This thorium system was selected instead of the more common U-235/ThO_2 option because of the judgement, on practical grounds, that reprocessing of uranium will precede reprocessing of thorium fuel, and that is highly desirable to avoid contamination of U-235 with U-232 and other uranium isotopes, which would increase the complexity and cost of U-235 re-enrichment and re-fabrication.

We have studied the effects of the fuel-to-moderator volume ratio (F/M), discharged fuel burnup (B) and number of staggered fuel batches (N) for the last core in each sequence (U-233/ThO_2 and Pu/UO_2) on the consumption of natural uranium (CNU) and on the fuel cycle cost (FCC) (calculated at the indifference value of bred fissile species) of each system. Consideration was given to the moderator-void and fuel-temperature coefficients of reactivity for these cores. In addition, other ways to improve the ore utilization and/or other core characteristics of LWR's are also briefly discussed.

6.2 Computational Methods

Methods and data verification in the range of present interest, 0.5 (current lattices) < F/M < 4.0 are limited by the scarcity of experiments with F/M > 1.0. Nevertheless the EPRI-LEOPARD (B-2) and LASER (P-3) programs used for the U-233/ThO_2 and Pu/UO_2 depletion calculations, respectively, were benchmarked against several of the most useful experiments.

Table 6.1 summarizes the main characteristics of some of the critical and exponential benchmark experiments analyzed with LEOPARD and LASER, and shows the average calculated values for the multiplication factor k. In terms of k, reasonably good results are obtained with both codes. However, for the plutonium experiments, LASER yields better results than LEOPARD because of its higher thermal energy cutoff (1.855 vs. 0.625 eV) and more accurate treatment of the 0.3 eV Pu-239 and the 1.0 eV Pu-240 resonances. It was found that in general, k's calculated by these codes decrease as F/M increases. This trend was attributed to the

TABLE 6.1

SUMMARY OF CALCULATIONS FOR BENCHMARK EXPERIMENTS

	RESULTS BASED ON[1]			
	EPRI - LEOPARD		LASER	
Fuel	$U\text{-}233/ThO_2$	$U\text{-}235/ThO_2$	Pu/UO_2	Pu/Al
ε[2] (w/o)	3.0	3.8-6.3	1.5-6.6	(9.1)[5]
F/M	0.01-1.0	0.1-0.8	0.4-0.9	0.5-1.0
D_2O (%)	0-99.3	0-82.0	0	99.0
ϕ_1/ϕ_2[3]	0.3-21.0	1.7-23.0	4.1-20.2	52.-210.
# of cases	16	16	12	7
$\bar{k}$	1.003 ± 0.012	1.009 ± 0.016	1.008 ± 0.008 (1.015 ± 0.012)[4]	0.991 ± 0.014 (0.952 ± 0.020)[4]

(1) cross section library of EPRI-LEOPARD is based on ENDF/B-IV, and for LASER, on ENDF/B-II for Pu nuclides and on the original LASER library for the other nuclides

(2) ε = fuel enrichment

(3) ϕ_1/ϕ_2 = epithermal-to-thermal flux ratio (based on LEOPARD-thermal energy cutoff = 0.625 eV).

(4) results based on EPRI-LEOPARD

(5) fissile plutonium concentration in the Pu/Al fuel (relative to plutonium + aluminum)

lack of proper treatment of resonance effects, since only the dominant fertile nuclide is spatially self-shielded, without any consideration given to resonance interference effects between nuclides.

The combination of thermal and fast reactor-physics methods (LEOPARD and SPHINX (D-2) + ANISN (E-2), respectively) gives better results in terms of k compared to LEOPARD for very epithermal thorium experiments (moderated by D_2O). It appears however that this method in contrast to LEOPARD, overshields the resonance absorption for both fertile and fissile nuclides.

The lack of uniform tight-lattice benchmark experiments and the difficulties in obtaining the true critical bucklings for those available (U-1) have, after due deliberation, led us to make only one major modification in LEOPARD: we have replaced the thorium metal-oxide correlation by a new prescription based on the resonance-integral correlation for thorium reported by Steen (S-3):

$$RI^{02}_{Steen} = 5.173 + 0.9298x + (0.04406\ x - 0.1269)T^{1/2}_{eff} \qquad (6.1)$$

This new correlation increases k for the epithermal thorium-benchmark experiments by as much as 1%. Moreover, for very tight lattices (F/M = 3.0), at operating temperatures, k is increased by as much as 3% because of the smaller contribution of the Doppler effect in the new correlation, bringing the results closer to SPHINX/ANISN results (the results based on EPRI-LEOPARD in Table 6.1 are based on this new correlation).

Based on sensitivity analyses we have concluded that a 10% error in the L-factors for the heavy nuclides can cause errors of less than 8 and 16% in the fissile inventory and in the consumption of fissile material,

respectively, for tight lattices (F/M = 3.0) of U-233/ThO_2 or Pu/UO_2. Similar errors can arise from a 10% error in the absorption cross sections for the lumped fission product.

The Simple Model (the SIMMOD Program) developed by Abbaspour (A-2) for calculating overall levelized fuel cycle costs assumes only equilibrium fuel batches and that revenue and depreciation charges occur at the mid-point of the irradiation period. Based on the author's comparisons with more sophisticated schemes (MITCOST II (C-4)), this model was judged to be accurate enough for the purposes of the present work.

6.3 Results

6.3.1 Fissile Inventory and Conversion Ratio

Table 6.2 gives the reload fissile enrichment (RFE) and the cycle-average conversion ratio (CR) for a 3-zone PWR fueled with U-233/ThO_2 or Pu/UO_2. The discharge burnup is fixed at 33 MWD/KgHM. The RFE increases with F/M for both fuels, reflecting decreased fissile cross sections in epithermal spectra. The conversion ratio also increases with F/M since increased absorption and fast fission in the dominant fertile elements relative to other cell components outweighs decreased values of fissile η in epithermal relative to thermal spectra.

For current lattices (F/M = 0.5) Pu/UO_2 requires slightly less enrichment than U-233/ThO_2 mainly because of: the higher thermal cross sections of the fissile plutonium isotopes compared to U-233; the smaller thermal cross section of U-238 compared to Th-232; and the larger fast fission effect for U-238 compared to Th-232 (1.09 vs. 1.02). The difference is not larger because the percentage of non-fissile isotopes was higher in the plutonium than in the U-233 fuel used. The

TABLE 6.2

CORE CHARACTERISTICS AS A FUNCTION OF FUEL-TO-MODERATOR RATIO

	Reload Enrichment w/o		Conversion Ratio Cycle-Average		Ore Consumption ST U_3O_8/Gwe • yr	
F/M	U-233/ThO_2	Pu/UO_2	U-233/ThO_2	Pu/UO_2	U-233/ThO_2	Pu/UO_2
0.5	2.8	2.7	0.76	0.72	103	106
1.0	3.0	6.2	0.82	0.85	100	90
2.0	4.2	8.4	0.87	0.94	99	71
3.0	5.4	8.8	0.91	0.99	96	44

BASIS:

(a) 75% capacity factor, 0.2 w/o Tails, 1% losses in reprocessing and in fabrication; successive recycle to extinction with worth-weighting for isotopic composition. On the same basis the once-through PWR would require 167 ST U_3O_8/Gwe • yr

(b) Initial isotopic compositions:

91 w/o U-233, 8 w/o U-234, 1 w/o U-235

54 w/o Pu-239, 26 w/o Pu-240, 14 w/o Pu-241, 6 w/o Pu-242

higher thermal eta of U-233 relative to Pu-239 provides a larger CR for U-233/ThO_2 fuel (and prevents the RFE for U-233/ThO_2 from going even higher) since this outweighs the fast fission differential.

For epithermal lattices, Pu/UO_2 requires considerably higher fissile enrichments than U-233/ThO_2 because of the much smaller resonance integral of Pu-239 relative to U-233. The very large fast fission effect in U-238 (plus Pu-240) compared to Th-232 (1.20 vs. 1.04 at F/M = 3.0), helps keep the RFE for Pu/UO_2 from rising even higher, and provides larger CR values than for U-233/ThO_2 despite the higher eta of U-233.

6.3.2 Consumption of Natural Uranium

Table 6.2 also shows the consumption of natural uranium when the subject reactors are operated in complete systems, namely the thorium system, U-235/UO_2 : Pu/ThO_2 : U-233/ThO_2 and the uranium system, U-235/UO_2 : Pu/UO_2. All cores use 3-batch fuel management, discharge fuel at 33 MWD/KgHM, and (except for the final core in each sequence) have F/M = 0.5.

The uranium system appears to be superior mainly because of the poor performance (CR = 0.72) of the Pu/ThO_2 core which dominates the U-233/ThO_2 core in the thorium system (and in part because of the smaller conversion ratios of the U-233/ThO_2 core compared to the Pu/UO_2 core at high values of F/M). Furthermore, increasing the F/M ratio of the Pu/ThO_2 core from 0.5 to 3.0 does not significantly improve the performance of the thorium system (since fast fission in Th-232 increases only slightly with F/M). In any event, at steady state, the uranium system can save as much as 60% (at F/M = 3.0) on ore use rate compared

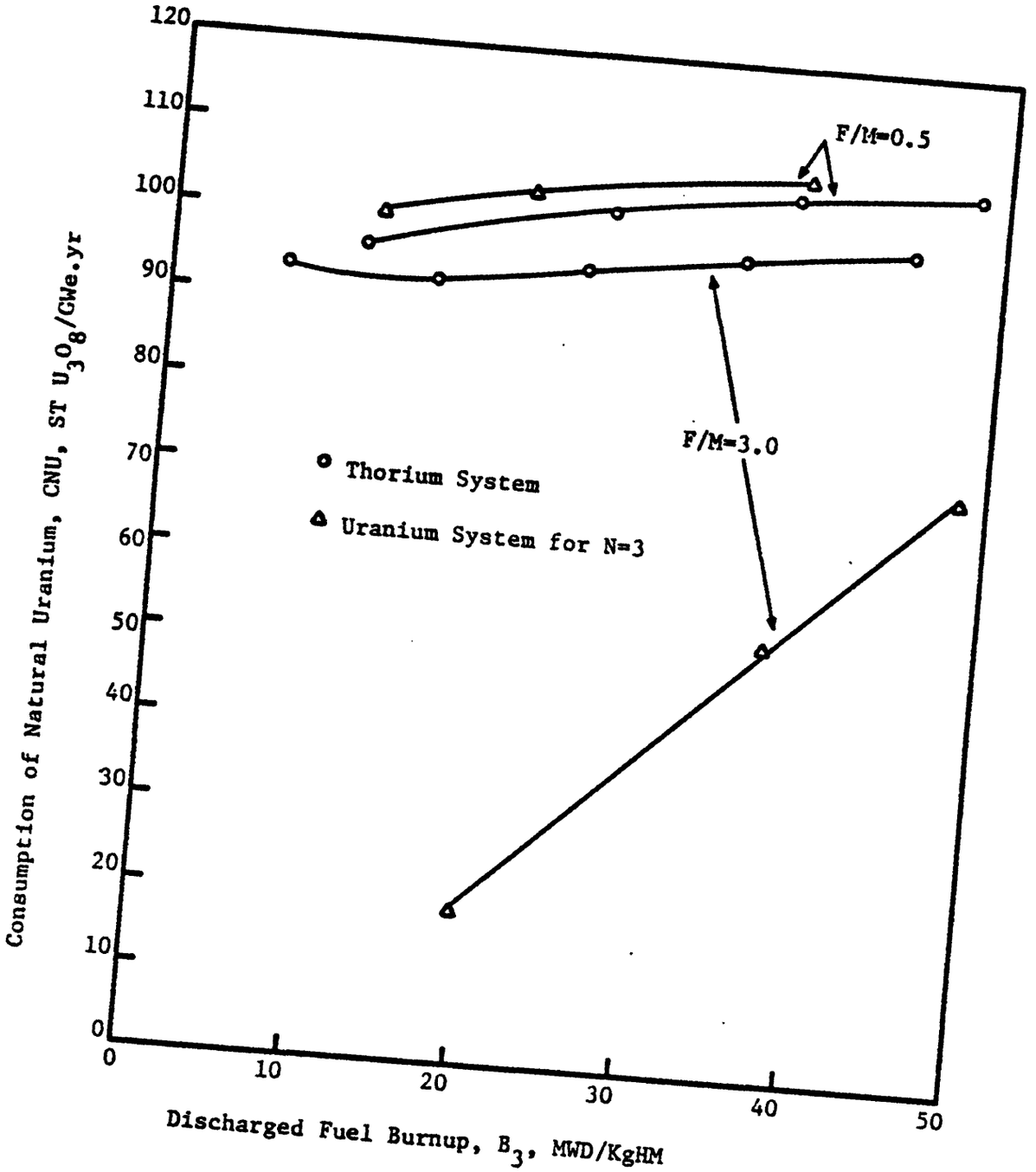

Fig. 6.1 SYSTEM CONSUMPTION OF NATURAL URANIUM AS A FUNCTION OF DISCHARGED FUEL BURNUP FOR THORIUM AND URANIUM FUEL CYCLES

to the same system (conventional recycle) with F/M = 0.5. On the same basis, the thorium system saves less than 10%.

Decreasing the discharged fuel burnup and increasing the number of core zones of the Pu/UO_2 core can increase ore savings from the quoted 60% to a value of 80% for the uranium system (Fig. 6.1). This improvement is due to decreased neutron losses to the fission product and control materials, which more than compensate for increased fuel re-processing and re-fabrication losses (provided that B is not too low, i.e. $B \geq 10$ MWD/KgHM). On the same basis, savings for the thorium system can be increased from ∿10% to only 15%.

The calculated CNU for these systems is very sensitive to fuel losses, to the type of isotopic weighting and also to the geometric buckling; especially at high F/M ratios and low discharged fuel burnups when the conversion ratio is near unity for the tight pitch cores. Errors in the CNU due to errors in the treatment of resonance cross sections and fission products for the tight pitch core are estimated to total less than 15%.

6.3.3 Reactivity Coefficients

The moderator void/temperature coefficients of reactivity (without soluble poison) are negative for all cases in Table 6.2 at BOC, which is in accord with the monotonic increase of the RFE with F/M. For thermal spectra (F/M = 0.5), the void reactivity coefficient of Pu/UO_2 is more negative than for $U\text{-}233/ThO_2$ (-3.8×10^{-3} vs. -1.7×10^{-3} $\Delta k/\%$ void) because the RFE for the latter fuel is less sensitive to the F/M ratio. The opposite is true for epithermal lattices (-0.5×10^{-3} vs. -3.8×10^{-3} $\Delta k/\%$ void at F/M = 3.0). Although the void reactivity coefficients

calculated with LASER for tight-pitch Pu/UO_2-fueled cores agree reasonably with fast reactor-physics methods (SPHINX + ANISN), the presence of large concentrations of Pu-240 in the fuel calls for more accurate models to properly account for differences in counterbalancing effects.

6.3.4 Fuel Cycle Costs

Fuel cycle calculations showed that, although the indifference values for the bred fissile materials vary widely with the parameters F/M, B and N for the last core in each sequence, the FCC for each system is rather insensitive to these variables, resulting in low economic impediments or low incentives depending on one's point of view. The underlying cause for this behavior of the FCC is the small amount of plutonium produced in the standard $U\text{-}235/UO_2$ core (only one-fifth of the initial mass of U-235) and the high discount rate assumed (10.25% yr^{-1}) which decreases the value of the discharged fuel. If one considers not merely fuel cost but the overall generation and/or system production costs of electricity, the use of low discharged fuel burnups becomes unattractive.

6.3.5 Alternative Concepts

A brief investigation was made into several core design concepts that could potentially reduce the consumption of natural uranium for LWR's and/or improve other core characteristics.

For standard F/M ratios ($F/M \approx 0.5$), neutron spectra as hard as those in tight pitch H_2O-moderated cores can be obtained by properly choosing the D_2O/H_2O ratio and, consequently, comparable ore savings can be achieved. Thermal-hydraulic and mechanical-design characteristics of the core can then be kept essentially the same as for today's standard LWR's.

The control of core reactivity by varying the effective F/M ratio is completely equivalent to the SSCR concept, since both versions very nearly eliminate neutron losses to control materials; but unlike the SSCR the Variable Fuel-to-Moderator Control Reactor (VFMCR) does not make use of the expensive D_2O.

The large mean free paths characteristic of tight pitch cores call for the use of radial and/or axial blankets of fertile material to reduce the neutron leakage. It is interesting to note that, if neutron losses due to leakage and due to absorption in the control materials are eliminated, the CNU for the uranium system can be reduced to very low values, even for high discharged fuel burnups. On the same basis, ore savings for the thorium system would also be significantly improved.

The use of the so-called denatured thorium-uranium cycle in LWR's has the advantage of producing roughly two-thirds less plutonium than the conventional uranium cycle while still holding the uranium enrichment below a weapons-safe level. In addition, it can reduce the consumption of uranium ore (at the expense of higher fissile inventories) to very nearly the level of a highly enriched system (uranium enriched to 93% in U-235, plus Th-232).

Because metallic thorium fuel stores less energy than UO_2 (or ThO_2) it can lead to smaller clad temperatures in the early stages of a LOCA; however this might not necessarily hold true in the final stages, and disadvantages might be worsened in other types of accidents.

Finally, the advantages of zircaloy over stainless steel as a cladding material for highly epithermal spectra appear to diminish considerably, since the ratio between the (one-group averaged) microscopic absorption σ_a's of SS and Zr decreases sharply with F/M (even becoming smaller than unity).

6.4 Conclusions

The use of tight-pitch (F/M > 0.5) PWR cores fueled with Pu/UO coupled to standard (F/M = 0.5) cores fueled with U-235/UO_2 can reduce (at steady-state) the consumption of natural uranium for this system by as much as 60% compared to the same system with conventional recycle (at F/M = 0.5). On the same basis however, the impact of tight pitch cores fueled with U-233/ThO_2 on uranium ore usage is less than 15% if this reactor is coupled to standard U-235/UO_2 cores via Pu/ThO_2-fueled cores, mainly because of the poor performance of the latter type of fuel which cannot be significantly remedied by going to a tighter lattice pitch.

Uranium ore usage could be further improved if neutron losses to control materials were minimized by increasing the number of staggered fuel batches in the core (from 3 to 6) and/or by using the spectral shift concept to control the core reactivity (by varying the concentration of D_2O in the moderator and/or by varying the effective F/M ratio of the core). Reducing neutron losses due to fission product absorptions and core leakage by decreasing the discharged fuel burnup (from 33 to $\sim$20 MWD/KgHM) and by using external blankets of fertile material would also help to bring down the consumption of natural uranium for these systems of coupled reactors.

Many practical questions must be answered before serious consideration can be given to use of tight pitch cores: thermal-hydraulic, mechanical and economic. While steady state DNBR is not calculated to be limiting, plant and core redesign to accomodate higher core pressure drops appears an inevitable requirement, and transient/accident limits await a definitive assessment. Some of these problems could be eliminated if, instead of

tightening the fuel lattice (of a H_2O-moderated core) to increase the fuel conversion ratio, an equivalent (fixed composition) D_2O/H_2O mixture was used as moderator while keeping the standard core design (F/M = 0.5). The moderator void/temperature coefficients of reactivity were calculated to be (slightly) negative for the tight pitch cores studied and we would expect similar numbers for equivalent D_2O/H_2O-moderated cores. Fuel cycle cost calculations showed that system fuel cycle costs (at the indifference value of bred fissile species) are quite insensitive to the fuel-to-moderator ratio - resulting in low impediments or low incentives depending on one's point of view.

Nevertheless, it is concluded that pursuit of this potential evolutionary change in PWR core design should be continued to a definitive conclusion, since near-breeder low-ore-usage fuel cycles are apparently attainable, with substantial import as regards the future competitive stance of the PWR with respect to the FBR.

Finally, the use of thorium in LWR cores in the manner investigated here (uniform lattices, using Pu/Th cores to produce U-233) appears to be less attractive than plutonium recycle into tight pitch uranium fueled cores. While thorium may offer advantages if it could be used in metallic form, the existence of several approaches to achieve the benefits of high F/M cores (use of D_2O/H_2O mixtures, stainless steel clad, variable F/M control) make it less likely that the (as yet unproven) advantages of metal fuel will prove decisive.

6.5 Recommendations

Benchmark experiments uniform lattices for several types of fuel combinations (mainly for U-233/ThO_2, Pu/UO_2 and Pu/ThO_2) and moderator compositions (mainly for pure H_2O but also for different D_2O/H_2O compositions) in the range of interest: $0.5 < F/M < 4.0$ and $2.0 < \varepsilon < 10.0$ w/o are clearly in order to verify the accuracy of reactor-physics methods and data for epithermal cores. Not only the critical bucklings should be measured, but also the lattice microscopic parameters ($\rho_{capture}^{fertile}$, $\rho_{fission}^{fissile}$, $\delta_{fissile}^{fertile}$ and the fertile capture rate-to-fissile fission rate ratio - the modified conversion ratio).

Irradiations of these fuels in epithermal lattices are also needed to check the accuracy of depletion models since, at high F/M ratios and low discharge burnups, the consumption of fissile material is also very sensitive to the model used to represent fission product effects. Three-dimensional diffusion-depletion calculations are called for to properly consider neutron leakage variation with fuel depletion, since neutron leakage is an important factor to be considered in tight pitch cores.

Alternative and complementary ways to further reduce uranium ore consumption and/or improve other core characteristics should be investigated. The use of mixtures of D_2O/H_2O can yield highly epithermal spectra in cores of current design. The use of the spectral shift concept to control core reactivity (by varying the concentration of D_2O in the moderator and/or by varying the effective F/M ratio) can reduce neutron losses as can the use of external blankets of fertile material. Thus a comparison of the alternatives of using tight pitch vs. D_2O dilution should be made to select the most promising approach.

Additional comparisons (for tight pitch cores) should be made between the use of: the denatured thorium-uranium cycle versus the conventional U-235/UO_2 cycle from a non-proliferation point of view; Th-metal versus UO_2 or ThO_2 fuels under LOCA and other transient/accident conditions; and finally, the use of stainless steel against zircaloy as a cladding material in tight-pitch cores.

It is important to reiterate that only one particular version of a thorium fuel cycle has been examined in the present work. Thus, the fact that it did not prove to be superior to the uranium-based fuel cycle should be interpreted with some caution: in particular, the direct use of highly enriched U-235 in thorium and/or the use of non-uniform lattices, as in the LWBR, must be considered independently on their own merits. With that caveat in mind, however, our results should be interpreted as confirming Edlund's claims as to the superiority of tight pitch Pu/U cores (E-1)(E-2) and the equivalent points raised in favor of D_2O moderated lattices by Radkowsky (R-2). We therefore recommend further evaluation of such concepts, with emphasis on accurate calculation of resonance absorption, assessment of means of reactivity control, system redesign to accomodate these lattices, and their thermal performance during transient and accident sequences.

APPENDIX A

PRELIMINARY DESIGN PARAMETERS FOR MAINE YANKEE*

MECHANICAL DESIGN PARAMETERS

Fuel Rod	
Fuel Material (Sintered Pellets)	UO_2
Pellet Diameter, Inch	0.382
Pellet Length, Approximate Inch	0.6
Fuel Density, Stacked, g/cc, % Theoretical	0.1, 92%
Clad Material	Zircaloy-4
Clad ID, Inch	0.388
Clad OD, Inch	0.440
Clad Thickness, Inch	0.026
Diametral Gap, Cold, Nominal, Inch	0.006
Active Length, Inch	137
Total Length, Inch	145.4
Fuel Assembly	
Number of Active Fuel Rods	176
Fuel Rod Array, Square	14 x 14
Fuel Rod Pitch, Inch	0.580
Spacers	
Type	Leaf Spring
Material	Zircaloy-4
Number Per Assembly	8
Weight of Fuel Assembly, Pound	1,300
Weight of Contained Uranium, kg U	401
Outside Dimensions	
Fuel Rod to Fuel Rod, Inch	7.980 x 7.980
Nominal Envelope, Inch	8.180 x 8.180
Control Element Assembly, CEA	
Number of Absorber Elements	5
Type	Cylindrical Rods
Array	Square Plus One Center
Sheath Material	Iconel Tube
Sheath Thickness	0.040
Neutron Absorber Material	B_4C
Corner Element Pitch, Inch	4.64
Active Length, Inch	137
Element Diameter, Inch	0.955
Standard CEA Weight, Pound	70
Total Operating Assembly Weight, Pound	187

* From the PSAR (M-5)

Core Arrangement	
Number of Fuel Assemblies in Core, Total	217
Number of Instrumented Assemblies	45
Number of CEA's	89
Number of Active Fuel Rods	38,192
CEA Pitch, Minimum, Inch	11.57
Fuel Rod Surface-to-Surface Between Fuel Assemblies, Inch	0.200
Outer Fuel Rod Surface to Core Shroud, Inch	0.180
Total Core Area, Ft^2	101
Core Equivalent Diameter, Inch	136
Core Circumscribed Diameter, Inch	143.3
Core Volume, Liters	32,610
Total Fuel Loading, MTU	87
Total Fuel Weight, Pound UO_2	218,000
Total Weight of Zircaloy, Pound	49,000

NUCLEAR DESIGN DATA*

Performance Characteristics	
Fuel Management	3-Batch
U-235 Enrichment (w/o)	
Batch 1	1.80
Batch 2	2.48
Batch 3	3.01
H_2O/UO_2 Volume Ratio, Unit Cell (Cold Dimensions)	1.61
Control Characteristics	
Keff (CEA's Control Rods Withdrawn, No Boron in Moderator)	
Cold, Clean	1.266
Hot, Clean, Zero Power	1.211
Hot, Clean, Full Power	1.178
Hot, Equilibrium Xe, Full Power	1.138
Control Elements (B_4C in Inconel Tubes)	
Number of Control Element Assemblies	89
Total Rod Worth, Hot, $\Delta\rho$, Percent Greater Than	9
Dissolved Boron Content for Criticality (CEA's Withdrawn)	
Cold, Clean, Ppm	1,300
Hot, Clean, Zero Power, Ppm	1,400
Hot, Clean, Full Power, Ppm	1,200
Hot, Equilibrium Xe, Full Power, Ppm	1,000

* Unless otherwise specified, the values are for the initial core.

Dissolved Boron Content Available for Refueling, Ppm	1,720
Boron Worth (Ppm/1 Percent $\Delta\rho$)	
Hot	80
Cold	60
Nuclear Power Peaking Factors	
Overall Nuclear Limits	
Heat Flux, F_Q^N	2.95
Enthalpy Rise, $F_{\Delta H}^N$	1.70
Reactivity Coefficients	
Moderator Temperature Coefficient	
Hot, Operating ($\Delta\rho$ / F)	0 to -2×10^{-4}
Room Temperature, CEA's Out ($\Delta\rho$ / F)	0.1×10^{-4} to -0.1×10^{-4}
Fuel Temperature Coefficient, Doppler ($\Delta\rho$ / F)	-1.8×10^{-5} to -1×10^{-5}
Full Power Reactivity Defect Due to Fuel Temperature Effects, Percent	1.6
Dissolved Boron Coefficient ($\Delta\rho$ /ppm)	-0.13×10^{-3} to -0.17×10^{-3}
Moderator Void Coefficient	
Hot ($\Delta\rho$ /Percent Void)	0 to -1.6×10^{-3}
Moderator Pressure Coefficient	
Hot ($\Delta\rho$ / Psi)	0 to $+2 \times 10^{-6}$

THERMAL HYDRAULIC PARAMETERS

General Characteristics	
Total Heat Output, Mwt	2,440
Total Heat Output, Btu Per Hour	8.33×10^9
Heat Generated in Fuel, Percent	97.5
Pressure	
Nominal, Psi Absolute	2,250
Minimum in Normal Operation, Psi Absolute	2,200
Maximum in Normal Operation, Psi Absolute	2,300
Nominal Coolant Inlet Temperature, F	550
Maximum Inlet Temperature, Normal Operation, F	555
Vessel Outlet Temperature, F	602
Core Bulk Outlet Temperature, F	603
Total Reactor Coolant Flow, Pound Per Hour	122×10^6
Total Coolant Flow Area*, Ft^2	53.2

* Guide tube areas not included

Coolant Flow Through Core, Pound Per Hour	119.5×10^6
Hydraulic Diameter Nominal Channel, Foot	0.04445
Average Mass Velocity, Pound Per Hour-Ft^2	2.23×10^6
Average Coolant Velocity in Core, Feet Per Second	13.8
Pressure Drop Across Core, Psi	9.5
Total Pressure Drop Across Vessel, Psi	42
Core Average Heat Flux, Btu Per Hour-Ft^2	162,000
Total Heat Transfer Area, Ft^2	50,200
Film Coefficient at Average Conditions, Btu Per Hour-Ft^2 - F	5,100
Average Film Temperature Difference, F	32
Average Linear Heat Rate of Rod, Kw Per Ft	5.6
Specific Power, Kw Per Kg	28.0
Power Density, Kw Per Liter	75.2
Design Overpower, Percent	112
Average Core Enthalpy Rise, 100 Percent Power, Btu Per Pound	69.7
Heat Flux Factors	
Total Nuclear Peaking Factor	2.95
Engineering Heat Flux Factor	1.05
Total Heat Flux Factor	3.10
Enthalpy Rise Factors, Nominal Conditions	
Heat Input Factors	
Nuclear Enthalpy Rise Factor	1.70
Engineering Factor on Hot Channel Heat Input	1.05
Total Heat Input Factor	1.79
Flow Factors	
Inlet Plenum Maldistribution	1.05
Fuel Rod Pitch, Bowing and Clad Diameter	1.065
Flow Mixing	0.92
Internal Leakage and Boiling Flow Redistribution	1.16
Total Flow Factor	1.20
Total Enthalpy Rise Factor = 1.79 x 1.20	2.14

	Full Power	Over-Power (112 Percent)
Hot Channel and Hot Spot Parameters		
Maximum Heat Flux (Btu Per Hour-Ft^2	501,000	516,000
Maximum Linear Heat Rate of Rod, Kw Per Foot	17.4	19.4

	Full Power	Over-Power (112 Percent)
Maximum UO_2 Temperature, Steady State, F	4,340	4,560
Maximum Clad Surface Temperature, F	658	664
Hot Channel Outlet Temperature, F	652	659
Hot Channel Enthalpy, Btu Per Pound	696.2	716.3
DNB Ratio, Steady State W-3 Correlation, q" DNBR	2.15	1.86

APPENDIX B

BENCHMARKING OF EPRI-LEOPARD AND ITS ENDF/B-IV CROSS SECTION LIBRARY AGAINST EXPERIMENTAL DATA

Tables B-1, B-3, B-5 and B-6 present the lattice parameters, and the calculated k values for benchmark U-233/ThO_2, U-233/ThO_2, U-235/UO_2 and U-235/U-metal lattices, respectively. Two k values are given for each thorium lattice based on the unmodified and modified EPRI-LEOPARD which includes the new metal-oxide resonance-integral correlation for thorium (Section 3.2.2).

Tables B-2 and B-4 compare the calculated and experimental values for the epithermal-to-thermal capture ratio in Th-232 (ρ_c^{02}) and other microscopic parameters for the U-233/ThO_2 and U-235/ThO_2 benchmark lattices of Tables B-1 and B-3, respectively.

TABLE B.1

CHARACTERISTICS OF AND CALCULATIONAL RESULTS FOR BENCHMARK U-233/ThO_2 LATTICES

Case #	F/M Volume Ratio	H+D / Th-232 Ratio	D_2O (%)	Lattice Pitch (in.)	Measured Buckling (m^{-2})	Calculated k Th-Correlation OLD	Calculated k Th-Correlation NEW (Steen)
1	0.11	31.3	0	1.3346	-1.22±0.3	0.9965	0.9970
2	0.15	23.1		1.1720	32.2±0.2	1.0072	1.0079
3	0.23	14.4		0.9707	69.8±1.0	1.0162	1.0173
4	0.33	10.1		0.8542	85.54±0.8	1.0166	1.0181
5	0.46	7.39		0.7706	90.35±1.6	1.0151	1.0172
6	0.58	5.77		0.7163	89.34±2.0	1.0117	1.0143
7	0.72	4.67		0.6767	86.06±1.3	1.0066	1.0097
8	1.00	3.36		0.6269	75.88±2.0	1.0017	1.0058
9	0.008	403.	99.25	4.520	11.29±0.20	0.9882	0.9885
10	0.012	273.	98.95	3.725	14.67±0.37	0.9948	0.9953
11	0.018	184.	99.34	3.079	19.13±0.27	0.9907	0.9914
12	0.026	126.	99.25	2.562	22.32±0.14	1.0026	1.0035
13	0.034	97.4	99.33	2.259	25.00±0.16	0.9971	0.9982
14	0.062	53.7	99.30	1.708	28.64±0.29	1.0014	1.0035
15	0.085	39.2	99.26	1.480	29.85±0.22	0.9972	1.0001
16	0.333	10.1	99.30	0.854	20.54±0.20	0.9638	0.9724
					Average k	1.0005 ±0.0132	1.0025 ±0.0122

Reference : (W-2)
Lattice Type : Hexagonal
Fuel Enrichment : 3.00 w/o (see Ref. (W-2) for detailed composition)
Fuel Density : 8.9618 g/cm^3
Pellet Diameter : 0.430 in.
Clad Material : Zircaloy-2
Clad OD : 0.499 in.
Clad Thickness : 0.0345 in.

TABLE B.2

COMPARISON BETWEEN CALCULATED AND EXPERIMENTAL

VALUES FOR ρ_c^{02} AND δ_{02}^{23} FOR BENCHMARK U-233/ThO_2 LATTICES

Case #	F/M Volume Ratio	D_2O (%)	ρ_c^{02} Measured: Cd Ratio Method	ρ_c^{02} Measured: Thermal Activation Method	ρ_c^{02} Calculated: OLD Th-Cor.	ρ_c^{02} Calculated: NEW Th-Cor.	δ_{02}^{23} Measured	δ_{02}^{23} Calculated: OLD Th-Cor.	δ_{02}^{23} Calculated: NEW Th-Cor.
1	0.11	0	0.170±0.007	-	0.151	0.148			
2	0.15		0.218±0.008	-	0.189	0.185	-		
3	0.23		-	-			-		
4	0.33		0.435±0.013	-	0.387	0.380	-		
5	0.46		0.607±0.026	-	0.530	0.521	-		
6	0.58		0.754±0.024	-	0.691	0.678	-		
7	0.72		0.928±0.038	-	0.876	0.859	-		
8	1.00		1.380±0.042	-	1.298	1.270	-		
9	0.008	99.25	0.089±0.005	-	0.074	0.072	-		
10	0.012	98.95	0.104±0.005	-	0.109	0.106	-		
11	0.018	99.34	0.166±0.006	-	0.164	0.160	-		
12	0.026	99.25	0.234±0.008	-	0.237	0.232	-		
13	0.034	99.33	0.297±0.011	-	0.312	0.306	-		

(cont'd)

TABLE B.2 - COMPARISON BETWEEN CALCULATED AND EXPERIMENTAL VALUES FOR ρ_c^{02} AND δ_{02}^{23} FOR BENCHMARK U-233/ThO_2 LATTICES (cont'd)

Case #	F/M Volume Ratio	D_2O (%)	ρ_c^{02} Measured: Cd Ratio Method	ρ_c^{02} Measured: Thermal Activation Method	ρ_c^{02} Calculated: OLD Th-Cor.	ρ_c^{02} Calculated: NEW Th-Cor.	δ_{02}^{23} Measured	δ_{02}^{23} Calculated: OLD Th-Cor.	δ_{02}^{23} Calculated: NEW Th-Cor.
14	0.062	99.30	0.559±0.018	0.634±0.060	0.586	0.574	0.0047±0.007	0.0021	0.0021
15	0.085	99.26	0.780±0.032	0.840±0.058	0.837	0.818	0.0056±0.007	0.0028	0.0028
16	0.332	99.30	5.190±0.540	4.660±0.19	5.52	5.29	0.0117±0.008	0.0096	0.0093
			Average		0.96	0.94	Average	0.59	0.58
			$\rho_c^{02}/\rho_{c\ exp.}^{02}$		±0.08	±0.08	$\delta_{02}^{23}/\delta_{02\ exp.}^{23}$	±0.20	±0.19

Reference (W-2)
Lattice Type (Hexagonal)

TABLE B.3

CHARACTERISTICS OF AND CALCULATIONAL RESULTS FOR BENCHMARK U-235/ThO_2 LATTICES

Case #	F/M Volume Ratio	H&D Th-232 Ratio	D_2O (%)	Enrichment (w%)	Fuel Density (g/cm^3)	Pellet Diameter (cm)	Clad Material	Clad OD (cm)	Clad Thickness (cm)	Lattice Pitch (cm)	Critical Buckling (m^{-2})	k OLD Th-Correlation	k NEW (Steen) Th-Correlation
1	0.62	5.90	0	3.78	8.35	0.660	SS	0.792	0.048	1.023	29.3	1.0169	1.0197
2	0.78	4.69								0.966	26.2	1.0044	1.0078
3	0.11	35.5	0	6.33	8.35	0.660	SS	0.792	0.048	1.933	57	1.0131	1.0137
4	0.25	15.0								1.367	94	1.0142	1.0154
5	0.46	8.2								1.115	84	1.0140	1.0161
6	0.62	6.06								1.023	72	1.0136	1.0163
7	0.78	4.82								0.966	61	1.0146	1.0178
8	0.17	20.9	0	3.85	8.45	0.594	Al	0.785	0.086	1.446	53.55	1.0204	1.0218
9	0.28	13.1								1.222	64.01	1.0238	1.0253
10	0.34	11.1	0	6.33	8.33	0.660	Al	0.782	0.036	1.222	114.2	1.0195	1.0211
11	0.60	6.21								1.023	94.25	1.0043	1.0069
12	0.72	5.22								0.978	83.51	1.0015	1.0045
13	0.70	5.33	55.38	6.33	8.33	0.660	Al	0.782	0.036	0.983	44.8	0.9971	1.0020
14			60.40								39.0	1.0038	1.0089
15			71.94								31.4	0.9762	0.9822
16			81.96								22.7	0.9543	0.9612
Reference (W-3) Lattice Type (square)										Average k		1.0057 ± 0.0179	1.0088 ± 0.0164

TABLE B.4

COMPARISON BETWEEN CALCULATED AND EXPERIMENTAL

VALUES FOR ρ_c^{02} AND ρ_f^{25} FOR BENCHMARK U-235/ThO_2 LATTICES

Case #	F/M Volume Ratio	D_2O (%)	ρ_c^{02} Measured	ρ_c^{02} Calculated (Th-Correlation) Old	ρ_c^{02} Calculated (Th-Correlation) New (Steen)	ρ_f^{25} Measured	ρ_f^{25} Calculated (Th-Correlation) Old	ρ_f^{25} Calculated (Th-Correlation) New (Steen)
1	0.62	0	-			0.157	0.178	0.178
2	0.78		1.28	1.242	1.215	0.210	0.224	0.224
3	0.11		-			-		
4	0.25		-			-		
5	0.46		-			-		
6	0.62		1.49	1.546	1.514	0.221	0.265	0.265
7	0.78		2.08	1.969	1.928	0.292	0.338	0.337
8	0.17		-			0.053	0.051	0.051
9	0.28		-			0.085	0.078	0.076
10	0.34		-			0.130	0.134	0.133
11	0.60		-			0.181	0.237	0.237
12	0.72		-			0.266	0.283	0.283
13	0.70	55.38	-			0.56	0.573	0.572
14		60.40	-			0.65	0.636	0.635
15		71.94	-			0.81	0.853	0.852
16		81.96	7	7.50	7.32	1.16	1.214	1.212
		Average		1.01	0.98	Average	1.07	1.07
		$\rho_c^{02}/\rho_{c\ exp.}^{02}$		±0.06	±0.06	$\rho_f^{25}/\rho_{f\ exp.}^{25}$	±0.11	±0.11

Reference (W-3)
Lattice Type (Square)

TABLE B.5

CHARACTERISTICS OF AND CALCULATIONAL RESULTS FOR BENCHMARK U-235/UO_2 LATTICES

Case #	Reference	Lattice Type	F/M Volume Ratio	H&D U-238 Ratio	D_2O (%)	Enrichment (w%)	Fuel Density (g/cm^3)	Pellet Diameter (cm)	Clad Material	Clad OD (cm)	Clad Thickness (cm)	Lattice Pitch (cm)	Critical Buckling (m^{-2})	Calculated k
1	B-1	S	0.59	5.16	0	3.0424	10.17	0.935	SS	1.057	0.0495	1.4318	74.27±0.29	1.0028
2		S	0.73	4.15	0	3.0424	10.17	0.935	Al	1.058	0.0480	1.3490	91.82±0.80	1.0003
3		S	0.78	3.90	0	3.0424	10.17	0.935	SS	1.057	0.0495	1.3256	61.99±0.39	1.0025
4			1.04	2.93								1.2400	47.44±0.27	1.0005
5		S	1.04	2.93	0	3.0424	10.17	0.935	Al	1.058	0.0480	1.2400	70.76±0.71	0.9991
6		H	1.32	2.30	0	3.0424	10.17	0.935	Al	1.058	0.0480	1.2700	55.38±0.24	0.9988
7			1.55	1.96								1.2340	47.70±0.93	0.9893
8			1.90	1.60								1.1957	36.00±0.74	0.9898
9			2.13	1.43								1.1772	29.66±0.42	0.9919
10			2.29	1.33								1.1660	24.36±0.10	1.0003
11			2.32	1.31								1.1642	25.91±0.14	0.9895
12	W-3	S	0.28	11.9	0	3.000	9.28	1.126	SS	1.270	0.072	2.196	69	0.9855
13			0.64	5.24								1.684	64	0.9948
14			0.87	3.83								1.554	51	0.9971
15		S	0.23	14.6	0	4.020	9.43	1.126	SS	1.270	0.072	2.381	92	0.9935

(cont'd)

TABLE B.5 - CHARACTERISTICS OF AND CALCULATIONAL RESULTS FOR BENCHMARK U-235/UO_2 LATTICES (cont'd)

Case #	Reference	Lattice Type	F/M Volume Ratio	H&D U-238 Ratio	D_2O (%)	Enrichment (w%)	Fuel Density (g/cm^3)	Pellet Diameter (cm)	Clad Material	Clad OD (cm)	Clad Thickness (cm)	Lattice Pitch (cm)	Critical Buckling ($\bar{m}^2$)	Calculated k
16			0.28	11.8								2.196	93	1.0110
17			0.64	5.21								1.684	86	1.0014
18			0.87	3.81								1.554	69	1.0061
19		S	0.88	3.76	0	4.020	9.46	1.126	SS	1.208	0.041	1.511	88.0	1.0000
20					49.66								44.0	0.9912
21					69.70								18.60	1.0018
22					73.77								14.30	0.9983
23					73.77								14.09	0.9997
24					76.50								10.77	1.0001
25					80.65								6.53	0.9945
26					89.14								-4.68	1.0005
												Average k		0.9977
														± 0.0058

TABLE B.6

CHARACTERISTICS OF AND CALCULATIONAL RESULTS FOR BENCHMARK U-235/U-METAL LATTICES

Case No.	Ref.	Lattice Type (*)	Fuel/H_2O Volume Ratio	H U-238 Ratio	Enrich-ment (at%)	Fuel Density (g/cm^3)	Pellet Diameter (in.)	Clad Material	Clad OD (in.)	Clad Thickness (in.)	Lattice Pitch (in.)	Critical Buckling (m^{-2})	Calculated k
1		S	1.16	1.17	0.26	18.95	1.28	Al	1.375	0.040	1.60	-121.6±3.4	0.9741
2			0.43	3.22							2.11	-130.2±1.6	0.8599
3			0.15	9.50							3.20	-186.2±3.4	0.6088
4		S	0.70	1.96	0.714	18.40	0.52	None	-	-	0.72	- 9.6±1.0	1.0089
5			0.50	2.78							0.80	- 3.2±1.0	0.9994
6		S	1.01	1.34	0.714	18.88	1.200	None	-	-	1.5	- 3.6±1.2	0.9977
7			0.50	2.77							1.846	- 2.1±1.2	0.9752
8			0.30	4.55							2.20	- 39.4±1.8	0.9640
9		S	1.16	1.17	0.714	18.95	1.28	Al	1.375	0.040	1.60	- 15.4±0.8	1.0165
10			0.43	3.22							2.11	- 19.3±0.8	0.9934
11			0.15	9.50							3.20	-118.9±1.4	0.8475
12		S	1.18	1.20	0.928	18.80	0.750	Al	0.805	0.021	0.94	- 6.1±2.3	1.0328
13			0.54	2.61							1.15	27.3±0.9	1.0045
14		S	1.69	0.84	0.928	18.67	1.20	Al	1.255	0.020	1.38	- 10.2±1.1	1.0053
15			1.12	1.28							1.50	11.1±1.6	1.0191

(cont'd)

TABLE B.6 - CHARACTERISTICS OF AND CALCULATIONAL RESULTS FOR BENCHMARK U-235/U-METAL LATTICES (cont'd)

Case No.	Ref.	Lattice Type (*)	Fuel/H_2O Volume Ratio	H / U-238 Ratio	Enrichment (at%)	Fuel Density (g/cm^3)	Pellet Diameter (in.)	Clad Material	Clad OD (in.)	Clad Thickness (in.)	Lattice Pitch (in.)	Critical Buckling (m^{-2})	Calculated k
16			0.71	2.00							1.68	24.1±1.2	1.0116
17			0.52	2.76							1.85	21.9±1.0	1.0024
18		H	0.83	1.71	0.95	18.9	1.336	Al	1.50	0.049	2.00	19.24±0.40	1.0211
19			0.68	2.06							2.10	22.57±0.32	1.0137
20			0.58	2.44							2.20	21.15±0.22	1.0111
21			0.44	3.24							2.40	14.74±0.34	0.9947
22		H	0.84	1.68	0.95	18.9	1.336	Fe	1.51	0.049	2.00	- 3.03±0.52	1.0159
23			0.69	2.04							2.10	1.69±0.75	1.0020
24			0.59	2.41							2.20	- 0.52±0.69	1.0005
25			0.44	3.21							2.40	- 8.00±0.71	0.9868
26		H	1.15	1.23	1.007	18.99	0.925	Al	1.002	0.035	1.26	13.77±0.42	1.0058
27			0.73	1.90							1.40	29.03±1.16	1.0138
28			0.57	2.43							1.50	34.70±0.19	1.0068
29			0.52	2.71							1.55	33.57±0.25	1.0084
30			0.47	2.99							1.60	30.12±0.21	1.0130
31		H	1.16	1.20	1.007	18.90	1.66	Al	1.73	0.028	2.20	16.39±0.36	1.0318
32			0.75	1.86							2.45	27.47±0.07	1.0176

(cont'd)

TABLE B.6 - CHARACTERISTICS OF AND CALCULATIONAL RESULTS FOR BENCHMARK U-235/U-METAL LATTICES (cont'd)

Case No.	Ref.	Lattice Type (*)	Fuel/H_2O Volume Ratio	H / U-238 Ratio	Enrichment (at%)	Fuel Density (g/cm^3)	Pellet Diameter (in.)	Clad Material	Clad OD (in.)	Clad Thickness (in.)	Lattice Pitch (in.)	Critical Buckling (m^{-2})	Calculated k
33			0.54	2.59							2.70	22.05±0.11	1.0005
34		H	0.67	2.12	1.027	18.898	0.250	Al	0.316	0.031	0.4190	12.14±1.03	-
35			0.50	2.83							0.4516	19.95±0.47	1.0058
36			0.33	4.24							0.5105	25.15±0.27	1.0071
37			0.25	5.66							0.5633	22.07±0.21	1.0055
38		H	1.00	1.41	1.027	18.898	0.387	Al	0.453	0.028	0.5674	3.23±0.80	1.0028
39			0.67	2.12							0.6244	19.70±0.34	1.0106
40			0.50	2.83							0.6767	29.02±0.34	1.0086
41			0.33	4.25							0.7706	31.39±0.19	1.0071
42			0.25	5.66							0.8542	25.68±0.24	1.0008
43		H	1.00	1.42	1.027	18.898	0.600	Al	0.666	0.028	0.8537	9.90±0.54	1.0155
44			0.67	2.12							0.9444	29.63±0.42	1.0089
45			0.50	2.83							1.0273	36.07±0.39	1.0072
46			0.33	4.24							1.1754	33.15±0.31	1.0007
47			0.25	5.66							1.3070	20.96±0.26	0.9935
48		H	0.75	1.89	1.027	18.898	0.750	Al	0.810	0.030	1.1293	28.9±0.5	1.0125
49			0.63	2.23							1.183	34.70±0.3	1.0090

(cont'd)

TABLE B.6 - CHARACTERISTICS OF AND CALCULATIONAL RESULTS FOR BENCHMARK U-235/U-METAL LATTICES (cont'd)

Case No.	Ref.	Lattice Type (*)	Fuel/H_2O Volume Ratio	H U-238 Ratio	Enrich-ment (at%)	Fuel Density (g/cm^3)	Pellet Diameter (in.)	Clad Material	Clad OD (in.)	Clad Thickness (in.)	Lattice Pitch (in.)	Critical Buckling (m^{-2})	Calculated k
50			0.55	2.59							1.2371	37.5±0.8	1.0067
51			0.43	3.30							1.336	36.73±0.48	1.0040
52			0.35	4.01							1.4285	32.88±0.18	0.9973
53			0.26	5.43							1.5977	18.6±0.60	0.9842
54		H	0.67	2.11	1.143	18.92	0.250	Al	0.316	0.031	0.4190	19.93±0.94	1.0029
55			0.50	2.81							0.4516	31.07±0.37	1.0024
56			0.33	4.22							0.5105	38.41±0.18	1.0036
57			0.25	5.63							0.5633	36.31±0.18	1.0031
58		H	1.00	1.41	1.143	18.92	0.387	Al	0.453	0.028	0.5674	12.03±0.91	0.9998
59			0.67	2.11							0.6244	31.21±0.35	1.0046
60			0.50	2.82							0.6767	42.26±0.51	1.0020
61			0.33	4.22							0.7706	46.18±0.37	1.0017
62			0.25	5.63							0.8542	40.14±0.17	0.9996
63		H	1.00	1.41	1.143	18.92	0.600	Al	0.666	0.028	0.8537	21.33±0.41	1.0067
64			0.67	2.11							0.9444	40.23±0.30	1.0083
65			0.50	2.81							1.0273	48.22±0.31	1.0059
66			0.33	4.22							1.1759	47.12±0.33	0.9990

(cont'd)

TABLE B.6 - CHARACTERISTICS OF AND CALCULATIONAL RESULTS FOR BENCHMARK U-235/U-METAL LATTICES (cont'd)

Case No.	Ref.	Lattice Type (*)	Fuel/H_2O Volume Ratio	H / U-238 Ratio	Enrichment (at%)	Fuel Density (g/cm^3)	Pellet Diameter (in.)	Clad Material	Clad OD (in.)	Clad Thickness (in.)	Lattice Pitch (in.)	Critical Buckling (m^{-2})	Calculated k
67			0.25	5.63							1.3070	36.03±0.16	0.9911
68		S	1.11	1.27	1.142	18.72	1.200	Al	1.255	0.020	1.50	30.0±2.1	1.0166
69			0.71	2.00							1.68	44.8±2.6	1.0143
70			0.52	2.75							1.85	43.6±1.0	1.0085
71		H	0.49	2.87	1.299	18.898	0.387	Al	0.453	0.028	0.679	53.55±0.48	1.0064
72			0.33	4.27							0.772	58.2±1.00	1.0088
73		H	1.00	1.42	1.299	18.898	0.387	Al	0.453	0.028	0.5674	20.98±0.46	1.0002
74			0.67	2.12							0.6244	40.51±0.30	1.0095
75			0.50	2.83							0.6767	52.19±0.36	1.0092
76			0.33	4.25							0.7706	59.25±0.33	1.0060
77			0.25	5.67							0.8542	54.69±0.36	1.0037
78		H	1.00	1.42	1.299	18.898	0.600	Al	0.666	0.028	0.8537	32.11±0.54	1.0039
79			0.67	2.12							0.9444	51.87±0.50	1.0087
80			0.50	2.83							1.0273	61.08±0.32	1.0069
81			0.33	4.25							1.1754	60.99±0.26	1.0025
82			0.25	5.66							1.3070	50.38±0.27	0.9962

(cont'd)

TABLE B.6 - CHARACTERISTICS OF AND CALCULATIONAL RESULTS FOR BENCHMARK U-235/U-METAL LATTICES (cont'd)

Case No.	Ref.	Lattice Type (*)	Fuel/H_2O Volume Ratio	H U-238 Ratio	Enrichment (at%)	Fuel Density (g/cm^3)	Pellet Diameter (in.)	Clad Material	Clad OD (in.)	Clad Thickness (in.)	Lattice Pitch (in.)	Critical Buckling (m^{-2})	Calculated k
83		H	0.83	1.64	1.44	18.90	1.336	Al	1.500	0.049	2.00	52.94±0.21	1.0270
84			0.68	1.98							2.10	56.78±0.27	1.0279
85			0.58	2.34							2.20	57.74±0.03	1.0259
86			0.43	3.11							2.40	51.15±0.05	1.0209
87			0.34	3.95							2.60	38.18±0.10	1.0110
												Average k**	1.006
													± 0.011

* S = Square; H = Hexagonal

** Does not include Cases No. 1, 2, 3, 11 and 34

Reference (H-1)

APPENDIX C

BENCHMARKING OF LASER AGAINST EXPERIMENTAL DATA

Tables C-1 and C-3 present the lattice parameters, and the k values calculated using LASER for benchmark Pu/UO_2 (H_2O) and Pu/Al (D_2O) lattices, respectively. For comparison, results from EPRI-LEOPARD for the same lattices are also given.

Tables C-2 and C-3 give the isotopic composition for the fuel used in the lattices of Tables C-1 and C-2, respectively.

TABLE C.1

CHARACTERISTICS OF AND CALCULATIONAL RESULTS FOR BENCHMARK Pu/UO_2 (H_2O) LATTICES

Case #	Lattice Type	Enrichment (w%)	F/M Volume Ratio	Fuel Density (g/cm^3)	Pellet Diameter (cm)	Clad Material	Clad OD (cm)	Clad Thickness (cm)	Lattice Pitch (cm)	Critical Buckling (m^{-2})	Calculated k LEOPARD	Calculated k LASER
1	H	1.5	0.91	9.59	0.9448	Zr-2	1.082	0.06858	1.397	48.0	1.0042	0.9977
2			0.64						1.524	65.1	1.0144	1.0006
3	H	2.0	0.40	9.54	1.2828		1.4352	0.0762	2.3622	103.3	1.0354	1.0165
4			0.40						2.3622	86.3	1.0343	1.0205
5			0.66						2.0320	63.1	1.0034	1.0028
6			0.40						2.3622	79.4	1.0190	1.0086
7	S	2.0	0.89	9.54	1.2828		1.4352	0.0762	1.7526	69.1	1.0126	1.0042
8			0.64						1.905	90.0	1.0162	1.0012
9	H	4.0	0.52	9.46	1.26366		1.4351	0.085598	2.159	94.7	1.0098	1.0104
10			0.39						2.3622	107.9	1.0189	1.0123
11	S	6.6	0.59	10.3334	0.857		0.993	0.05840	1.3208	108.8	0.9943	0.9996
12			0.46						1.4224	121.5	1.0186	1.0153
									Average k		1.0151 ± 0.0119	1.0075 ± 0.0075

Reference (G-1)

TABLE C.2

ISOTOPIC COMPOSITION OF Pu FUEL USED IN EXPERIMENTS

WITH PuO_2 /UO_2 LATTICES (at %)

Cases	Pu-239	Pu-240	Pu-241	Pu-242	Pu-238
1-2	91.41	7.83	0.73	0.03	
3	91.62	7.65	0.70	0.03	
4	81.11	16.54	2.15	0.20	
5-6	71.76	23.50	4.08	0.66	
7-8	91.65	7.62	0.70	0.031	
9-10	75.38	18.10	5.08	1.15	0.28
11-12	90.54	8.54	0.88	0.04	

Reference (G-1)

TABLE C.3

CHARACTERISTICS OF AND CALCULATIONAL RESULTS FOR

BENCHMARK Pu/Al (D_2O) LATTICES

Case #	Lattice	F/M Ratio	D_2O (%)	Pitch (cm)	Measured Buckling (m^{-2})	Calculated k LEOPARD	Calculated k LASER
1	2-i	0.96	99.10	2.1682	15.68±0.41	0.9790	1.0086
2	2-a		99.26		15.45±0.20	0.9819	1.0107
3	2-m	0.65	98.86	2.3987	17.25±0.21	0.9518	0.9822
4	5-a		99.05		20.68±0.14	0.9385	0.9782
5	5-m		98.96		20.75±0.14	0.9387	0.9789
6	7-a	0.49	98.92	2.6093	23.78±0.13	0.9360	0.9958
7	7-m		98.89		23.75±0.15	0.9370	0.9805
					Average k	0.9518	0.9907
						±0.0203	±0.0142

Reference : (O-2)
Lattice Type : Hexagonal
Pellet Diameter : 0.6 in.
Clad Material : Zr-2
Clad OD : 0.680 in.
Clad Thickness : 0.028 in.

TABLE C.4

ISOTOPIC COMPOSITION OF THE FUEL FOR Pu/Al (D_2O) LATTICES

Isotope	(Atom/cm^3) x 10^{23}
Pu-239	0.006550
Pu-240	0.000639
Pu-241	0.000095
Pu-242	0.000007
Al	0.581522
Fe	0.000006
Si	0.000029
C	0.000016
Ga	0.000004

Reference (O-2)

APPENDIX D

CHARACTERISTICS OF, AND MASS FLOW RESULTS FOR, THE U-235/UO_2 AND Pu/ThO_2 - FUELED CORES

In this appendix the characteristics of, and mass flow results for, the U-235/UO_2 and Pu/ThO_2-fueled cores calculated using EPRI-LEOPARD - are documented (Table D.2). Nomenclature for the symbols used in Appendices D, E and F are given in Table D.1.

TABLE D.1

MEANING AND UNITS OF SYMBOLS USED
IN APPENDICES D, E AND F

Symbol	Units	Meaning
F/M	-	Fuel-to-moderator volume ratio
ε	w %	Fuel enrichment
N	-	Number of staggered fuel batches (zones) used in the core
B_N	MWD/KgHM	Discharged burnup for an N-zone core
CR	-	Cycle-average fuel conversion ratio
SP(*)	KW/KgHM	Specific power
PY	\$/lb U_3O_8	Price of yellowcake
CNU(**)	ST U_3O_8/GWe.yr	Consumption of natural uranium ore per installed GWe per calendar year
FCC	mill/KWhre	Fuel cycle cost (at indifferences values of bred fissile species)
C23	\$/Kg	Indifference value of "equivalent" U-233
C49	\$/Kg	Indifference value of "equivalent" Pu-239

* the average specific power for the U-233/ThO_2 and Pu/UO_2 cores are 30.6 and 27.9 Kw/KgHM, respectively

** availability-based capacity factor = 0.83 and 0.2 w/o tails assay

TABLE D.2

MASS FLOWS FOR THE U-235/UO_2 AND Pu/ThO_2 CORES*

Fuel Type	U-235/UO_2	Pu/ThO_2	Pu/ThO_2
F/M	0.5	0.5	3.0
ε(w/o)	2.75	3.71	9.50
B_3	33.1	33.5	33.9
CR	0.64	0.72	0.83
SP	28.4	30.4	30.1
	CHARGED MASSES (Kg/MTHM)**		
Th-232	-	945.3	859.9
U-235	27.50		
U-238	972.5		
Pu-239	-	29.44	75.42
Pu-240	-	14.25	36.47
Pu-241	-	7.69	19.71
Pu-242	-	3.30	8.46
	DISCHARGED MASSES (Kg/MTHM)**		
Th-232	-	926.3	829.6
Pa-233	-	0.73	1.02
U-233	-	11.08	21.56
U-234	-	0.96	0.96
U-235	4.93	0.14	0.07
U-236	3.59	0.01	0.003
U-238	947.7		
Pu-239	4.61	4.63	48.92
Pu-240	2.40	7.94	35.20
Pu-241	1.21	6.84	15.13
Pu-242	0.55	4.87	8.41

*based on EPRI-LEOPARD calculations

**Discharged mass (*) are per metric ton heavy metal in the as-charged fuel

APPENDIX E

RESULTS FOR THE U-235/UO_2 : Pu/ThO_2 : U-233/ThO_2 SYSTEM OF COUPLED REACTORS.

In this appendix the charged and discharged masses calculated using EPRI-LEOPARD are presented for the U-233/ThO_2-fueled cores (Tables E.1 to E.6). The consumption of natural uranium and fuel cycle costs for the U-235/UO_2 : Pu/ThO_2 : U-233/ThO_2 system of coupled reactors are also given (Tables E.7 to E.12) together with the cycle-average fuel conversion ratio and discharged fuel burnup for the U-233/ThO_2 core.

TABLE E.1

Charged and Discharged Masses for the U-233/ThO_2 (F/M = 0.5) Core

N ↓	ε (w/o)	2.0	2.5	3.0	3.5	4.0	4.5
	Charged Masses (Kg/MTHM)						
	U-233	19.76	24.71	29.69	34.63	39.15	44.50
	U-234	1.72	2.15	2.63	3.06	3.49	3.91
	U-235	0.24	0.29	0.34	0.38	0.43	0.48
	Th-232	978.3	972.9	967.3	961.9	956.9	951.1
	Discharged Masses (Kg/MTHM)						
1	U-233	17.32	18.83	19.80	20.64	21.27	21.93
	Pa-233	1.13	1.04	0.99	0.94	0.91	0.88
	U-234	2.36	3.48	4.39	5.12	5.76	6.41
	U-235	0.38	0.68	0.97	1.24	1.49	1.77
	U-236	0.02	0.06	0.12	0.17	0.22	0.29
	Th-232	971.8	959.7	949.6	941.1	933.6	925.3
3	U-233	16.55	16.81	16.84	16.63	16.45	16.08
	Pa-233	1.18	1.13	1.11	1.09	1.09	1.08
	U-234	2.80	4.15	5.04	5.73	6.24	6.70
	U-235	0.50	0.95	1.32	1.63	1.88	2.12
	U-236	0.04	0.15	0.27	0.40	0.54	0.72
	Th-232	966.8	949.4	936.3	924.0	913.8	901.5
6	U-233	16.50	16.70	16.26	15.96	15.53	15.18
	Pa-233	1.18	1.14	1.13	1.12	1.13	1.12
	U-234	2.83	4.19	5.19	5.83	6.30	6.68
	U-235	0.51	0.97	1.40	1.71	1.95	2.13
	U-236	0.05	0.16	0.32	0.48	0.68	0.88
	Th-232	966.4	948.6	932.0	918.6	905.5	892.5

TABLE E.2

Charged and Discharged Masses for the U-233/ThO_2 (F/M = 1.0) Core

N ↓	ε (w/o)	2.0	2.5	3.0	3.5	4.5	5.0
	Charged Masses (Kg/MTHM)						
	U-233	19.76	24.71	29.69	34.63	44.50	49.47
	U-234	1.72	2.15	2.63	3.06	3.91	4.34
	U-235	0.24	0.29	0.34	0.38	0.48	0.53
		978.3	972.9	967.3	961.9	951.1	945.7
	Discharged Masses (Kg/MTHM)						
1	U-233	18.31	20.94	22.89	24.30	26.84	27.96
	Pa-233	1.17	1.14	1.07	1.02	0.95	0.92
	U-234	2.05	3.28	4.20	5.00	6.31	6.91
	U-235	0.34	0.73	1.10	1.48	2.16	2.49
	U-236	0.01	0.05	0.10	0.17	0.30	0.37
	Th-232	974.8	961.0	950.3	940.2	922.7	914.4
3	U-233	18.04	19.72	20.45	20.93	21.30	21.35
	Pa-233	1.26	1.19	1.14	1.11	1.08	1.06
	U-234	2.30	3.89	4.93	5.68	6.82	7.27
	U-235	0.42	1.04	1.61	2.06	2.86	3.18
	U-236	0.02	0.12	0.25	0.39	0.70	0.88
	Th-232	972.2	952.5	937.0	924.1	900.2	889.0
6	U-233	17.97	19.31	19.71	19.86	19.72	20.27
	Pa-233	1.28	1.20	1.17	1.15	1.12	1.09
	U-234	2.39	4.11	5.18	5.90	6.89	7.27
	U-235	0.44	1.18	1.80	2.28	3.01	3.24
	U-236	0.02	0.15	0.33	0.52	0.94	1.03
	Th-232	971.1	948.7	930.8	915.7	887.8	881.4

TABLE E.3

Charged and Discharged Masses for the U-233/ThO_2 (F/M = 1.5) Core

N ↓	ε (w/o)	2.5	3.0	3.5	4.0	4.5	5.0
	Charged Masses (Kg/MTHM)						
	U-233	24.71	29.69	34.63	39.15	44.50	49.47
	U-234	2.15	2.63	3.06	3.49	3.91	4.34
	U-235	0.29	0.34	0.38	0.43	0.48	0.53
	Th-232	972.9	967.3	961.9	956.9	951.1	945.7
	Discharged Masses (Kg/MTHM)						
1	U-233	22.77	25.85	28.33	30.31	32.47	34.29
	Pa-233	1.23	1.16	1.10	1.06	1.02	0.99
	U-234	2.73	3.77	4.61	5.32	6.04	6.70
	U-235	0.53	0.93	1.30	1.65	2.02	2.36
	U-236	0.02	0.06	0.11	0.17	0.23	0.29
	Th-232	966.5	954.6	944.0	934.9	924.8	915.7
3	U-233	22.38	24.54	25.93	26.93	27.93	28.68
	Pa-233	1.27	1.20	1.16	1.13	1.10	1.08
	U-234	3.08	4.39	5.36	6.09	6.80	7.41
	U-235	0.69	1.33	1.92	2.40	2.88	3.30
	U-236	0.04	0.14	0.26	0.39	0.53	0.68
	Th-232	962.4	945.5	930.5	918.3	905.0	893.2
6	U-233	22.22	24.10	25.14	25.90	26.43	26.91
	Pa-233	1.27	1.21	1.18	1.15	1.13	1.11
	U-234	3.25	4.61	5.62	6.33	7.03	7.58
	U-235	0.78	1.50	2.16	2.66	3.19	3.60
	U-236	0.05	0.18	0.34	0.50	0.71	0.90
	Th-232	960.2	941.5	924.4	910.8	895.0	882.0

TABLE E.4

Charged and Discharged Masses for the U-233/ThO_2 (F/M = 2.0) Core

N ↓	ε (w/o)	3.0	3.5	4.0	4.5	5.0	5.5
	Charged Masses (Kg/MTHM)						
	U-233	29.69	34.63	39.15	44.50	49.47	54.39
	U-234	2.63	3.06	3.49	3.91	4.34	4.77
	U-235	0.34	0.38	0.43	0.48	0.53	0.57
	Th-232	967.3	961.9	956.9	951.1	945.7	940.3
	Discharged Masses (Kg/MTHM)						
1	U-233	27.75	31.24	34.03	37.01	39.54	41.86
	Pa-233	1.26	1.20	1.15	1.11	1.08	1.05
	U-234	3.20	4.11	4.89	5.67	6.39	7.06
	U-235	0.63	0.99	1.33	1.68	1.99	2.29
	U-236	0.02	0.06	0.10	0.16	0.21	0.27
	Th-232	960.6	949.2	939.4	928.6	918.9	909.5
3	U-233	27.38	30.15	32.16	34.13	35.66	36.96
	Pa-233	1.28	1.23	1.19	1.16	1.13	1.11
	U-234	3.55	4.71	5.61	6.49	7.24	7.93
	U-235	0.82	1.41	1.90	2.41	2.85	3.24
	U-236	0.05	0.13	0.23	0.35	0.47	0.60
	Th-232	956.2	940.3	927.0	912.6	899.7	887.5
6	U-233	27.22	29.77	31.49	33.07	34.32	35.29
	Pa-233	1.29	1.24	1.20	1.17	1.15	1.13
	U-234	3.72	4.93	5.89	6.79	7.53	8.21
	U-235	0.92	1.58	2.15	2.72	3.18	3.60
	U-236	0.06	0.17	0.30	0.46	0.62	0.79
	Th-232	953.9	936.5	921.2	904.7	890.6	876.8

TABLE E.5

Charged and Discharged Masses for the U-233/ThO_2 (F/M = 2.5) Core

N ↓	ε (w/o)	3.5	4.0	4.5	5.0	5.5	6.0
	Charged Masses (Kg/MTHM)						
	U-233	34.63	39.15	44.50	49.47	54.39	59.36
	U-234	3.06	3.49	3.91	4.34	4.77	5.20
	U-235	0.38	0.43	0.48	0.53	0.57	0.67
	Th-232	961.9	956.9	951.1	945.7	940.3	934.8
	Discharged Masses (Kg/MTHM)						
1	U-233	32.89	36.55	40.39	43.61	46.54	49.27
	Pa-233	1.28	1.25	1.19	1.16	1.12	1.09
	U-234	3.56	4.34	5.17	5.94	6.67	7.39
	U-235	0.66	0.93	1.26	1.55	1.82	2.11
	U-236	0.02	0.05	0.09	0.13	0.18	0.24
	Th-232	955.6	946.0	934.5	924.2	914.2	904.4
3	U-233	32.63	35.80	38.91	41.32	43.34	45.12
	Pa-233	1.31	1.27	1.22	1.19	1.16	1.14
	U-234	3.86	4.89	5.90	6.79	7.62	8.40
	U-235	0.84	1.30	1.78	2.21	2.60	2.97
	U-236	0.04	0.11	0.20	0.30	0.40	0.52
	Th-232	951.5	937.7	922.4	908.5	895.2	882.3
6	U-233	32.56	35.55	38.37	40.45	42.20	43.66
	Pa-233	1.32	1.27	1.23	1.20	1.18	1.16
	U-234	3.97	5.10	6.20	7.14	7.97	8.76
	U-235	0.90	1.44	2.01	2.50	2.91	3.31
	U-236	0.05	0.13	0.26	0.39	0.52	0.68
	Th-232	950.0	934.3	916.7	900.8	886.3	871.8

TABLE E.6

Charged and Discharged Masses for the U-233/ThO_2 (F/M = 3.0) Core

N ↓	ε (w/o)	4.0	4.5	5.0	5.5	6.0	6.5
	Charged Masses (Kg/MTHM)						
	U-233	39.15	44.50	49.47	54.39	59.36	64.27
	U-234	3.49	3.91	4.34	4.77	5.20	5.67
	U-235	0.43	0.48	0.53	0.57	0.67	0.72
	Th-232	956.9	951.1	945.7	940.3	934.8	929.3
	Discharged Masses (Kg/MTHM)						
1	U-233	37.72	42.29	46.16	49.66	53.01	55.97
	Pa-233	1.26	1.28	1.24	1.20	1.16	1.13
	U-234	3.82	4.69	5.50	6.28	6.99	7.77
	U-235	0.62	0.92	1.19	1.44	1.68	1.91
	U-236	0.02	0.05	0.08	0.12	0.16	0.21
	Th-232	952.3	940.4	929.6	919.1	909.6	899.6
3	U-233	37.55	41.84	45.19	48.00	50.33	52.38
	Pa-233	1.34	1.30	1.26	1.22	1.19	1.17
	U-234	4.07	5.17	6.16	7.10	8.03	8.90
	U-235	0.76	1.21	1.61	1.98	2.37	2.68
	U-236	0.03	0.09	0.16	0.25	0.36	0.46
	Th-232	948.8	933.1	918.6	904.5	889.9	876.6
6	U-233	37.51	41.67	44.80	47.33	49.48	51.21
	Pa-233	1.35	1.30	1.26	1.23	1.20	1.18
	U-234	4.20	5.38	6.46	7.47	8.39	9.29
	U-235	0.84	1.33	1.81	2.23	2.62	2.97
	U-236	0.04	0.11	0.21	0.33	0.45	0.58
	Th-232	946.9	929.8	913.2	896.9	881.7	866.8

TABLE E.7

Consumption of Natural Uranium and Fuel Cycle Cost for the U-235/UO_2 : Pu/ThO_2 (F/M = 0.5) : U-233/ThO_2 (F/M = 0.5) System

N ↓	PY* ↓ ($/lb U_3O_8)	ε (w/o)	2.0	2.5	3.0	3.5	4.0	4.5
1		B_1	6.7	15.5	23.0	29.4	35.0	41.2
		CR	0.85	0.75	0.68	0.64	0.60	0.57
		CNU	100.2	105.2	108.0	109.7	110.7	111.6
	40	FCC	6.94	6.93	6.92	6.92	6.92	6.92
		C23	-16.0	- 3.6	3.6	7.87	10.5	12.6
		C49	13.5	14.8	15.6	16.1	16.3	16.6
	100	FCC	11.70	11.68	11.67	11.67	11.66	11.66
		C23	- 9.6	8.5	18.7	24.3	27.7	30.0
		C49	37.9	39.8	40.9	41.5	41.8	42.1
3		B_3	11.6	26.2	37.5	48.3	57.3	68.5
		CR	0.87	0.80	0.74	0.71	0.68	0.66
		CNU	95.7	101.3	104.4	106.1	107.2	108.0
	40	FCC	6.94	6.92	6.91	6.91	6.91	6.90
		C23	- 9.7	7.3	15.3	19.9	22.1	23.5
		C49	14.2	16.0	16.8	17.3	17.5	17.7
	100	FCC	11.69	11.66	11.65	11.64	11.64	11.64
		C23	1.4	27.3	38.6	44.8	47.1	48.3
		C49	39.1	41.8	43.0	43.6	43.9	44.0
6		B_6	13.3	30.0	44.4	56.9	68.5	82.5
		CR	0.88	0.81	0.77	0.74	0.72	0.71
		CNU	93.1	99.0	102.2	104.0	105.0	105.7
	40	FCC	6.94	6.92	6.91	6.90	6.90	6.90
		C23	- 7.8	10.5	19.6	23.7	25.7	26.5
		C49	14.4	16.3	17.3	17.7	17.9	18.0
	100	FCC	11.69	11.66	11.64	11.63	11.64	11.64
		C23	4.7	32.7	46.0	51.2	53.2	53.3
		C49	39.4	42.4	43.8	44.3	44.5	44.5

* See Table D.1 for symbol explanation and units

TABLE E.8

Consumption of Natural Uranium and Fuel Cycle Cost for the U-235/UO_2 : Pu/ThO_2 (F/M = 0.5) : U-233/ThO_2 (F/M = 1.0) System

N ↓	PY* ↓ ($/lb U_3O_8)	ε (w/o)	2.0	2.5	3.0	3.5	4.5	5.0
1		B_1	3.2	12.1	19.3	26.3	38.3	44.1
		CR	0.96	0.85	0.77	0.73	0.66	0.64
		CNU	97.2	100.4	104.6	106.9	109.5	110.3
	40	FCC	6.95	6.94	6.93	6.92	6.92	6.92
		C23	-20.5	- 7.2	0.3	5.5	11.0	12.5
		C49	13.1	14.5	15.3	15.8	16.4	16.5
	100	FCC	11.71	11.69	11.68	11.67	11.66	11.66
		C23	-17.5	2.2	12.8	20.1	27.2	29.0
		C49	37.1	39.2	40.3	41.0	41.8	42.0
3		B_3	5.6	20.4	32.7	43.2	63.3	72.9
		CR	0.97	0.88	0.82	0.78	0.72	0.70
		CNU	88.9	95.9	100.6	103.3	106.1	107.0
	40	FCC	6.95	6.93	6.92	6.91	6.91	6.91
		C23	-17.4	1.3	11.4	16.7	21.6	22.4
		C49	13.4	15.4	16.4	17.0	17.5	17.6
	100	FCC	11.70	11.67	11.66	11.65	11.64	11.64
		C23	-12.1	16.9	31.9	39.3	45.2	45.6
		C49	37.6	40.7	42.3	43.0	43.7	43.7
6		B_6	6.4	24.0	38.8	51.6	76.0	86.7
		CR	0.98	0.89	0.84	0.80	0.75	0.74
		CNU	86.9	94.2	98.7	101.4	104.2	104.9
	40	FCC	6.94	6.92	6.91	6.91	6.90	6.90
		C23	-16.6	4.5	15.5	20.9	24.9	24.8
		C49	13.5	15.7	16.9	17.4	17.9	17.8
	100	FCC	11.70	11.67	11.65	11.64	11.64	11.64
		C23	-10.5	22.5	38.9	46.4	50.8	49.7
		C49	37.8	41.3	43.0	43.8	44.3	44.1

* See Table D.1 for symbol explanation and units

TABLE E.9

Consumption of Natural Uranium and Fuel Cycle Cost
for the U-235/UO_2 : Pu/ThO_2 (F/M = 0.5) :
U-233/ThO_2 (F/M = 1.5) System

N ↓	PY* ↓ ($/lb U_3O_8)	ε (w/o)	2.5	3.0	3.5	4.0	4.5	5.0
1		B_1	5.8	12.8	19.3	24.9	31.2	37.0
		CR	0.94	0.86	0.81	0.77	0.74	0.71
		CNU	96.9	100.7	103.8	105.6	107.2	108.2
	40	FCC	6.94	6.93	6.93	6.92	6.92	6.92
		C23	-13.8	- 5.4	0.3	4.0	7.0	9.2
		C49	13.8	14.7	15.3	15.6	16.0	16.2
	100	FCC	11.70	11.69	11.68	11.67	11.67	11.67
		C23	- 9.3	2.9	10.9	16.2	20.4	23.2
		C49	37.9	39.2	40.1	40.6	41.1	41.4
3		B_3	9.5	21.5	32.7	42.0	52.2	61.5
		CR	0.96	0.89	0.84	0.81	0.78	0.76
		CNU	91.5	96.6	100.1	102.2	104.0	105.2
	40	FCC	6.94	6.93	6.92	6.91	6.91	6.91
		C23	-10.0	2.1	9.8	14.1	17.2	18.9
		C49	14.2	15.4	16.3	16.7	17.0	17.2
	100	FCC	11.69	11.67	11.66	11.66	11.65	11.65
		C23	- 2.7	15.8	27.3	33.5	37.6	39.7
		C49	38.6	40.6	41.8	42.4	42.9	43.1
6		B_6	11.4	25.3	38.7	49.4	62.4	73.0
		CR	0.96	0.90	0.86	0.83	0.80	0.78
		CNU	89.2	95.0	98.4	100.6	102.3	103.6
	40	FCC	6.94	6.92	6.91	6.91	6.91	6.91
		C23	- 8.2	4.9	13.3	17.5	20.6	21.7
		C49	14.4	15.7	16.6	17.1	17.4	17.5
	100	FCC	11.69	11.67	11.66	11.65	11.65	11.64
		C23	0.5	20.6	33.3	39.2	43.5	44.5
		C49	39.0	41.1	42.4	43.0	43.5	43.6

* See Table D.1 for symbol explanation and units

TABLE E.10

Consumption of Natural Uranium and Fuel Cycle Cost for the U-235/UO_2 : Pu/ThO_2 (F/M = 0.5) : U-233/ThO_2 (F/M = 2.0) System

N ↓	PY* ↓ ($/lb U_3O_8)	ε (w/o)	3.0	3.5	4.0	4.5	5.0	5.5
1		B_1	6.1	12.3	17.8	24.0	29.7	35.3
		CR	0.96	0.90	0.85	0.81	0.78	0.76
		CNU	98.0	99.9	102.0	104.2	105.6	106.7
	40	FCC	6.94	6.93	6.93	6.92	6.92	6.92
		C23	-11.3	- 5.0	- 0.8	3.0	5.6	7.6
		C49	14.0	14.7	15.2	15.5	15.8	16.0
	100	FCC	11.70	11.69	11.68	11.68	11.67	11.67
		C23	- 7.4	1.8	8.0	13.3	17.0	19.7
		C49	38.1	39.1	39.8	40.3	40.7	41.0
3		B_3	10.0	20.6	29.8	40.0	49.4	58.5
		CR	0.97	0.91	0.88	0.84	0.82	0.80
		CNU	92.5	95.6	98.4	100.8	102.5	103.7
	40	FCC	6.94	6.93	6.92	6.92	6.91	6.91
		C23	- 7.9	1.1	6.8	11.4	14.3	16.2
		C49	14.4	15.3	15.9	16.4	16.7	34.4
	100	FCC	11.69	11.68	11.67	11.66	11.66	11.65
		C23	- 1.5	12.4	21.0	27.8	31.9	16.9
		C49	38.8	40.2	41.1	41.8	42.3	42.5
6		B_6	12.0	24.2	35.3	47.7	58.5	69.2
		CR	0.97	0.92	0.89	0.86	0.83	0.81
		CNU	90.4	94.0	96.8	99.3	101.0	102.3
	40	FCC	6.93	6.92	6.92	6.91	6.91	6.91
		C23	- 6.3	3.4	9.8	14.6	17.2	18.9
		C49	14.6	15.6	16.3	16.8	36.9	17.2
	100	FCC	11.69	11.67	11.66	11.66	11.65	11.65
		C23	1.3	16.4	26.1	33.3	17.0	39.0
		C49	39.1	40.6	41.7	42.4	42.8	43.0

* See Table D.1 for symbol explanation and units

TABLE E.11

Consumption of Natural Uranium and Fuel Cycle Cost
for the U-235/UO_2 : Pu/ThO_2 (F/M = 0.5) :
U-233/ThO_2 (F/M = 2.5) System

N ↓	PY* ↓ ($/lb U_3O_8)	ε (w/o)	3.5	4.0	4.5	5.0	5.5	6.0
1		B_1	5.6	10.2	16.2	21.8	27.4	33.0
		CR	0.98	0.93	0.89	0.85	0.82	0.80
		CNU	98.5	98.8	100.8	102.5	104.0	105.2
	40	FCC	6.94	6.93	6.93	6.93	6.92	6.92
		C23	-10.1	- 5.9	- 1.6	1.5	4.0	6.0
		C49	- 7.0	14.6	15.1	15.4	15.6	15.9
	100	FCC	11.70	11.69	11.68	11.68	11.68	11.67
		C23	14.2	- 0.9	5.4	10.0	13.6	16.5
		C49	38.2	38.8	39.5	40.0	40.3	40.6
3		B_3	9.2	17.6	27.6	37.0	46.3	55.5
		CR	0.99	0.95	0.91	0.88	0.85	0.83
		CNU	92.3	93.6	96.6	98.9	100.7	102.1
	40	FCC	6.94	6.93	6.92	6.92	6.92	6.91
		C23	- 7.5	- 1.0	4.8	8.9	11.8	13.9
		C49	14.4	15.1	15.7	16.2	16.5	16.7
	100	FCC	11.69	11.68	11.67	11.67	11.66	11.66
		C23	- 2.4	7.6	16.4	22.6	27.0	30.0
		C49	38.7	39.7	40.6	41.3	41.8	42.1
6		B_6	10.5	20.7	32.8	44.3	54.9	65.8
		CR	0.99	0.95	0.92	0.89	0.86	0.84
		CNU	90.4	91.8	95.0	97.3	99.2	100.7
	40	FCC	6.93	6.93	6.92	6.92	6.91	6.91
		C23	- 6.6	0.9	7.4	11.8	14.6	16.5
		C49	14.5	15.3	16.0	16.5	16.8	17.0
	100	FCC	11.69	11.68	11.67	11.66	11.66	11.65
		C23	- 0.9	10.8	20.8	27.6	31.7	34.4
		C49	38.8	40.1	41.1	41.8	42.2	42.5

* See Table D.1 for symbol explanation and units

TABLE E.12

Consumption of Natural Uranium and Fuel Cycle Cost
for the U-235/UO_2 : Pu/ThO_2 (F/M = 0.5) :
U-233/ThO_2 (F/M = 3.0) System

N ↓	PY* ↓ ($/lb U_3O_8)	ε (w/o)	4.0	4.5	5.0	5.5	6.0	6.5
1		B_1	3.9	9.6	15.1	20.6	25.5	31.1
		CR	1.01	0.96	0.92	0.89	0.85	0.83
		CNU	102.0	97.9	99.2	100.9	102.7	104.0
	40	FCC	6.94	6.93	6.93	6.93	6.93	6.92
		C23	-10.2	- 5.5	- 2.0	0.8	2.9	4.9
		C49	14.2	14.6	15.0	15.3	15.5	15.7
	100	FCC	11.70	11.69	11.69	11.68	11.68	11.68
		C23	- 8.2	- 1.3	3.9	8.1	11.1	14.0
		C49	38.1	38.8	39.3	39.8	40.1	40.4
3		B_3	7.0	16.1	25.1	34.4	44.6	53.8
		CR	1.02	0.97	0.94	0.90	0.88	0.85
		CNU	93.6	92.3	94.7	97.0	98.9	100.6
	40	FCC	6.94	6.93	6.92	6.92	6.92	6.92
		C23	- 8.2	- 1.8	3.1	7.0	10.3	12.4
		C49	14.4	15.0	15.6	16.0	16.3	16.5
	100	FCC	11.69	11.68	11.68	11.67	11.67	11.66
		C23	- 4.7	5.2	12.7	18.7	23.8	27.0
		C49	38.4	39.5	40.3	40.9	41.4	41.8
6		B_6	8.5	19.0	30.1	41.4	52.3	63.4
		CR	1.02	0.95	0.94	0.91	0.89	0.86
		CNU	90.3	90.2	92.8	95.3	97.6	99.3
	40	FCC	6.94	6.93	6.92	6.92	6.92	6.91
		C23	- 7.2	- 0.2	5.3	9.6	12.6	14.7
		C49	14.5	15.2	15.8	16.2	16.5	16.8
	100	FCC	11.69	11.68	11.67	11.67	11.66	11.66
		C23	- 3.0	7.8	16.6	23.2	27.7	30.9
		C49	3.9	39.7	40.7	41.4	41.8	42.2

* See Table D.1 for symbol explanation and units

APPENDIX F

RESULTS FOR THE U-235/UO_2 : Pu/UO_2 SYSTEM OF COUPLED REACTORS.

In this appendix the charged and discharged masses calculated using LASER are presented for the Pu/UO_2-fueled cores (Tables F.1 to F.4). The consumption of natural uranium and fuel cycle costs for the U-235/UO_2 : Pu/UO_2 system of coupled reactors are also given (Tables F.5 to F.8) together with the cycle-average fuel conversion ratio and discharged fuel burnup for the Pu/UO_2 core.

TABLE F.1

Charged and Discharged Masses for the PU/UO_2 (F/M = 0.5) Core

N ↓	ε (w/o)	1.5	2.0	3.0	4.0
	Charged Masses (Kg/MTHM)				
	U-235	1.98	1.93	1.93	1.89
	U-238	978.9	971.5	956.7	942.1
	Pu-239	10.36	14.33	22.31	30.28
	Pu-240	4.98	6.90	10.75	14.55
	Pu-241	2.70	3.74	5.80	7.87
	Pu-242	1.13	1.58	2.48	3.34
	Discharged Masses (Kg/MTHM)				
1	U-235	1.43	1.26	1.11	1.01
	U-236	0.10	0.13	0.17	0.19
	U-238	972.7	962.0	941.5	922.0
	Pu-239	7.75	9.33	12.25	15.05
	Pu-240	5.18	6.91	10.00	12.82
	Pu-241	2.79	3.83	5.78	7.57
	Pu-242	1.50	2.17	3.38	4.44
3	U-235	1.17	0.95	0.73	
	U-236	0.15	0.19	0.23	
	U-238	969.2	956.3	931.7	
	Pu-239	6.80	7.63	8.93	
	Pu-240	5.09	6.47	8.57	
	Pu-241	2.75	3.62	5.04	
	Pu-242	1.72	2.53	4.00	
6	U-235	1.06	0.83	0.58	
	U-236	0.17	0.21	0.25	
	U-238	967.5	953.7	926.7	
	Pu-239	6.44	7.07	7.74	
	Pu-240	5.02	6.22	7.78	
	Pu-241	2.71	3.49	4.54	
	Pu-242	1.82	2.69	4.29	

TABLE F.2

Charged and Discharged Masses for the PU/UO_2 (F/M = 1.0) Core

N ↓	ε (w/o)	4.0	5.0	6.0	7.0
	Charged Masses (Kg/MTHM)				
	U-235	1.89	1.84	1.84	1.79
	U-238	942.1	927.4	912.6	897.9
	Pu-239	30.28	38.23	46.18	54.15
	Pu-240	14.55	18.39	22.22	26.10
	Pu-241	7.87	9.93	11.99	14.04
	Pu-242	3.34	4.24	5.14	6.04
	Discharged Masses (Kg/MTHM)				
1	U-235	1.76	1.53	1.40	1.26
	U-236	0.04	0.09	0.13	0.15
	U-238	938.6	917.8	897.6	877.5
	Pu-239	29.33	35.08	40.29	44.91
	Pu-240	14.24	17.35	20.33	23.16
	Pu-241	8.28	10.81	13.02	14.99
	Pu-242	3.36	4.26	5.14	6.01
3	U-235	1.69	1.38	1.18	1.02
	U-236	0.05	0.13	0.18	0.21
	U-238	936.8	912.4	888.3	866.2
	Pu-239	28.90	33.58	37.37	40.92
	Pu-240	14.08	16.75	19.11	21.47
	Pu-241	8.46	11.09	13.18	14.91
	Pu-242	3.37	4.30	5.20	6.05
6	U-235	1.67	1.32	1.10	0.95
	U-236	0.06	0.14	0.20	0.22
	U-238	936.1	910.0	884.4	862.3
	Pu-239	28.73	32.97	36.27	39.69
	Pu-240	14.01	16.48	18.60	20.89
	Pu-241	8.52	11.18	13.17	14.81
	Pu-242	3.38	4.32	5.23	6.07

TABLE F.3

Charged and Discharged Masses for the PU/UO_2 (F/M = 2.0) Core

N ↓	ε (w/o)	7.0	8.0	9.0
	Charged Masses (Kg/MTHM)			
	U-235	1.79	1.75	1.75
	U-238	897.9	883.2	868.5
	Pu-239	54.15	62.13	70.08
	Pu-240	26.10	29.92	33.74
	Pu-241	14.04	16.10	18.19
	Pu-242	6.04	6.89	7.78
	Discharged Masses (Kg/MTHM)			
1	U-235	1.62	1.39	1.25
	U-236	0.05	0.11	0.15
	U-238	891.3	868.2	846.0
	Pu-239	53.27	59.03	63.90
	Pu-240	25.15	27.55	29.80
	Pu-241	14.56	16.94	18.98
	Pu-242	5.96	6.73	7.56
3	U-235	1.53	1.22	1.04
	U-236	0.08	0.16	0.20
	U-238	887.6	859.3	834.0
	Pu-239	52.82	57.48	61.23
	Pu-240	24.64	26.26	27.93
	Pu-241	14.79	17.11	18.88
	Pu-242	5.93	6.67	7.47
6	U-235	1.49	1.15	0.99
	U-236	0.09	0.18	0.22
	U-238	886.1	855.3	830.2
	Pu-239	52.65	56.85	60.49
	Pu-240	24.44	25.73	27.38
	Pu-241	14.86	17.13	18.80
	Pu-242	5.91	6.64	7.44

TABLE F.4

Charged and Discharged Masses for the PU/UO_2 (F/M = 3.0) Core

N ↓	ε (w/o)	8.0	9.0	10.0
	Charged Masses (Kg/MTHM)			
	U-235	1.75	1.75	1.70
	U-238	883.2	868.5	853.7
	Pu-239	62.13	70.08	78.07
	Pu-240	29.92	33.74	37.59
	Pu-241	16.10	18.19	20.24
	Pu-242	6.89	7.78	8.68
	Discharged Masses (Kg/MTHM)			
1	U-235	1.49	1.30	1.14
	U-236	0.08	0.13	0.16
	U-238	872.2	847.5	824.6
	Pu-239	61.06	66.58	71.21
	Pu-240	28.04	29.82	31.57
	Pu-241	16.92	19.26	21.16
	Pu-242	6.78	7.60	8.43
3	U-235	1.37	1.10	0.98
	U-236	0.11	0.18	0.20
	U-238	865.9	835.6	813.7
	Pu-239	60.54	64.95	69.21
	Pu-240	27.07	27.94	29.71
	Pu-241	17.19	19.29	20.93
	Pu-242	6.73	7.53	8.36
6	U-235	1.31	1.04	0.92
	U-236	0.13	0.20	0.21
	U-238	863.1	831.2	809.1
	Pu-239	60.33	64.41	68.49
	Pu-240	26.66	27.30	28.97
	Pu-241	17.28	19.24	20.77
	Pu-242	6.72	7.50	8.33

TABLE F.5

Consumption of Natural Uranium and Fuel Cycle Cost for the U-235/UO_2 : Pu/UO_2 (F/M = 0.5) System

N ↓	PY* ↓ ($/lb U_3O_8)	ε (w/o)	1.5	2.0	3.0	4.0
1		B_1	8.3	13.9	24.2	34.0
		CR	0.72	0.70	0.68	0.67
		CNU	103.6	106.9	110.5	112.7
	40	FCC	7.25	7.11	6.99	6.95
		C49	-17.0	- 3.4	8.4	12.8
	100	FCC	12.10	11.93	11.80	11.75
		C49	- 3.1	13.6	27.0	31.4
3		B_3	12.8	21.4	38.1	
		CR	0.74	0.73	0.71	
		CNU	99.9	103.3	107.0	
	40	FCC	7.15	6.99	6.87	
		C49	- 7.51	8.2	20.5	
	100	FCC	11.93	11.73	11.58	
		C49	13.8	33.8	48.0	
6		B_6	14.8	24.6	44.9	
		CR	0.75	0.74	0.73	
		CNU	98.4	101.8	105.4	
	40	FCC	7.11	6.95	6.83	
		C49	- 3.54	12.5	24.9	
	100	FCC	11.86	11.65	11.51	
		C49	20.8	41.2	55.4	

* See Table D.1 for symbol explanation and units

TABLE F.6

Consumption of Natural Uranium and Fuel Cycle Cost for the U-235/UO_2 : Pu/UO_2 (F/M = 1.0) System

N ↓	PY* ↓ ($/lb U_3O_8)	ε (w/o)	4.0	5.0	6.0	7.0
1		B_1	4.0	11.6	19.4	27.8
		CR	0.91	0.88	0.84	0.81
		CNU	92.1	86.7	92.5	97.7
	40	FCC	7.16	7.10	7.06	7.03
		C49	- 8.6	- 2.4	1.6	4.6
	100	FCC	12.13	12.04	11.98	11.94
		C49	- 6.5	2.5	8.4	12.7
3		B_3	6.0	18.1	31.1	42.7
		CR	0.91	0.89	0.85	0.82
		CNU	82.2	82.2	89.5	95.4
	40	FCC	7.15	7.06	7.01	6.98
		C49	- 7.2	1.1	6.6	9.5
	100	FCC	12.11	11.98	11.90	11.85
		C49	- 4.0	8.6	17.0	21.2
6		B_6	6.8	20.9	35.9	47.8
		CR	0.91	0.89	0.85	0.83
		CNU	79.3	81.0	88.8	94.8
	40	FCC	7.14	7.05	6.99	6.97
		C49	- 6.7	2.4	8.24	10.7
	100	FCC	12.10	11.96	11.87	11.83
		C49	- 3.1	11.0	19.9	23.3

* See Table D.1 for symbol explanation and units

TABLE F.7

Consumption of Natural Uranium and Fuel Cycle Cost for the U-235/UO_2 : Pu/UO_2 (F/M = 2.0) System

N ↓	PY* ↓ ($/lb U_3O_8)	ε (w/o)	7.0	8.0	9.0
1		B_1	7.0	17.3	27.7
		CR	1.00	0.95	0.91
		CNU	74.2	71.7	81.8
	40	FCC	7.11	7.07	7.04
		C49	- 3.5	0.5	3.4
	100	FCC	12.08	12.02	11.97
		C49	- 1.4	4.9	9.49
3		B_3	11.0	27.5	42.2
		CR	1.00	0.95	0.91
		CNU	56.1	65.5	78.9
	40	FCC	7.09	7.04	7.01
		C49	- 1.9	3.7	7.0
	100	FCC	12.05	11.96	11.91
		C49	1.3	10.4	15.7
6		B_6	12.6	31.9	46.6
		CR	1.00	0.95	0.91
		CNU	51.4	64.3	78.4
	40	FCC	7.09	7.03	7.00
		C49	- 1.4	4.8	7.8
	100	FCC	12.04	11.94	11.90
		C49	2.2	12.4	17.1

* See Table D.1 for symbol explanation and units

TABLE F.8

Consumption of Natural Uranium and Fuel Cycle Cost for the U-235/UO_2 : Pu/UO_2 (F/M = 3.0) System

N ↓	PY* ↓ ($/lb U_3O_8)	ε (w/o)	8.0	9.0	10.0
1		B_1	11.7	23.9	35.6
		CR	1.04	0.98	0.94
		CNU	38.9	54.3	71.0
	40	FCC	7.09	7.05	7.03
		C49	- 1.4	2.3	4.9
	100	FCC	12.05	11.99	11.95
		C49	1.6	7.5	11.6
3		B_3	18.3	37.3	48.6
		CR	1.03	0.98	0.94
		CNU	19.7	51.3	70.1
	40	FCC	7.07	7.02	7.00
		C49	0.7	5.7	7.4
	100	FCC	12.01	11.93	11.91
		C49	5.2	13.3	16.0
6		B_6	21.2	42.2	54.0
		CR	1.03	0.98	0.94
		CNU	15.8	51.3	69.8
	40	FCC	7.06	7.01	6.99
		C49	1.6	6.6	8.2
	100	FCC	12.00	11.92	11.89
		C49	6.7	15.0	17.4

* See Table D.1 for symbol explanation and units

REFERENCES

A-1 Abtahi, F., "Out-of-Reactor Aspects of Thorium Utilization in Light Water Reactors", Ph.D. Thesis, MIT, Nucl. Eng. Dept. (July 12, 1977)

A-2 Abbaspour, A.T. and Driscoll, M.J., "The Fuel Cycle Economics of Improved Uranium Utilization in Light Water Reactors", MIT-EL 79-001, MITNE-224 (January, 1979).

A-3 Amster, H. and Suarez, R., "The Calculation of Thermal Constants Averaged over a Wigner Wilkins Flux Spectrum: Description of the SOFOCATE Code, "WAPD-TM-39 (January, 1957).

B-1 Boynton, A. R., et. al., "High-Conversion Critical Experiment Program", Reactor Physics Division Annual Report, July 1, 1963 to June 30, 1964, ANL-7010, pp. 33-43 (1965)

B-2 Barry, R. F., "LEOPARD - A Spectrum Dependent Non-Spatial Depletion Code", WCAP-3269-26 (September, 1963).

B-3 Bohl, H., Gelbard, E., and Ryan, G., "MUFT-4 - Fast Neutron Spectrum Code for the IBM-704", WAPD-TM-72 (July, 1957)

B-4 Bell, M. J., "ORIGEN - The ORNL Isotope Generation and Depletion Code", ORNL-4628 (May, 1973)

B-5 Bondarenko, I. I., "Group Constants for Nuclear Reactor Calculations", Consultants Bureau Enterprises, Inc., 227 West 17th St., New York, NY, 10011 (1964)

B-6 Borg, R. C. and Ott, K. O., "A Stationary Definition of the Doubling Time for Breeder Reactor Fuel", Trans. Am. Nucl. Soc., 23, 533 (1976)

B-7 Boyd, W. A., "Thermal-Hydraulics Analysis of Tight Lattice Light Water Reactors", SM Thesis, MIT Nucl. Eng. Dept. (May 1977)

B-8 Beecher, N., Benedict, M., "Which for Minimum Fuel Cost - Zircaloy or Stainless Clad?", Nucleonics, Vol. 17, No. 7, 64, (July, 1959)

C-1 Correa, F., "Utilization of Thorium in PWR Reactors", SM Thesis, University of São Paulo, Brazil, 1976; English Translation Available as ERDA-TR-214

C-2 Celnik, J., et. al., "Representation of Fission Products in Thermal Power Reactors Containing UO_2 and Plutonium Recycle Fuel", Trans. Am. Nucl. Soc., 10, 516 (1967)

C-3 Cobb, W. R. and Eich, W. J., "A New Cell Depletion Code for LWR Analysis", Trans. Am. Nucl. Soc., 24, 442 (1976)

C-4 Croff, A. G., "MITCOST-II - A Computer Code for Nuclear Fuel Cycle Costs", N.E. Thesis, MIT Nucl. Eng. Dept. (1974)

C-5 Cadwell, W. R., "PDQ-7 Reference Manual", WAPD-TM-678 (January, 1967)

C-6 Correa, F. and Driscoll, M. J., "Effect of the Th-232/U-238 Ratio on the Conversion Ratio of PWR's", Special Problem Report, MIT Nucl. Eng. Dept. (August, 1977)

D-1 DOE, ORNL/TM-6331, "The Economics and Utilization of Thorium in Nuclear Reactors", (May, 1978)

D-2 Davis, W. J., et. al., "SPHINX - A One Dimensional Diffusion and Transport Nuclear Cross Section Processing Code", WARD-XS-3045-17 (August, 1977)

E-1 Edlund, M. C., "Physics of the Uranium - Plutonium Fuel Cycle in Pressurized Water Reactors", Trans. Am. Nucl. Soc., 25, 136 (November, 1976)

E-2 Edlund, M. C., "High Conversion Ratio Plutonium Recycle in Pressurized Water Reactors", Annals of Nuclear Energy, Vol. 2, pp. 801 to 807, Pergamon Press (1975)

E-3 Engle, Jr., W. W. , "A User's Manual for ANISN - A One Dimensional Discrete Ordinates Transport Code with Anisotropic Scattering", K-1693 (March 30, 1967)

E-4 England, T. R., "CINDER - A One Point Depletion and Fission Product Program", WAPD-TM-334 (revised), BAPL (June, 1964)

E-5 Edlund, M. C., "Developments in Spectral Shift Reactors", Proc. Third U.N. Conf. on Peaceful Uses of Atomic Energy, 6, 314 (1964)

F-1 Fujita, E. K., Driscoll, M. J. and Lanning, D. D., "Design and Fuel Management of PWR Cores to Optimize the Once-Through Fuel Cycle", MIT-EL 78-017, MITNE-215 (August, 1978)

F-2 Feiveson, H. A. and Taylor, T. B., "Security Implications of Alternative Fission Futures", Bull. At. Sci., 32, 10-14 (1976)

G-1 Garel, K. C. and Driscoll, M. J., "Fuel Cycle Optimization of Thorium and Uranium Fueled PWR Systems", MIT-EL 77-018, MITNE-204 (October, 1977)

G-2 Garrison, J. D. and Roos, B. W., "Fission-Product Capture Cross Sections", Nucl. Sci. Eng., 12, 115-135 (1962)

G-3 Graves, H. W., Jr., "Nuclear Fuel Management", John Wiley and Sons, Inc., New York, pg. 273 (1979)

H-1 Hellens, R. L. and Price, G. A., "Reactor Physics Data for Water-Moderated Lattices of Slightly Enriched Uranium", Reactor Technology - Selected Reviews, TID-8540 (1964)

H-2 Hardy, Jr., J., et. al., "Measurement and Analysis of Parameters in Tight ^{232}Th - ^{235}U and ^{232}Th - ^{233}U Lattices Moderated with Heavy Water", Nucl. Sci. Eng., 55, 401-417 (1974)

H-3 Honeck, H. C., "THERMOS - A Thermalization Transport Theory Code for Reactor Lattice Calculations", BNL-5826 (1961)

K-1 Kasten, P. R., et. al., "Assessment of the Thorium Fuel Cycle in Power Reactors", ORNL/TM-5565 (January, 1977)

K-2 Kidman, R. B., and MacFarlane, R. E., "LIB-IV, A Library of Group Constants for Nuclear Reactor Calculations", LA-6260-MS, Los Alamos Scientific Laboratory (March, 1976)

L-1 Safety Analysis Report for the Light Water Breeder Reactor, Volume 4 (1975)

M-1 Milani, et.al., "BNU Series of ^{233}U Fueled Critical Experiments", WAPD-TM-1117 (January, 1975)

M-2 Milani, et. al., "^{233}U Oxide-Thorium Oxide Detailed Cell Critical Experiments", WAPD-TM-1101 (October, 1974)

M-3 Momsen, B. F., "An Analysis of Plutonium Recycle Fuel Elements in San Onofre-I", Nucl. Eng. Thesis, MIT Nucl. Eng. Dept. (May, 1974)

M-4 Maudlin,, P. J., Borg, R. C. and Ott, K. O., "Transitory Fuel Growth Rates for Fast Breeder Reactors", Trans. Am. Nucl. Soc., 26, 235 (1977)

M-5 Maine Yankee Atomic Power Company, "Preliminary Safety Analysis Report Volume I, Maine Yankee Atomic Power Station", (September, 1967)

N-1 Nininger, R. D. and Bowie, S. H. U., "Technological Status of Nuclear Fuel Resources", Trans. Am. Nucl. Soc., 25, 35 (1976)

N-2 Nuclear News, 22, No. 2 (February, 1979)

O-1 Oosterkamp, W. J., and Correa, F., "Thorium Utilization in the Angra dos Reis PWR", IEA, 419, Trans. Am. Nucl. Soc., 21, 261 (1976)

O-2 Ozer, O., "Analysis of Exponential Experiments with Lattices of Plutonium in Heavy Water", Nucl. Sci. Eng., 43, 286-302 (1971)

O-3 Olsen, A.R., et. al., "Irradiation Behavior of Thorium-Uranium Alloys and Compounds", IAEA Technical Report Series No. 52, Utilization of Thorium in Power Reactors (1966); also available as ORNL/TM-1142 (1965)

P-1 Peterson, S., et. al., "Properties of Thorium, Its Alloys and Its Compounds", IAEA Technical Report Series No. 52, Utilization of Thorium in Power Reactors (1966)

P-2 Perry, A. M. and Weinberg, A. M., "Thermal Breeder Reactors", An. Rev. Sci., 22, 317-54 (1972)

P-3 Poncelet, C. G., "LASER - A Depletion Program for Lattice Calculations Based on MUFT and THERMOS", WCAP-6073 (April, 1966)

R-1 Robbins, T. R., "Preliminary Evaluation of a Variable Lattice Fuel Assembly and Reactor Design Concept", ORNL/Sub-79/13576/1 (1979)

R-2 Radkowsky, A., et. al., "Epithermal to Intermediate Spectrum Pressurized Heavy Water Breeder Reactor", U. S. Patent 3, 859, 165; Official Gazette of the United States Patent Office, Volume 930, Number 1 (January 7, 1975)

S-1 Shapiro, N. L., et. al., "Assessment of Thorium Fuel Cycles in Pressurized Water Reactors", EPRI-NP-359 (February, 1977)

S-2 Strawbridge, L. E. and Barry, R. F., "Criticality Calculations for Uniform Water-Moderated Lattices", Nucl. Sci. Eng., 23, 58-73 (1965)

S-3 Steen, N. M., "An Evaluation of the Radioactive Neutron Capture Cross Sections of Thorium-232 for the Range 0.0 eV to 15 MeV", WAPD-TM-971 (December, 1970)

S-4 Spierling, H., "The Value of Recycle Plutonium in Pressurized Water Reactors", Ph.D. Thesis, MIT Nucl. Eng. Dept. (February, 1972)

S-5 Suich, J. E. and Honeck, H. C.,"The HAMMER System: Heterogeneous Analysis by Multigroup Methods of Exponentials and Reactors", DP-1064 (1967)

S-6 Sege, C. A., et. al., "The Denatured Thorium Cycle - An Overview" Nucl. Technol., 42, 144-149 (Feb. 1979)

U-1 Ullo, J. J., et. al., "Review of Thorium - U-233 Cycle Thermal Reactor Benchmark Studies", Proc. Thermal Reactor Data Seminar, Brookhaven National Lab. (May, 1978)

U-2 USAEC, The Use of Thorium in Nuclear Power Reactors, WASH 1097 (June, 1969)

W-1 Williamson, H. E., et. al., "Assessment of Utilization of Thorium in BWRs", ORNL/SUB-4380/5, NEDG-24073 (January, 1978)

W-2 Windsor, H. H., et. al., "Exponential Experiments with Lattices of Uranium-233 Oxide and Thorium Oxide in Light and Heavy Water", Nucl. Sci. Eng. 42, 150-161 (1970)

W-3 Wehmeyer, D. B., "Analysis of Water Moderated UO_2 and ThO_2 Lattices", BAW-1257 (May, 1962)

Z-1 Zorzoli, G. B., "The Use of Metallic Thorium for LWBRs and LWRs", Nucl. Technol., 20, 109-13 (1973)